Transdermal Delivery of a DTPA Penta-ethyl Ester Prodrug for Continuous Decorporation of Transuranic Elements

Yong Zhang

A dissertation submitted to the faculty of the University of North Carolina at Chapel Hill in partial fulfillment of the requirements for the degree of Doctor of Philosophy in the UNC Eshelman School of Pharmacy.

Chapel Hill
2013

Approved By:

Michael Jay, Ph.D.

Richard J. Kowalsky, Pharm.D.

Zhi Liu, Ph.D.

Russell J. Mumper, Ph.D.

William C. Zamboni, PharmD, Ph.D.

©2013
Yong Zhang
ALL RIGHTS RESERVED

ABSTRACT

YONG ZHANG: Transdermal Delivery of a DTPA Penta-ethyl Ester Prodrug for Continuous Decorporation of Transuranic Elements
(Under the direction of Prof. Michael Jay, Ph.D.)

The penta-ethyl ester of diethylenetriamine pentaacetic acid (DTPA), a DTPA prodrug designated as C2E5, was designed for transdermal delivery for radionuclide decorporation. The C2E5 was first screened with a prototype cream formulation and a hydrocarbon base ointment. C2E5 experienced rapid degradation in the cream matrix and C2E5 ointment formulations underwent phase separation due to components incompatibility. Non-aqueous gel matrix comprised of ethyl cellulose/Miglyol 840® was utilized to formulate C2E5.

The C2E5 non-aqueous gel prepared by direct mixing method failed to yield a uniform and pharmaceutically acceptable gel. Solvent evaporation method was conceived and applied to prepare the C2E5 non-aqueous gels. The thermal, rheological and *in vitro* release studies of a formulation containing 40% C2E5, 20% ethyl cellulose and 40% Miglyol 840 prepared using the solvent evaporation method demonstrated that the gel had acceptable content uniformity, flow properties and C2E5 release profile suitable for transdermal delivery. Topical application of the gel at a 200 mg C2E5/kg dose level in rats achieved higher plasma exposures of several active metabolites compared with neat C2E5 oil at the same dose level.

The C2E5 non-aqueous gels comprised of 40% C2E5, 40-45% Miglyol 840 and 15-20% ethyl cellulose prepared by solvent evaporation method were further evaluated by mass balance study and *in vivo* decorporation study in rodents. When the aforementioned C2E5 gels were spiked with [^{14}C]-C2E5 and applied to rat skin at a dose of 200 mg

C2E5/kg, over 60% of the applied dose was absorbed within a 24 h period. Radioactivity was observed in urinary and fecal excretions for over three days after removal of the gel. Using an ^{241}Am wound contamination model, transdermal C2E5 gels were able to enhance total body elimination and reduce the liver and skeletal burden of ^{241}Am in a dose-dependent manner. The efficacy achieved by a single 1000 mg/kg dose to contaminated rats was statistically comparable to the intravenous Ca-DTPA treatment.

In conclusion, transdermal delivery of the DTPA penta-ethyl ester prodrug achieved enhanced decorporation of ^{241}Am in contaminated rats. The effectiveness of this treatment, favorable sustained release profile and ease of administration support its use following nuclear and radiological emergencies.

DEDICATION

To my wife, Hui Li, for her love, understanding, support and encouragement.

For the loving memory of my parents, Fengge Zhang and Congqiao Di.

ACKNOWLEDGEMENTS

For the past five years, many people have helped me during my PhD study at UNC Eshelman School of Pharmacy. First of all, I would like to thank my advisor, Dr. Michael Jay, for giving me the opportunity to join his lab and trusting me to work on this research project. His work ethics, teachings, and encouragement have inspired me and carried me through my PhD study. I will remember what I have learned from him throughout my personal and professional life.

I would like to thank my committee members, Dr. Richard J. Kowalsky, Dr. Zhi Liu, Dr. Russell J. Mumper, and Dr. William C. Zamboni for their time and effort in guiding me through my study. I gratefully acknowledge the help and insightful discussions with Jay lab members, especially Dr. Matthew P. Sadgrove and Dr. Yu-Tsai Yang, as well as the faculty and students, past and present, of the Division of Molecular Pharmaceutics. I would also like to thank Dr. Richard Superfine, Dr. Joseph DeSimone, Dr. Nancy Monteiro, Dr. Jeremy Cribb, Ms. Nadira Williams, Ms. Sarah White who helped me with instrument access and training. In addition, I would like to thank the administration staff of MOPH and ESOP for their help during my study at UNC.

Last but not least, I would like to thank my wife, Hui Li, for her love, understanding and endless support. I also want to thank my two boys, Leon and Roger, for bringing joy and happiness to my life. I'm grateful to my parents-in law and family members for their constant support during these years.

TABLE OF CONTENTS

LIST OF TABLES xii

LIST OF FIGURES xiii

LIST OF ABBREVATIONS AND SYMBOLS xvi

CHAPTER 1 INTRODUCTION

1.1 General Introduction 1

1.2 Decorporation of Internalized Transuranic Elements 3

1.2.1 Mechanism of Radiation Induced Damage 3

1.2.2 Transuranic Elements 4

1.2.3 Treatment for Internalized Transuranic Elements 5

1.3 Transdermal Drug Delivery 9

1.4 Transdermal Delivery of DTPA Prodrug by Matching Biokinetics of Internalized Transuranic Elements 11

1.5 Hypothesis and Specific Aims 17

1.5.1 Hypothesis 17

1.5.2 Specific Aims 17

1.6 Summary 18

CHAPTER 2 FORMULATION DEVELOPMENT OF PENTA-ETHYL ESTER OF DTPA FOR TRANSDERMAL DELIVERY

2.1 Introduction....30

2.2 Materials and Method....32

2.2.1 Materials....32

2.2.2 Preparation of C2E5 Cream Formulations....33

2.2.3 Preparation of C2E5 Ointment Formulations....34

2.2.4 Preparation of C2E5 Non-aqueous Gels....34

2.2.5 High Pressure Liquid Chromatography (HPLC) Assay for C2E5....35

2.2.6 Viscosity Measurement of C2E5 Non-aqueous Gels....36

2.2.7 Thermal Analysis by Differential Scanning Calorimetry (DSC)....36

2.2.8 Scanning Electron Microscope (SEM) Imaging....36

2.2.9 Americium Decorporation in a Rodent Wound Model of Contamination....37

2.2.10 Statistical Analysis....38

2.3 Results....39

2.3.1 Stability of C2E5 Cream and Ointment Formulations....39

2.3.2 Stability of C2E5 Non-aqueous Gels....40

2.3.3 Viscosity of C2E5 Non-aqueous Gels....40

2.3.4 Thermal Analysis by Differential Scanning Calorimetry (DSC)....41

2.3.5 Scanning Electron Microscope (SEM) Imaging....41

2.3.6 Radionuclide Decorporation 42

2.4 Discussion 43

2.5 Conclusion....47

CHAPTER 3 NON-AQUEOUS GEL FOR TRANSDERMAL DELIVERY OF PENTA-ETHYL ESTER OF DTPA

3.1 Introduction....56

3.2 Materials and Method 60

3.2.1 Materials 60

3.2.2 Preparation of C2E5 Non-aqueous Gels 60

3.2.3 Differential Scanning Calorimetry (DSC) 61

3.2.4 Scanning Electron Microscope (SEM) Imaging 62

3.2.5 Rheological Measurements....62

3.2.6 In Vitro Release of C2E5 Non-aqueous Gel 63

3.2.7 Absorption of C2E5 Administered as a Neat Oil or as a Non-aqueous Gel....65

3.2.8 Statistical Analyses 68

3.3 Results 69

3.3.1 Preparation of C2E5 Non-aqueous Gels 69

3.3.2 Thermal Analysis by DSC 69

3.3.3 Scanning Electron Microscope (SEM) Imaging....70

3.3.4 Rheological Measurements Results 70

3.3.5 *In Vitro* Release of C2E5 Non-aqueous Gel 71

3.3.6 Absorption of C2E5 Administered as a Neat Oil or as a Non-aqueous Gel 71

3.4 Discussion 73

3.5 Conclusion 77

CHAPTER 4 RADIONUCLIDE DECORPORATION: MATCHING THE BIOKINETICS OF ACTINIDES BY TRANSDERMAL DELIVERY OF PRO-CHELATORS

4.1 Introduction 89

4.2 Materials and Method 92

4.2.1 Materials 92

4.2.2 Preparation of C2E5 Non-aqueous Gels 92

4.2.3 *In Vivo* Studies 93

4.2.4 Statistical Analysis 97

4.3 Results 98

4.3.1 Preparation of C2E5 Non-aqueous Gels 98

4.3.2 Absorption & Mass Balance of [^{14}C]-Labeled C2E5 Non-aqueous Gels 98

4.3.3 *In Vivo* Radionuclide Decorporation 99

4.4 Discussion 100

4.5 Conclusion 105

CHAPTER 5 GENERAL CONCLUSIONS AND FUTURE WORK

4.1 General Conclusions 114

4.2 Future Work.....115

APPENDICES.....116

APPENDIX A DTPA Derivatives Synthesized for the Dissertation Research.....117

APPENDIX B Non-aqueous Gel for the Transdermal Delivery of a DTPA Penta-ethyl Ester Prodrug.....118

APPENDIX C Transdermal Prodrug Delivery for Radionuclide Decorporation: Non-aqueous Gel Formulation Development and *In Vitro* and *In Vivo* Assessment.....129

REFERENCES.....140

LIST OF TABLES

Table 1.1 Transuranic elements, their synthesis and isotopes.....20

Table 1.2 Relevant physicochemical properties of C2E5 and its metabolites.....21

Table 2.1 C2E5 cream formulation composition, physical appearance and stability results after storage at 25 ± 2°C and 60 ± 5% relative humidity for 2 months.....48

Table 2.2 Ethyl cellulose-containing C2E5 non-aqueous gel formulation composition, related physical characterization data and stability results after storage at 25 ± 2°C and 60 ± 5% relative humidity for 3 months.....49

Table 2.3 Distribution of Americium-241 in excreta 7 days after different treatments immediate post contamination at a dose of 200 mg C2E5/kg.....50

Table 3.1 Rheological properties of a 40% C2E5 non-aqueous gel at different temperatures.....79

Table 3.2 Pharmacokinetic parameters of C2E3 and C2E2 after application of neat C2E5 oil or 40% C2E5 non-aqueous gel at a C2E5 dose of 200 mg/kg (n=4) and the enhancement ratio of C2E3 and C2E2 based on the formula $AUC_{0\text{-}24h}$ (C2E5 gel) /$AUC_{0\text{-}24h}$ (Neat C2E5). 80

Table 4.1 Percent of administered dose in various tissues 6 days after administration of [^{14}C]-labeled C2E5 non-aqueous gels at a dose of 200 mg C2E5/kg (n=6).....107

Table 4.2 ^{241}Am recovered in samples seven days following single dose treatments 24 h post i.m. contamination of rats with ^{241}Am nitrate (% of ID of ^{241}Am) 108

LIST OF FIGURES

Figure 1.1 Structures of DTPA, the prodrug C2E5 and its metabolites 22

Figure 1.2 Clearance of ^{14}C-DTPA following intravenous administration 23

Figure 1.3 Estimated blood levels (from Fig 1.2) following a 1 g i.v. dose of DTPA to a 70 kg man 24

Figure 1.4 Simulated Blood Concentration Profiles Following Daily i.v. Administration of DTPA vs. Biokinetics of Initially Insoluble Radionuclides (A) and Biokinetics of Highly Soluble Radionuclides (B) 25

Figure 1.5 Anticipated Blood Concentration Profiles Following Transdermal Administration of DTPA Penta-ethyl Prodrug vs. Biokinetics of Initially Insoluble Radionuclides (A) and Biokinetics of Highly Soluble Radionuclides (B).DA standard calibration curve in deionized water……. 26

Figure 1.6 Estimated DTPA/^{241}Am ratio in the circulation as a function of infusion rate at steady state assuming [^{241}Am] = 2 x 10^{-10} M, k = 0.693 h^{-1} and Vd = 6 L ……. 27

Figure 1.7 A graphic description for decorporation of [^{241}Am]-americium nitrate contaminated rats with C2E5 transdermal formulations. 28

Figure 2.1 Structures of DTPA (A) and its prodrug C2E5 (B).....51

Figure 2.2 DSC traces of pre-dried EC10 (A) and a C2E5 non-aqueous gel formulation consisting of 10% EC10, 30% C2E5 and 60% Miglyol 840 (B) from -10°C to 160°C at a scanning rate of 10°C min^{-1} 52

Figure 2.3 SEM images of EC10 particles (A and B) and a C2E5 non-aqueous gel formulation consisting of 10% EC10, 30% C2E5 and 60% Miglyol 840 (C and D) at magnifications of ~500 X and 3,000 X 53-54

Figure 2.4 Daily excretion of ^{241}Am in excreta after a single dose of topical application of 40% C2E5 non-aqueous gels (n=6) versus untreated control (n=4) (Data are means ± S.D.). (C2E5 gel group, -●-; untreated control, -■-)……. 55

Figure 3.1 Structures of DTPA, the prodrug C2E5 and its metabolites 81

Figure 3.2 DSC spectrum of C2E5 non-aqueous gel comprised of 20% EC10, 40% C2E5 and 40% Miglyol 840 by solvent evaporation method from -10°C to 160°C at a scanning rate of 10°C min^{-1}…….. 82

Figure 3.3 SEM images of (A–B) C2E5 non-aqueous gel comprised of 20% EC10, 40% C2E5 and 40% Miglyol 840 by solvent evaporation method at three magnifications (~500 X and 3,000 X)…….. 83

Figure 3.4 Continuous shear rheogram showing shear rate vs. shear stress at 25 °C and 32 °C of C2E5 non-aqueous gel comprised of 20% EC10, 40% C2E5 and 40% Miglyol 840 prepared using the solvent evaporation method ……. 84

Figure 3.5 Relationship between square root of time and cumulative amount of C2E5 released through a cellulose membrane into 0.1 M phosphate buffer after application of C2E5 non-aqueous gel (n=5) ……. 85

Figure 3.6 Plot showing the concentration of C2E3 detected in rat plasma versus time for the neat C2E5 oil and the 40% C2E5 non-aqueous gel (Data are means ± S.D.) (n=4) 86

Figure 3.7 Plot showing the concentration of C2E2 detected in rat plasma versus time for the neat C2E5 oil and the 40% C2E5 non-aqueous gel (Data are means ± S.D.) (n=4) 87

Figure 4.1 Release-time profile of soluble, colloidal and particulate radionuclides (including actinides such as ^{238}Pu, ^{239}Pu, ^{241}Am and ^{242,244}Cm) following i.m. injected in rats 109

Figure 4.2 Structures of C2E5 and its metabolites.....110

Figure 4.3 Daily excretion of radioactivity in urine and feces after topical application of [^{14}C]-labeled 40% C2E5 non-aqueous gels (Data are means ± SD) (n=6). (Urinary excretion, –■–; fecal excretion, –●–)…… 111

Figure 4.4 Daily excretion of ^{241}Am in urine (A) or in feces (B) after a single dose of the decorporation agents at different dose levels and application areas 24 h post contamination. Significant (*p < 0.05, **p < 0.01, and ***p < 0.001) by Dunnett's test. (Untreated control, –■–; 200 mg/kg applied to 6 cm^2, –●–; 600 mg/kg applied to 6 cm^2, –♦–; 1,000 mg/kg to 6 cm^2, –▲–; 600 mg/kg to 18 cm^2, –■–)…… 112

Figure 4.5 Daily ^{14}C excretion and ^{241}Am decorporation via urine (A) and feces (B) by C2E5 gel formulations at 200 mg/kg dose applied 24 h post contamination. (Urinary excretion of ^{14}C, –■–; fecal excretion of ^{14}C, –●–; Urinary excretion of ^{241}Am, –■–; fecal excretion of ^{241}Am, –●–)…….....113

LIST OF ABBREVIATIONS AND SYMBOLS

ANOVA	analysis of variance
AUC	area under the curve
Brij 58	polyoxyl 20-cetyl ether
C_{max}	maximum concentration
CAT	catalase
DNA	deoxyribonucleic acid
DTPA	diethylenetriaminepentaacetic acid
DSC	Differential Scanning Calorimetry
EC7	ETHOCEL® Std 7 FP Premium
EC10	ETHOCEL® Std 10 FP Premium
EC100	ETHOCEL® Std 100 FP Premium
EDTA	ethylenediaminetetraacetic acid
GSH	glutathione
h	hour
HOPO	hydroxypyridinonate
HPLC	high-pressure liquid chromatography
IACUC	Institutional Animal Care and Use Committee
ICP-MS	inductively coupled plasma mass spectrometry
ICRP	International Commission on Radiological Protection
IDA	Iminodiacetic acid
i.p.	intraperitoneal
IPA	isopropyl alcohol
i.v.	intravenous
kg	kilogram

LC-MS	liquid chromatography–mass spectrometry
LC-MS/MS	liquid chromatography–tandem mass spectrometry/mass spectrometry
LSC	liquid scintillation counting
mg	milligram
min	minute
mL	milliliter
M_r	molecular mass
MS	mass spectrum
NCRP	National Council on Radiation Protection and Measurements
NDA	new drug application
ng	nanogram
NMR	nuclear magnetic resonance
NTA	nitrilotriacetic acid
PBS	phosphate buffered saline
RBE	relative biological effectiveness
RNS	reactive nitrogen species
ROS	reactive oxygen species
SAMMS	self-assembled monolayer on mesoporous supports
s.c.	subcutaneous
SD	Sprague-Dawley
S.D.	standard deviation
SEM	scanning electron microscope
SNS	Strategic National Stockpile
SOD	superoxide dismutase
$t_{1/2}$	half-life
V_d	volume of distribution

vs.	versus
WMD	weapons of mass destruction
α	alpha
β	beta
γ	gamma
µg	microgram
µL	microliter

CHAPTER 1: INTRODUCTION

1.1 GENERAL INTRODUCTION

The United States and many other countries face increasing threats from terrorist groups with respect to the use of weapons of mass destruction (WMD) against civilian populations. Of particular concern is that some of these groups are intensifying their efforts to acquire and develop nuclear and radiological weapons. The Nuclear Trafficking Abstracts Database reports an increasing number of incidents in the diversion of nuclear and radioactive materials (1). These materials can be used to make Radiation Dispersal Devices (RDD) which when spread by means of conventional explosives constitutes what is referred to as a “dirty bomb”. Among the radionuclides of greatest concern that may be incorporated in an RDD are isotopes of Americium (Am), Plutonium (Pu) and Curium (Cm). Furthermore, the accidents of nuclear power plants and radionuclides such as Chernobyl in April 1986 (2) and Goiânia accident in September 1987 (3), as well as Fukushima Daiichi in March 2011 (4), which all involved the release of a substantial amount of radioactive materials into the environment, have heightened the awareness that many nations need to be prepared for such cataclysmic events.

Since radioactivity was discovered by the French scientist Henri Becquerel in 1896 (5), great progress has been made to harness the power of this phenomenon. Radioactivity, also known as radioactive decay or nuclear decay, is the process by which an unstable atomic nucleus undergoes spontaneous decay or disintegration accompanied by the emission of particles of ionizing radiation. The three major radioactive decay modes are

alpha decay, beta decay, and gamma decay. Alpha decay, or α-decay, is a type of radioactive decay in which an atomic nucleus emits a helium nucleus (He^{2+}, also known as an alpha particle, α particle). Beta decay, or β-decay, is a type of radioactive decay in which an atomic nucleus emits a beta particle (an electron or a positron, β particle). Gamma decay, γ-decay, is a type of radioactive decay in which an unstable daughter nucleus, which is produced from the original atomic nucleus as a result of alpha or beta decay, emits photons (γ ray) when it moves from an excited state to a lower energy state. Gamma decay from excited states may also be produced as a result of nuclear reactions such as neutron capture, nuclear fission, or nuclear fusion. High-energy β particles and γ rays are high in penetration depth but low in ionizing power on their travelling path, whereas α particles are low in penetration depth but high in ionizing power on their travelling path. Alpha particles can cause substantial injury and subsequent health effects only when they are internalized because the helium nuclei are not highly penetrating as a result of their relative large size and charge. When a human is exposed to a large dose of radiation, be it in the form of direct contact in close range or internalized as a result of inhalation, ingestion, injection or absorption through intact skin or wound, it could result in the acute radiation syndrome (ARS), as well as delayed health effects of radiation exposure. The International Commission on Radiological Protection (ICRP) and the National Council on Radiation Protection and Measurements (NCRP) have published a series of publications and reports on topics such as radiation risk evaluation, recommendations on the limit of radiation exposure, and protection against ionizing radiations (6, 7).

1.2 DECORPORATION OF INTERNALIZED TRANSURANIC ELEMENTS

1.2.1 Mechanism of Radiation-induced Damage

The radiation-induced damage to biological systems can be classified into two mechanisms by which radiation ultimately affect cells, direct and indirect effects (8). Direct effects of radiation refer to the fact that radiation interacts with the atoms of the deoxyribonucleic acid (DNA) molecule, or some other cellular component critical to the survival of the cell, which can lead to cell death and apoptosis in the short term, and mutations and cancer in the long term (9-13). Indirect effects of radiation refer to the fact that radiation can cause the radiolytic decomposition of water molecules in the cell and form reactive oxygen species (ROS) and reactive nitrogen species (RNS), which can interact with DNA and other important cellular components and result in cell death, apoptosis, mutations and cancer (9-13).

Radiation-protective agents, which include prophylactic agents that are administered before potential radiation exposure, and mitigating agents (mitigators) that are administered during or after radiation exposure, have been developed to prevent or reduce radiation-related damage (14). Because the major damage at the cellular level caused by radiation is related to the ROS and RNS generated by ionizing radiation (9, 11), a substance that could manage or help to reduce the oxidative stress would alleviate the detrimental effect of the radiation (15, 16). This class of substance includes endogenous glutathione (GSH), glutamine, catalase (CAT), superoxide dismutase (SOD) and antioxidant nutrients such as vitamin C and E, phytochemicals and herbal preparation (17). The history, development, and recent progress on radiation-protective agents have been reviewed in detail by Weiss and Landauer (17), Seed (18), Xiao and Whitnall (19), Hosseinimehr (20), Mönig and colleagues (21).

Because alpha particles are low in penetration depth but high in ionizing power on their travelling path, they are very dangerous to living cells due to the high relative biological effectiveness (RBE) of alpha radiation to cause biological damage only when they are internalized. It is estimated that chromosome damage caused by alpha particle emitters (such as transuranics or actinides) is an average of about 20 times more detrimental, and in some experiments up to 1000 times more damaging, than an equivalent amount of gamma or beta radiation (12). Russian dissident and ex-Federal Security Service officer Alexander V. Litvinenko was believed to be killed by the powerful alpha emitter polonium-210 in 2006 (a milligram of ^{210}Po emits as many alpha particles per second as 4.215 grams of ^{226}Ra) (22). Internalized transuranic radionuclides impose even greater damage to nearby living cells because not only do alphas themselves cause damage, but alpha recoil (the phenomenon that the parent nucleus needs to recoil after alpha emission due to the conservation of momentum) cause approximately equal ionization along the path. This alpha recoil process may in turn be especially damaging to genetic material, since many soluble transuranic elements that emit alphas carry positive charge and these positive cations are chemically attracted to the net negative charge of DNA, causing the recoiling transuranic nucleus to be in close proximation to the DNA (23).

1.2.2 Transuranic Elements

The transuranic elements (also known as transuranium elements) are the chemical elements with atomic numbers greater than 92 (the atomic number of uranium). All of these elements are unstable and decay radioactively into other elements. The first several transuranic elements were discovered at the Radiation Laboratory (now Lawrence Berkeley National Laboratory) by Edwin McMillan, Glenn Seaborg, Albert Ghiorso and their colleagues during 1945-1974 at the University of California, Berkeley. The transuranic

elements of the actinides family, their synthesis and isotopes are presented in Table 1-1 (24, 25). Due to cost and production difficulties, none of the elements beyond californium (Cf) has industrial applications (26). In comparison, isotopes of transuranic elements of Am, Pu and Cm have wide applications in nuclear power plants and other fields, such as in smoke detectors. As a result of their abundant availability, it makes the isotopes of transuranic elements of Am, Pu and Cm among the radionuclides of great concern for incorporation in RDD.

1.2.3 Treatment for Internalized Transuranic Elements

After the terrorist attacks on September 11, 2001 in the U.S., a renewed effort has been undertaken for the development of medical countermeasures for radiological/nuclear, biological, and chemical threats. There is an interest in developing and procuring therapeutic agents for national stockpiles. For this purpose, a U.S. research focus has primarily been initiated and led by the U.S. Department of Health and Human Services through the National Institute of Allergy and Infectious Diseases (NIAID) and the Biomedical Advanced Research and Development Authority (BARDA). In 2005, NIH published a Strategic Plan and Research Agenda for Medical Countermeasures against Radiological and Nuclear Threats that provided the research and development objectives of radionuclide decorporation agents. This was followed by the 2007 publication of the "*Implementation Plan for Chemical, Biological, Radiological and Nuclear Threats"* by the Public Health Emergency Medical Countermeasures Enterprise (27). The US Food and Drug Administration (FDA) has issued several guidance documents to facilitate this effort, including guidelines for a new drug application (NDA) for calcium and zinc DTPA products (28), guidelines for the development and testing of decorporation agents (29), and guidelines for animal models used to address

efficacy under the animal rule (30). These coordinated efforts have resulted in a number of reports, books and new drug candidates in the pipeline (31-33).

1.2.3.1 Diethylenetriaminepentaacetic Acid (DTPA)

DTPA (Figure 1.1) is a synthetic polyamino carboxylic acid with eight coordinate bond forming sites that can sequester metal ions and form highly stable DTPA-metal ion complexes. DTPA has wide industrial and medical applications including control of water hardness, medical imaging and decorporation of internally deposited radionuclides (34). In August 2004, FDA approved the calcium and zinc salts of DTPA manufactured by Hameln Pharmaceuticals GmbH, of Hameln, Germany for treatment of internal contamination with americium, curium and plutonium (35), which was based on the extensive experience in the treatment of nuclear workers who were contaminated with plutonium or americium and treated with Ca-DTPA and Zn-DTPA documented at the Radiation Emergency Assistance Center/Training Site (REAC/TS) and other studies (36-38). Ca-DTPA and Zn-DTPA treatment has established the usefulness of DTPA treatment in effectively reducing the body burden of internalized Pu, Am and Cm isotopes. These drugs are known to form very stable chelates with metal ions by exchanging calcium or zinc for a metal with greater binding affinity, radioactive actinides in particular. These chelates are then excreted by glomerular filtration into the urine. The approved Ca-DTPA and Zn-DTPA products are supplied as sterile solutions (dose = 1 g/5 mL). Akorn Pharmaceutical Inc. provides the FDA approved DTPA product in the US via an exclusively licensed and supply agreement with Hameln Pharmaceuticals GmbH. These products may be obtained from the REAC/TS in the event of a nuclear emergency. Over 4,600 doses these drugs have been administered for investigational use over the past 45 years. The Medical Preparedness and Response Sub-Group of the Department of Homeland Security Working Group on Radiological Dispersal

Device (RDD) Preparedness recommends that these drugs be administered in 1 g daily unfractionated doses either by slow intravenous push, intravenous infusion, or inhalation in a nebulizer (1:1 dilution with water or saline). The package insert states that following intravenous administration, these agents are rapidly distributed with almost no accumulation in specific organs (39). No significant amounts of Ca- or Zn-DTPA penetrate into erythrocytes or other cells and there is little or no binding by the renal parenchyma. The oral bioavailability of these compounds is low. The low permeability of DTPA and Ca-DTPA classifies them as Class III compounds (high solubility, low permeability) in the Biopharmaceutical Classification System (BCS).

1.2.3.2 Improved DTPA formulations and Other Decorporation Agents under Development

NCRP Report No. 65 summarized the treatment options for internalized radionuclides (40). Due to the fact that effective treatments for internal radionuclide contamination exist for only a few radionuclides, the Public Health Emergency Medical Countermeasures Enterprise has prioritized development of broad-spectrum, and novel or improved radionuclide decorporation agents (27). Because DTPA treatment is contraindicated for decorporating uranium, as well as unsuitable for a mass casualty scenario (31, 41), a pharmaceutical approach to improved DTPA formulations and a chemical approach to new classes of decorporation agents have been pursued to solve these challenges (31).

The pharmaceutical approach to improved DTPA formulations focuses on development of DTPA formulations suitable for delivery routes other than i.v. or inhalation, namely oral or other routes that are convenient to administer, suitable for mass casualty scenario and offer significant logistic advantages (42). Our group has developed a series of

DTPA prodrugs for enhanced delivery of DTPA via the oral route (31, 43-46), and the transdermal route (47, 48). The latter is the focus of this dissertation. The enhanced decorporation of transuranic elements by this prodrug approach has been demonstrated in an i.v. contamination model (44, 45), simulated wound model (45, 48), and inhalation models on rodents (unpublished results). Dr. Gita Shankar and colleagues at SRI International (Menlo Park, CA) are developing an orally bioavailable formulation of DTPA using gastrointestinal absorption enhancers (49), and demonstrated the enhanced decorporation over untreated control in i.v. contamination model on rodents (50). Dr. James Talton and colleagues at Nanotherapeutics Incorporated (Alachua, FL) have developed an enteric-coated NanoDTPA® formulation for oral delivery and demonstrated enhanced decorporation of transuranic elements over untreated control in i.v. contamination model on rodents (51, 52).

The chemical approach to new classes of decorporation agents of transuranic elements focuses on the development of new chemical entities (NCE) and currently available biomaterials (31). Dr. Scott Miller and his colleagues at University of Utah have developed triethylenetetramine-hexaacetic acid based decorporation agents, which are structurally similar to DTPA and belong to the class of amphipathic polyaminocarboxylic acid compound family, and enhanced decorporation was achieved for the removal of plutonium and americium in rodents (53, 54). Siderophore-based actinide-sequestering agents are one major class of NCEs under investigation, which siderophore stands for “iron carrier” in Greek (55). Dr. Raymond Bergeron and colleagues at University of Florida have developed desferrithiocin and its derivatives, which are siderophore analogs, for decorporation of uranium isotopes (56, 57). Dr. Kenneth Raymond’s group at University of California at Berkeley, along with Patricia Durbin’s group at Lawrence Berkeley National Laboratory, has done extensive research in synthesizing novel siderophore-based actinide decorporation agents (58-60), and identified two lead hydroxypyridinonate (HOPO) compounds,

octadentate 3,4,3-LI-1,2-HOPO and tetradentate 5-LIO-Me-3,2-HOPO, as effective and safe decorporating agents for actinides in rodents (61-71). In terms of applying biomaterials for radionuclide decorporation, chitosan and its derivatives are currently being developed for the decorporation of ingested radionuclides by Dr. Tatiana Levitskaia at the Pacific Northwest National Laboratory (31). Dr. Charles Timchalk and colleagues of the Pacific Northwest Laboratory have designed a self-assembled monolayer on mesoporous supports (SAMMS), which are hybrid materials of mesoporous silica (SiO_2), for decorporation evaluation of ingested radionuclides and the radionuclides in the systemic circulation (31).

1.3 TRANSDERMAL DRUG DELIVERY

Transdermal drug delivery possesses many advantages over the parenteral and oral routes. These include the delivery of a steady-state profile that reduces side effects related to fluctuations in plasma drug concentration, reduced dosing frequency, avoidance of first-pass metabolism, and improved patient compliance due to its convenient and non-invasive means of self-administration (72-74). It may also offer benefits to special populations such as patients with needle phobia, those who are unconscious or too nauseated to take oral medications, pediatric patients and the elderly. The latter two populations are specific areas of concern to the FDA related to the development of radionuclide decorporation agents (29). The factors that affect transdermal absorption of drugs may include physiological and pharmaceutical factors such as the degree of hydration and thickness of the skin, the exposure time, skin immunology, the concentration of drug applied and the surface area over which the drug is applied (72-76). Also of critical importance are the physicochemical properties of drugs such as molecular weight and solubility, and the partition coefficient (log P) where the affinity of the drug for the skin must be greater than its affinity for the vehicle in which it is delivered. The ideal drug properties for passive transdermal delivery are aqueous

solubility > 1 mg/mL, molecular weight < 500 Da and a log P value of 2-4 (depending on molecular weight) (72-76). Passive diffusion of a drug across the stratum corneum can determined from Fick's Law (Eq. 1-1). According to the following equation:

$$J_{ss} = \left(\frac{D * K_p}{h}\right) * A * C_{veh} \qquad (Eq. 1-1)$$

where J_{ss} = steady-state flux (mg/h); D = drug diffusivity (cm^2/h); h= membrane thickness (cm); K_p = drug's membrane-vehicle partition coefficient; C_{veh} = initial drug concentration (mg/cm^3) in the vehicle; and A = surface area (cm^2). According to Fick's Law, transdermal fluxes can be improved by increasing drug diffusivity, partitioning into the stratum corneum, the surface area of application and the drug concentration in the formulation. It has been demonstrated that for relatively small molecules, e.g., a series of non-steroidal anti-inflammatory agents, the log P values correlate well with the area under the plasma-time curve (AUC) values (77).

Previous research reports have shown that to be a successful transdermal drug delivery candidate, a balance of lipophilicity and hydrophilicity is highly desirable because the drug needs to be reabsorbed into an aqueous environment after it penetrates through the stratum corneum (75, 76). A recent paper by Mark Prausnitz's group at Georgia Institute of Technology demonstrated that transdermal delivery of molecules is limited by the full epidermis, not just the stratum corneum (78).

1.4 TRANSDERMAL DELIVERY OF DTPA PRODRUG BY MATCHING BIOKINETICS OF INTERNALIZED TRANSURANIC ELEMENTS

Mass contamination scenarios call for effective and prompt medical countermeasures for the affected populations. Current DTPA treatment options do not meet the challenge imposed by a mass casualty setting in that skilled medical professionals are required to administer Ca/Zn-DTPA by i.v. injection and multiple injections may be required due to the short plasma half-life of DTPA. Crawley and Haines studied the clearance of ^{14}C-labeled DTPA in rats after intravenous administration and observed that the amount of radioactivity retained in tissues 24 hours after administration was <1% of the administered radioactivity, and that over 99% was excreted up to 9 days after administration (79). Chromatographic analysis of the excreted radioactivity demonstrated that ^{14}C-DTPA was intact and had not been metabolically degraded. A separate study was conducted in which plasma and urine were analyzed for ^{14}C content following the i.v. administration of ^{14}C-DTPA to human subjects. The results showed that DTPA was rapidly distributed in the extracellular fluid volume and was cleared through the kidneys by glomerular filtration. Greater than 99% of the administered dose was collected in the urine within 24 hours of administration (see Figure 1.1 which was obtained from Akorn Inc's package insert for Pentetate Calcium Trisodium Injection) (39). Based on a dose of 1 g/70 kg, we can project the plasma concentration of DTPA (Figure 1.2). From these data, we can calculate that the elimination half-life is tri-phasic with a mean of 60 min and that there is very little tissue distribution of DTPA after i.v. injection. Thus, a 1 g dose in 70 kg subject is expected to yield a C_{max} of ~ 142 µg/mL and a blood concentration of 34 ng/mL 12 hours after administration.

In contrast, the release rates of internalized Am, Pu and Cm contaminants from wound sites to the systemic circulation in various animal species range from 0.052 to 6.3% of the administered radionuclides per day, a relatively slow and steady transfer process (80).

The release profiles of inhaled transuranic material based on ICRP Publication 66 respiratory tract model and the biokinetic data from the contamination cases are highly dependent on the physical and chemical forms of the inhaled transuranic radionuclides, varying from highly soluble forms to insoluble forms (81-87). Simulated blood concentration profiles following daily i.v. administration of DTPA versus biokinetics of internalized transuranic radionuclides could be scenarios as depicted in Figure 1.4 as initially insoluble radionuclides (A) and highly soluble radionuclides (B). Furthermore, it has been suggested that a chelating agent must be maintained at a concentration of at least 10 to 25 μM in both extracellular and intercellular fluids for a sustained duration to ensure an optimal chelation effect of transuranic radionuclides (88). In comparing the short half-life and rapid clearance of DTPA after i.v. administration to the slow and sustained introduction of radio-actinides into the systemic circulation (80), there is a mismatch between the pharmacokinetic profile of intravenously administered DTPA and the biokinetic profile of transuranic radionuclides. This mismatch leads to a period where DTPA plasma concentrations are below the effective concentration required to chelate radionuclides in the systemic circulation and, thus, may limit the effectiveness of the current parenteral DTPA treatments. Previous efforts have addressed this mismatch and produced encouraging results.

There are a number of reports in which DTPA salts have been used for the decorporation of ^{241}Am in animal models in which the Am is in various chemical forms (89). Several studies have demonstrated that if the ^{241}Am can be chelated before it accumulates in liver and bone, its decorporation can be greatly enhanced (90). Once in these tissues, ^{241}Am becomes firmly bound and clears very slowly. The clearance of ^{241}Am from rat liver has been approximated using bi-exponential functions with half-lives of 5.8 and 150 days (91), which is also a slow and sustained release process. Based on this observation, Guilmette and Muggenburg conducted a study in which they used an osmotic pump for the continuous infusion of Zn-DTPA in dogs that had been contaminated with the moderately

soluble $^{241}AmO_2$ by inhalation. They compared this treatment to controls as well as to dogs that received i.v. daily doses of Ca-DTPA (bi-weekly after the first 4 days) and assessed the decorporation efficiency by measuring the % initial pulmonary burden remaining as a function of time. The results of this study clearly demonstrated that continuous infusion of DTPA was significantly more effective in preventing the translocation of inhaled $^{241}AmO2$ from lung to extra-pulmonary tissues such as liver and bone compared to bi-weekly intravenously administered DTPA. The infusion therapy approach led to 60- and 200-fold reductions in the absorbed radiation doses to the bone and liver, respectively, and blocked over 98% the ^{241}Am that otherwise would have deposited in liver and bone (92). From a pharmacokinetic perspective, this is logical as the dissolution rate of $^{241}AmO_2$ which is necessary for its absorption into the circulation, is much less than the clearance of DTPA from the circulation (93). DTPA has been entrapped in various liposome formulations for prolonged circulation after i.v. administration, and improved decorporation of ^{238}Pu was achieved (94, 95). However, these approaches involve parenteral administration, thus making them unsuitable for mass casualty scenarios after a major nuclear/radiological emergency. As a result, a non-parenteral delivery system which can provide sustained levels of chelators in the circulation that match the biokinetic profile of actinides after inhalation or wound contamination is an attractive approach to address this problem.

It is highly desirable to deliver DTPA to the circulation at a zero-order rate to better match actinide biokinetic profiles and thus achieve optimal radionuclide decorporation over an extended duration, as the results from the previous studies have shown. Due to its low partition coefficient (log P = -4.90) and high melting point (219-220ºC), DTPA is not a good candidate for transdermal delivery (73, 96). Prodrug strategies have been widely applied to drug candidates and compounds with undesirable physicochemical properties and absorption permeability, by converting certain functional groups into pro-moieties and thus transforming the molecules suitable for oral, topical and transdermal, and other routes of

delivery (97-102). Applying the prodrug strategy to the DTPA molecule, the five highly ionizable carboxylic groups were converted into 5 ethyl ester groups via Fischer esterification reaction (43, 44). The penta-ethyl ester of DTPA, designated as C2E5, was designed and synthesized as a new radionuclide decorporation prodrug to overcome the limitations of the current DTPA treatments (31, 43, 44). C2E5 possesses physicochemical properties suitable for transdermal delivery. It has a molecular weight of 533.6, water solubility of 3.0 mg/mL at pH 7.1 and 20.3 mg/mL at pH 5.7, and a log P value of 3.3, and a log D value of 2.2 at pH 6.0., and it is a Newtonian liquid with a viscosity of 175 cP at 25ºC (44). The structures of C2E5 as well as its potential degradation products and metabolites including DTPA tetra-ethyl ester (C2E4), DTPA tri-ethyl ester (C2E3), DTPA di-ethyl ester (C2E2), DTPA mono-ethyl ester (C2E1), and the fully de-esterified DTPA are shown in Figure 1.1. Simulated blood concentration profiles following daily i.v. administration of DTPA versus biokinetics of internalized transuranic radionuclides are depicted in Figure 1.4 as initially insoluble radionuclides (A) and highly soluble radionuclides (B).

Many prodrugs tested for topical and transdermal delivery were ester prodrugs (102-107). After permeation through the stratum corneum, the ester prodrugs were metabolized by the enzymes in the epidermis and dermis, including mainly esterases and cytochrome P450 (108-113). Studies on the esterase distribution of skin have shown that the stratum corneum has little or no activity, the epidermis has the highest esterase activity, and the dermis has reduced activity relative to the epidermis (114). Selected niacin ester prodrugs were able to achieve high blood levels of niacin sufficient to reduce serum cholesterol and improve blood lipid profiles and it was evident that esterases in the skin were capable of rapidly converting the prodrug to the pharmacologically active niacin (104). The action of skin esterases was also exploited in the development of testosterone esters where it was demonstrated that testosterone propionate was rapidly converted to testosterone during the skin permeation process (115). Because the transdermal drug delivery is limited by the full

epidermis, not just the stratum corneum (78), it's highly desirable that a lipophilic ester prodrug first penetrates through the stratum corneum and then is converted by esterases in the epidermis into more hydrophilic metabolites and/or parent drug which need to be reabsorbed into an aqueous environment before entering into systemic circulation. Preliminary data on C2E5 metabolism suggest that C2E5 molecules undergo step wise de-esterification *in vivo* (116, 117), and it's anticipated that many of the partially hydrolyzed C2E5 metabolites could bind internalized transuranic radionuclides (118-122). Relevant physicochemical properties of C2E5 and its metabolites are shown in Table 1.2. Anticipated blood concentration profiles following transdermal administration of DTPA penta-ethyl prodrug versus biokinetics of internalized transuranic radionuclides could be two scenarios as depicted in Figure 1.5 as initially insoluble radionuclides (A) and highly soluble radionuclides (B).

If a victim of nuclear terrorism inhaled $^{241}AmO_2$ and/or was contaminated with ^{241}Am particles via wound and the amount of ^{241}Am that diffused into the circulation resulted in an average of 1 μCi in the bloodstream, then the concentration of Am in the bloodstream would be approximately 2 x 10^{-10} M. Thus, if we made the over-simplified assumption that the circulation was a well-stirred reactor and knowing the stability constant for DTPA binding with Am (10^{22} M), we can calculate the steady-state concentration of DTPA required to chelate the Am in the circulation to prevent its uptake into liver and bone. Figure 1.6 shows the DTPA/^{241}Am ratio in the circulation as a function of infusion rate of DTPA at steady state, where the steady state concentration (C_{ss}) is defined as $C_{ss} = R/V_dk$, where R = infusion rate, V_d is the volume of distribution and k is the elimination rate constant. The red data point on this figure represents the infusion rate Guilmette used in rat studies (30 μmole/kg/day) extrapolated to a 70 kg man, i.e., 2.1 mmole/day (~800 mg/day). This figure shows that even at infusion rates of 0.1 μmole/hour/70 kg, the DTPA/^{241}Am ratio would be >100 at steady state. This represents a daily dose of just only 1 mg/day. Of course, this model does not

take into account the physiological complexities of the circulatory system, local pH effects or the presence of biomacromolecules (proteins, indirect acids and bases) and other metals. Our group has studied the transmetallation between DTPA-lanthanide chelates, which have stability constants similar to actinides, and the two most physiologically relevant divalent ions, Cu^{2+} and Zn^{2+} (Ca^{2+} and Fe^{2+} do not compete with Am^{3+} for DTPA because the $K_{Am\text{-}DTPA}$ >> $K_{Ca\text{-}DTPA}$ and $K_{Fe\text{-}DTPA}$) (93). Based on these studies, we expect the exchange between Am-DTPA and Cu^{2+} and Zn^{2+} at physiological concentrations to be ~1% (123). Thus, this model can provide initial guidance in the development of formulations for the continuous delivery of DTPA and related chelators. The intravenous doses of Ca- and Zn-DTPA are large (14.3 mg/kg), however, calculations based on known kinetic parameters indicate that delivery rates of the DTPA prodrug required to maintain effective steady state concentrations of DTPA may be achieved by much lower daily doses. It is not uncommon for 10 g of a topical formulation to be applied to the skin for systemic delivery of a therapeutic agent, as in the case of AndroGel® (testosterone gel) (105). In addition, there are examples where ester prodrugs have been administered topically in relatively large doses for systemic delivery of therapeutic agents. Jacobson et al described the topical administration of niacin esters in which the dose of the prodrugs, applied as a 1-10% lotion, ranged from 34 to 340 mg/kg (103). Because DTPA penta-ethyl ester is a liquid oil, formulations containing up to 50% of the DTPA penta-ethyl prodrug can be prepared and 10-20 g of this semisolid formulation can be applied to the skin of an individual that has been contaminated with ^{241}Am to achieve zero order release of DTPA in bloodstream.

1.5 HYPOTHESIS AND SPECIFIC AIMS

1.5.1 Hypothesis

Transdermal administration of DTPA penta-ethyl ester prodrug, designated as C2E5, achieves comparable enhanced decorporation of ^{241}Am to i.v. administration of DTPA in rats contaminated with intramuscularly injected [^{241}Am]-americium nitrate.

1.5.2 Specific Aims

Aim I: Develop C2E5 Transdermal Formulations with Suitable Stability Profile.

The objective of Specific Aim I is to 1) develop viable transdermal C2E5 formulations by screening non-proprietary oil-in-water emulsion-based cream and hydrocarbon base ointment formulation prototypes, and exploring other semisolid formulations; and 2) evaluate the physical and chemical stability of prepared C2E5 formulations for at least 6 month under storage stability conditions at 25 ± 2°C and 60 ± 5% relative humidity and at 4 ± 2°C.

Aim II: Characterize and Evaluate the Candidate C2E5 Transdermal Formulations.

The objective of Specific Aim II is to 1) characterize the candidate C2E5 formulations with Differential Scanning Calorimetry (DSC) and Scanning Electron Microscopy (SEC); 2) evaluate the rheological properties of the candidate C2E5 formulations; and 3) perform *in vitro* release testing of the selected C2E5 transdermal formulations with Franz diffusion cell.

.

Aim III: Evaluate C2E5 Transdermal Formulations by Pharmacokinetic, Absorption and Mass Balance Studies in Rats.

The objective of Specific Aim III is to 1) perform a pharmacokinetic study using the selected C2E5 transdermal formulations to determine the pharmacokinetic parameters in rats; and 2) perform absorption and mass balance studies with [^{14}C]-labeled C2E5 transdermal formulation in rats.

Aim IV: Determine Efficacy of C2E5 Transdermal Formulations with Animal Model.

The objective of Specific Aim IV is to determine the efficacies of the selected C2E5 transdermal formulations using a wound contamination model with [^{241}Am]-americium nitrate in rats at different C2E5 dose levels after ^{241}Am contamination.

1.6 SUMMARY

In this dissertation, various C2E5 transdermal formulation prototypes were prepared and tested for C2E5 stability under normal storage stability conditions. The non-aqueous gel matrix comprised of ethyl cellulose and Miglyol 840® proved to stabilize C2E5 in the matrix. In addition, C2E5 non-aqueous gel was characterized by DSC and SEC, and *in vitro* release profile of the formulation was evaluated with Franz diffusion cell. The pharmacokinetic study, and absorption and mass balance study, as well as efficacy studies using a simulated wound contamination model in rats, were conducted in rats. A graphic description of decorporation of [^{241}Am]-americium nitrate contaminated rats with C2E5 transdermal formulations is presented in Figure 1.7. The semisolid formulations containing C2E5 are

applied to the clipped dorsal skin of rats which have been contaminated with intramuscularly injected [^{241}Am]-americium nitrate on the thigh. The C2E5 molecules penetrate through the stratum corneum and are converted to its metabolites by esterases in the skin. The C2E5 metabolites chelate with ^{241}Am to form stable complexes for enhanced elimination from the body. Detailed results are discussed in the following chapters.

Table 1.1 Transuranic elements, their synthesis and isotopes.

Element	Symbol	Year of Discovery	Method	Isotopes
Neptunium	Np	1940	Bombarding ^{238}U by neutrons	^{235}Np, ^{236}Np, ^{237}Np, ^{239}Np
Plutonium*	Pu	1941	Bombarding ^{238}U by deuterons	**^{238}Pu***, ^{239}Pu, ^{240}Pu, ^{241}Pu, ^{242}Pu, ^{244}Pu
Americium*	Am	1944	Bombarding ^{239}Pu by neutrons	**^{241}Am***, ^{242m}Am, ^{243}Am
Curium*	Cm	1944	Bombarding ^{239}Pu by α-particles	**^{242}Cm***, ^{243}Cm, **^{244}Cm***, ^{245}Cm, ^{246}Cm, ^{247}Cm, ^{248}Cm, ^{249}Cm, ^{250}Cm
Berkelium	Bk	1949	Bombarding ^{241}Am by α-particles	^{245}Bk, ^{246}Bk, ^{247}Bk, ^{248}Bk, ^{249}Bk
Californium	Cf	1950	Bombarding ^{242}Cm by α-particles	^{248}Cf, ^{249}Cf, ^{250}Cf, ^{251}Cf, ^{252}Cf, ^{253}Cf, ^{254}Cf
Einsteinium	Es	1952	As a product of nuclear explosion	^{252}Es, ^{253}Es, ^{254}Es, ^{255}Es
Fermium	Fm	1952	As a product of nuclear explosion	^{252}Fm, ^{253}Fm, ^{255}Fm, ^{257}Fm
Mendelevium	Md	1955	Bombarding ^{253}Es by α-particles	^{257}Md, ^{258}Md, ^{260}Md
Nobelium	No	1965	Bombarding ^{243}Am by ^{15}N or ^{238}U with α-particles	^{253}No, ^{254}No, ^{255}No, ^{257}No, ^{259}No
Lawrencium	Lr	1961–1971	Bombarding ^{252}Cf by ^{10}B or ^{11}B and of ^{243}Am with ^{18}O	^{254}Lr, ^{255}Lr, ^{256}Lr, ^{259}Lr, ^{260}Lr, ^{261}Lr, ^{262}Lr

* The common transuranic elements and readily available isotopes are highlighted in bold.

Table 1.2 Relevant physicochemical properties of C2E5 and its metabolites.

Species	Properties					
	Molecular Wt. (Dalton)	Log P or Clog P*	Hydrogen bond donor	Hydrogen bond acceptor	Binding sites	Structurally similar common chelator
C2E5	533.61	3.3	0	13	3	IDA
C2E4	505.56	2.5	1	13	4	NTA
C2E3	477.50	0.3	2	13	5	N-hydroxyl EDTA
C2E2	449.45	-1.9	3	13	6	EDTA
C2E1	421.40	-2.4	4	13	7	N/A
DTPA	393.35	-4.9	5	13	8	DTPA

* The Clog P values for the C2E5 metabolites were obtained from ChemBioDraw Ultra 12.0; IDA: Iminodiacetic acid; NTA: nitrilotriacetic acid; EDTA: ethylenediaminetetraacetic acid; DTPA: diethylenetriaminepentaacetic acid, N/A: Not available.

.

Figure 1.1 Structures of DTPA, the prodrug C2E5 and its metabolites.

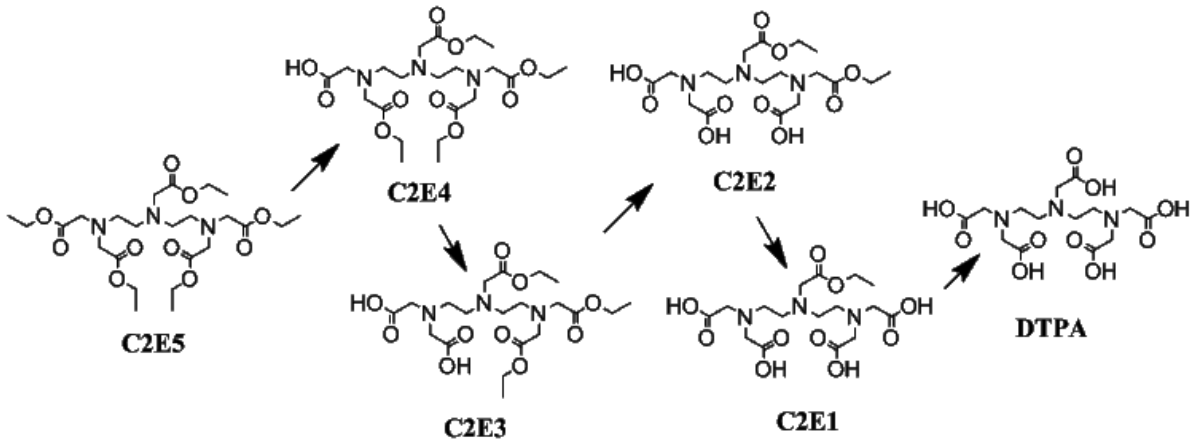

Figure 1.2 Clearance of ^{14}C-DTPA following intravenous administration.

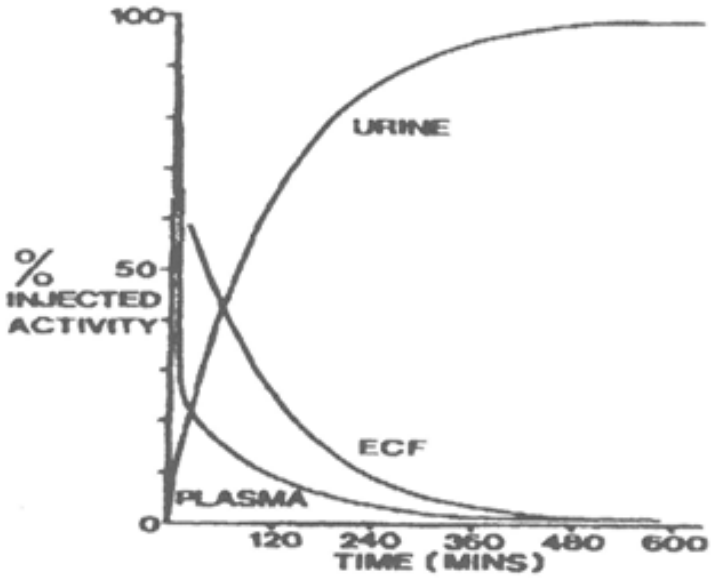

Figure 1.3 Estimated blood levels (from Fig 1.2) following a 1 g i.v. dose of DTPA to a 70 kg man.

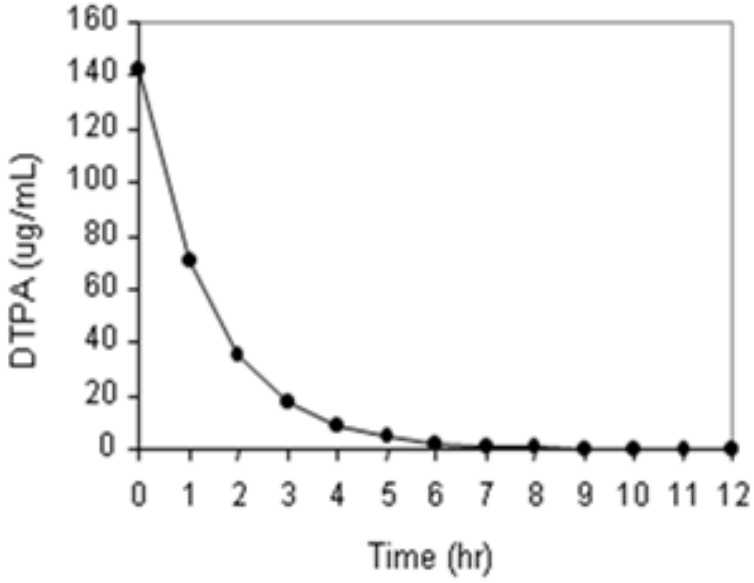

Figure 1.4 Simulated Blood Concentration Profiles Following Daily i.v. Administration of DTPA vs. Biokinetics of Initially Insoluble Radionuclides (A) and Biokinetics of Highly Soluble Radionuclides (B).

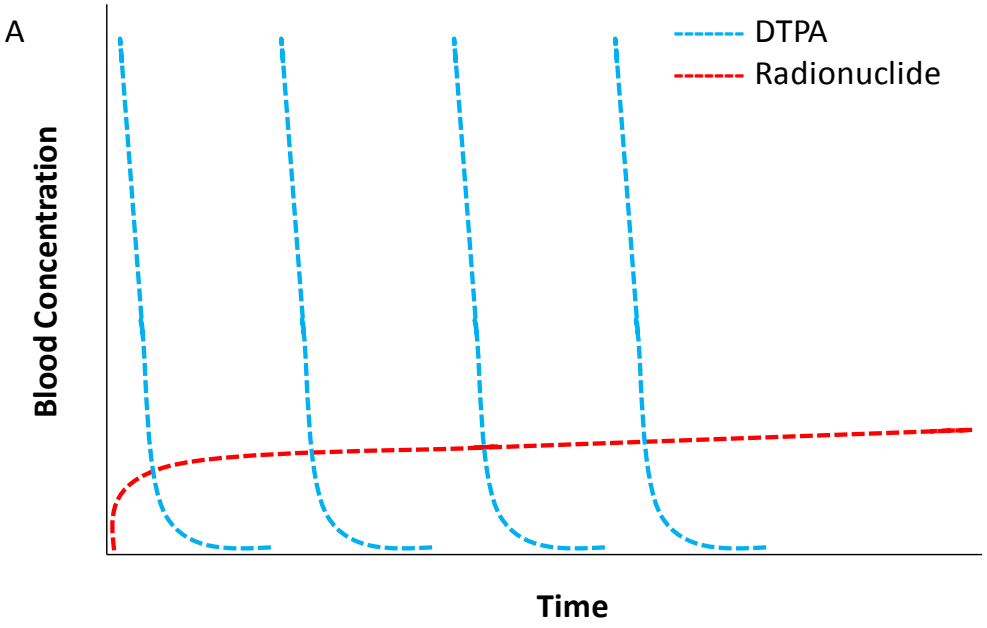

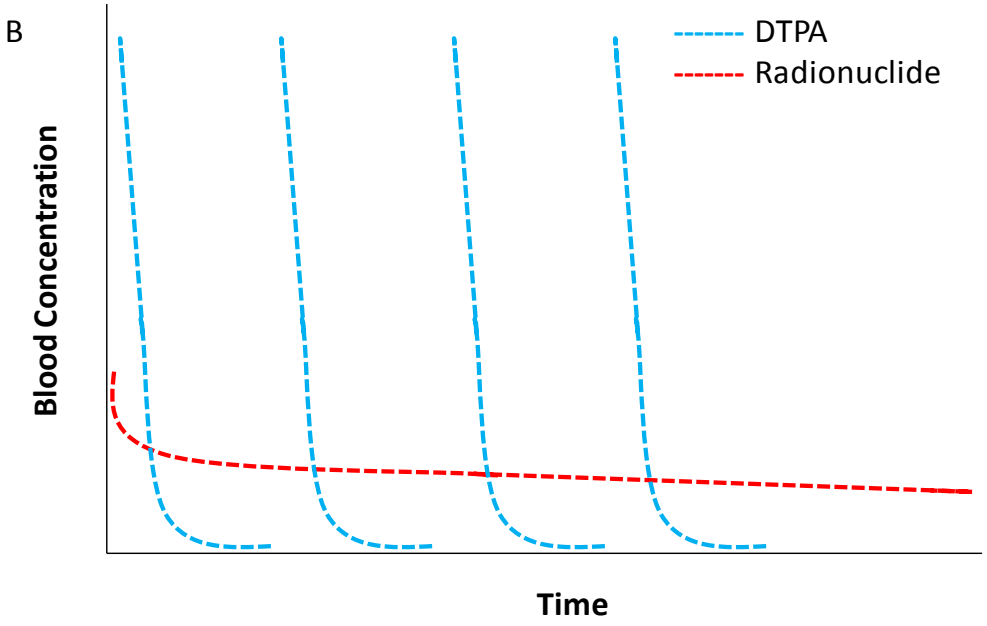

Figure 1.5 Anticipated Blood Concentration Profiles Following Transdermal Administration of DTPA Penta-ethyl Prodrug vs. Biokinetics of Initially Insoluble Radionuclides (A) and Biokinetics of Highly Soluble Radionuclides (B).

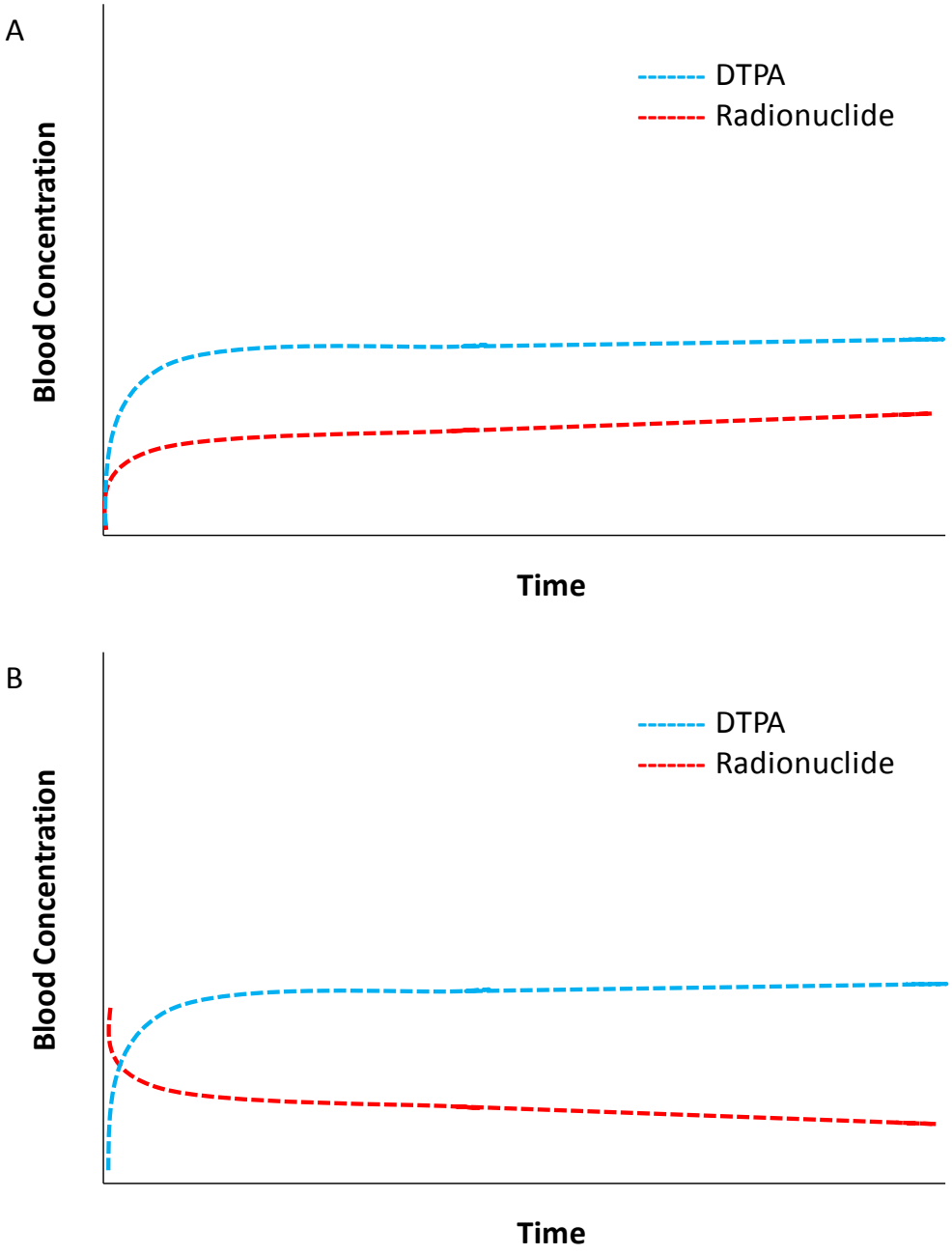

Figure 1.6 Estimated DTPA/^{241}Am ratio in the circulation as a function of infusion rate of DTPA at steady state assuming [^{241}Am] = 2 x 10^{-10} M, k = 0.693 h^{-1} and V_d = 6 L.

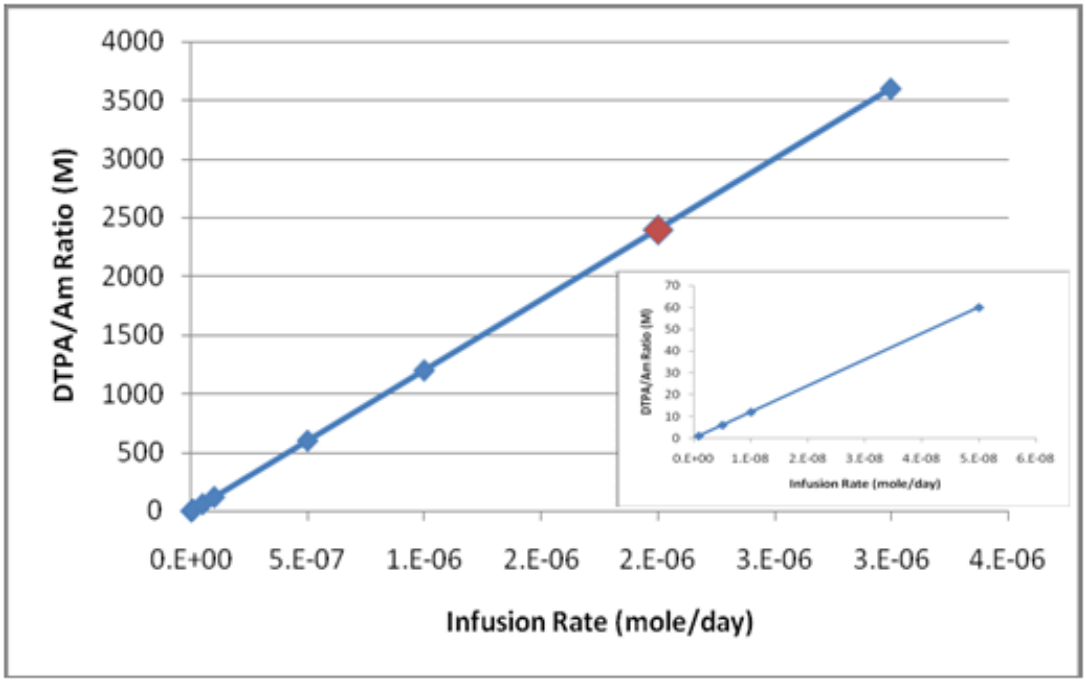

Figure 1.7 A graphic description for decorporation of [^{241}Am]-americium nitrate contaminated rats with C2E5 transdermal formulations.

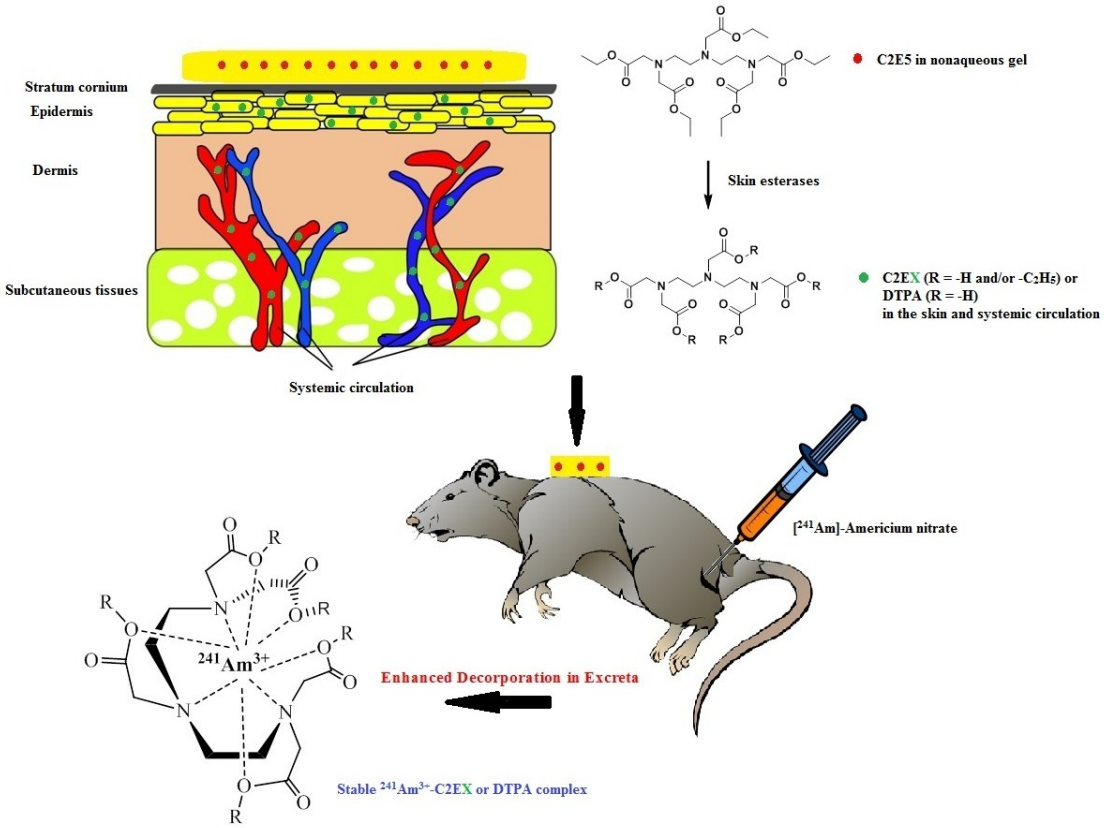

CHAPTER 2: FORMULATION DEVELOPMENT OF PENTA-ETHYL ESTER OF DTPA FOR TRANSDERMAL DELIVERY

The penta-ethyl ester of diethylenetriamine pentaacetic acid (DTPA), a DTPA prodrug designated as C2E5 intended for transdermal delivery for radionuclide decorporation, was first screened with a prototype cream formulation and a hydrocarbon base ointment with C2E5 concentration ranging from 1% to 20%. C2E5 experienced rapid degradation in the cream matrix and C2E5 ointment formulation underwent phase separation due to components incompatibility. Non-aqueous gel matrix comprised of ethyl cellulose/Miglyol 840® was utilized to formulate C2E5 at different ethyl cellulose and C2E5 content levels. Differential Scanning Calorimetry (DSC) and Scanning Electron Microscope (SEM) imaging were applied for analysis of the prepared C2E5 gel formulation. C2E5 was stabilized in the non-aqueous gel matrix and ethyl cellulose solubilization by dispersion media was confirmed by DSC and SEM results. Selected C2E5 non-aqueous gel formulations were evaluated in a rodent ^{241}Am wound contamination model at a dose level of 200 mg C2E5/kg. The enhanced decorporation over no treatment control on total decorporation, decorporation by urine, and decorporation by feces was 142%, 181% and 86%, respectively. The non-aqueous gel matrix comprised of ethyl cellulose/Miglyol 840 was successfully employed to stabilize the hydrolysis prone C2E5. C2E5 was delivered transdermally and achieved enhanced decorporation for the proof of hypothesis.

2.1 INTRODUCTION

The United States and many other countries face increasing threats from terrorist groups with respect to the use of weapons of mass destruction against civilian populations. Of particular concern is that some of these groups are intensifying their efforts to acquire and develop nuclear and radiological weapons, such as Radiological Dispersal Devices (RDD) which, when spread by means of conventional explosives, constitutes what is referred to as a “dirty bomb”. Among the radionuclides of greatest concern that may be incorporated in an RDD are isotopes of americium (Am), curium (Cm) and plutonium (Pu). Internalization of these radioactive materials may result in acute radiation sickness or chronic injuries including an increased risk of developing tumors.

The calcium (Ca) and zinc (Zn) trisodium salts of diethylenetriamine pentaacetic acid (DTPA) are the only agents that have been approved by the US Food and Drug Administration (FDA) as chelating agents for internal contamination by Am, Cm and Pu radionuclides. The primary goal of these agents is to chelate those radionuclides before they become fixed in tissues such as liver and bone while enhancing their elimination. Due to the fact that Ca-DTPA and Zn-DTPA are highly hydrophilic and have a low oral bioavailability of 2-3% (124), these products must be prepared as sterile injectable solutions. Most sterile injectable products are expensive to manufacture and require administration by a skilled professional, which render current Ca/Zn-DTPA treatment unsuitable for facile use in a mass casualty situation. Furthermore, there is a mismatch between the pharmacokinetic profile of intravenously (i.v.) administered DTPA and the biokinetic profile of transuranic radionuclides (90, 92, 94). Stevens and colleagues studied the clearance of ^{14}C-labeled DTPA in man after i.v. administration and observed that the intravenously administered ^{14}C-labeled DTPA was quantitatively excreted intact in urine within 24 hours (125). The total body clearance of ^{14}C-labeled DTPA in rats 24 h after i.v. injection has been reported to range from 94% to

100% with half-lives from 0.28 to 0.53 h with no metabolic degradation (79, 94). In contrast, the release rates of internalized Am, Pu and Cm contaminants from wounds sites to the systemic circulation in various animal species range from 0.052 to 6.3% of the injected dose per day, a relatively slow and steady transfer process (80). It has been suggested that a chelating agent must be maintained at a concentration of at least 10 to 25 μM for a sustained duration to ensure an optimal chelation effect of transuranic radionuclides, both in extracellular and intercellular fluids (88). A sustained DTPA plasma concentration cannot be achieved by i.v. Ca/Zn-DTPA and is not readily achievable by conventional sustained-release oral dosage forms. In addition, there are some patient populations that cannot take drugs orally, e.g., patients experiencing severe nausea following radiation exposure and very young pediatric patients.

A zero-order release profile can be achieved via transdermal drug delivery (72, 73). Topical and transdermal drug delivery provides many clinical advantages over the oral route, such as avoidance of first path metabolism, sustained release of drug with more uniform plasma concentration, and improved patient acceptance and compliance (72, 73). To be a good topical and transdermal drug delivery candidate, the compound needs to possess suitable physicochemical properties, such as a molecular weight generally less than 500 Dalton, a partition coefficient (log P) between 1 and 3, and a melting point below 200ºC (72, 73). DTPA is highly hydrophilic (log P = -4.90) with high melting point (219 - 220ºC), thus making it unsuitable for transdermal delivery (96). We have reported on the preparation of a lipophilic DTPA prodrug, designated as C2E5, in which the 5 carboxylic groups on DTPA were esterified with ethanol. C2E5 is a clear, light yellow, slightly viscous Newtonian liquid with a viscosity of ~175 cP (175 mPa s) and possesses desirable physicochemical properties for transdermal delivery (43, 44). The structures of C2E5 and the parent compound (DTPA) are depicted in Figure 1. Transdermal delivery of C2E5 may provide a sustained release of DTPA in the circulation following metabolism of the prodrug

by esterases present in the skin and plasma. The semisolid dosage forms for topical and transdermal drug delivery include creams, ointments, gels, and lotions. Unlike transdermal patches which require highly specialized expertise on patch design and sophisticated manufacturing systems, semisolid dosage forms can easily be screened in a lab setting. Previous reports showed that approximately 68% of C2E5 remained intact for the neat C2E5 oil containing 0.6% α-tocopherol stored at 25°C/80% relative humidity for three months (46), indicating that C2E5 is prone to degradation. The aims of these studies were to screen candidate cream, ointment and gel dosage forms to identify a semisolid matrix to stabilize and be compatible with C2E5, investigate the relevant physical properties of a lead C2E5 formulation, and evaluate the decorporation efficiency of the lead C2E5 formulation in a simulated ^{241}Am wound contamination model.

2.2 MATERIALS AND METHODS

2.2.1 Materials

Miglyol 812® and Miglyol 840® were gifts from Sasol (Witten, Germany). The Capmul MCM® was a gift from Abitec Corp (Columbus, Ohio). Ethylcellulose polymers of increasing chain length with ethoxyl content of 48.0-49.5% [ETHOCEL® Std 7 FP Premium (EC7), ETHOCEL® Std 10 FP Premium (EC10), and ETHOCEL® Std 100 FP Premium (EC100)] were gifts from Dow Chemical (Midland, MI, USA). C2E5 was prepared based on the Fischer esterification method by reacting DTPA with ethanol under reflux in the presence of a hydrochloric acid catalyst delivery (44). Propylene glycol (USP), sorbitol, 70% solution (USP), sorbic acid (NF), butylated hydroxytoluene (NF), simethicone (USP), white petrolatum (USP), cetostearyl alcohol (NF), polyoxyethylene (20) cetyl ether (Brij 58®), glyceryl monostearate (cosmetic grade), polyethylene glycol 400 monostearate (NF),

butylated hydroxyanisole (NF), 1N NaOH solution, acetonitrile, trifluoroacetic acid, anhydrous ethanol, and isopropyl alcohol were purchased from VWR International (Radnor, PA) and Fisher Scientific (Fairlawn, NJ). [^{241}Am]-Americium nitrate solution for intramuscular (i.m.) contamination of adult female Sprague-Dawley (SD) rats was prepared from [^{241}Am]-Americium chloride (Eckert & Ziegler Isotope Products, Valencia, CA) by dilution with a solution of concentrated nitric acid. Double-distilled water was obtained from a Milli-Q system (Millipore, Billerica, MA, USA).

2.2.2 Preparation of C2E5 Cream Formulations

The oil-in-water emulsion-based cream formulation was comprised of an aqueous phase (85.2% w/w of base cream; Components: distilled water, 79.8% w/w; propylene glycol, 3.0% w/w; sorbitol, 70% solution, 2.0% w/w; sorbic acid, 0.2% w/w; butylated hydroxytoluene, 0.1% w/w; simethicone, 0.1% w/w) and an oil phase (14.8% w/w of base cream, Components: petrolatum, 5.6% w/w; cetostearyl alcohol, 4.4% w/w; Brij 58, 4.0% w/w; glyceryl monostearate, 0.2% w/w; polyethylene glycol 400 monostearate, 0.6% w/w). The topical cream was prepared by first preparing the aqueous phase in a 200 mL glass jar. The ingredients were weighed into the jar and subsequently heated to 70°C in a water bath. When all ingredients were fully dissolved, the pH was adjusted to 3.5, 4.5 or 5.5 by addition of a 1N NaOH solution. The oil phase was prepared by weighing the various components into a 100 mL beaker and then heating at 60°C. The emulsion was formed by decanting the melted oil phase into the jar containing the aqueous phase and which was equipped with a Caframo BDC1850 mechanical stirrer (Caframo Ltd., Wiarton, ON, Canada). The mixer was positioned in the center of the jar approximately 1/3 from the bottom and the stirring speed was set at 1000 RPM. The emulsion was stirred for 30 min while heated at 70°C. The heating was then stopped and the emulsion was stirred for an additional 2 hours. The final

emulsion was prepared by direct addition of C2E5 and subsequent mixing for 5 minutes at 500 RPM so that the final concentration of C2E5 was 1%, 5%, 10% or 15% w/w. All emulsions were sealed in vials with an airtight cap, covered with aluminum foil to protect from light, and stored at room temperature for stability testing.

2.2.3 Preparation of C2E5 Ointment Formulations

The non-aqueous hydrocarbon base ointment was comprised of white petrolatum (79.9% w/w), Miglyol 812 (15.4% w/w), Capmul MCM (4.6% w/w) and butylated hydroxyanisole (0.1% w/w). The base ointment was prepared by liquefying the white petrolatum using heat while mixing and then adding the Miglyol 812, Capmul MCM and butylated hydroxyanisole; a white ointment was produced upon cooling. C2E5 containing ointment formulations with C2E5 concentrations of 5%, and 10% and 20% w/w were prepared by adding the C2E5 directly to the base ointment and then mixing for 5 minutes at 1000 RPM using a Caframo BDC1850 mechanical stirrer with a mixer with 8 points and 1 inch in diameter. The final C2E5 containing ointment formulations were transferred to 20 mL scintillation vials, sealed with an airtight cap, covered with aluminum foil to protect from light, and stored at room temperature for subsequent stability testing.

2.2.4 Preparation of C2E5 Non-aqueous Gels

The C2E5 non-aqueous gels were prepared according to a previously described method with minor modifications (126). Miglyol 840 and C2E5 were first heated to 60°C, followed by the slow addition of the fine particles of EC7, EC10 and EC100 into the solvent under constant stirring. The EC, Miglyol 840 and C2E5 mixtures were held under stirring until the mixtures turned into clear viscous solutions, typically in 2 to 12 hours. Non-aqueous

gels were formed after cooling to ambient temperature. Four formulations were prepared from each EC polymer: 7%, 8%, 14% and 16% w/w for EC7, and 7%, 8%, 10% and 12% w/w for EC10 and EC100. The non-aqueous gel samples were put under vacuum to remove air bubbles trapped in the gels and subsequently crimped with an airtight cap, covered with aluminum foil to protect from light, and stored at room temperature for stability testing.

2.2.5 High Pressure Liquid Chromatography (HPLC) Assay for C2E5

The C2E5 concentration in these cream, ointment and non-aqueous gel formulations was determined using a Shimadzu Prominence HPLC system equipped with an Alltech 3300 Evaporative Light Scattering Detector (ELSD). A reverse-phase gradient separation was performed using a Chromolith® FastGradient RP-18e column (50 × 2.0 mm) coupled with an Alltima Alltech HP All-Guard Cartridge (C18, 5µm particle size, 2.1 x 7.5 mm) at 40°C and at a flow rate of 0.25 mL/min. The solvents that comprised the mobile phase were water with 0.1% trifluoroacetic acid (A) and acetonitrile with 0.1% trifluoroacetic acid (B). The linear gradient for the mobile phase mixture (A:B) was first an equilibration phase at 95:5 for 1 min, then from 95:5 to 5:95 over 9 min, followed by an equilibration phase at 95:5 for 10 min, and ending with a reversal to 95:5 in 3 min and an equilibration phase of 95:5 for 3 min. The ELSD was operated at 40°C with 1.9 L/min nitrogen gas flow and the retention time of C2E5 was 9 min. The extraction of C2E5 from the cream, ointment and non-aqueous gel samples was followed the method of Tashtoush with minor modifications (127). Approximately 50 - 200 mg of the formulation samples were weighed into a 50 mL conical centrifugation tube, followed by addition of 20 -30 mL of acetonitrile. The mixture was then vortexed for 1-10 minute followed by centrifugation for 5 min at 10,000xg at 20ºC. One mL of the supernatant was filtered through a 0.2 µm polyvinylidene difluoride (PVDF) filter into an HPLC vial for analysis. A 10 µL injection for each sample was performed. Samples were

held at ambient temperature during analysis and analyzed using standard curves over a concentration range of 0.05 – 1.00 mg/mL which had a power regression fit of $R^2 \geq 0.997$.

2.2.6 Viscosity Measurement of C2E5 Non-aqueous Gels

The apparent viscosity of the C2E5 non-aqueous gels were measured at a shear rate of 1000 s^{-1} at 25ºC using an Brookfield R/S Plus rheometer (Brookfield Engineering, Middleboro, MA), which was equipped with a 25 mm diameter cone and plate assembly. The gel samples were carefully loaded to the lower plate to reduce shearing effects and equilibrated for 5 min at 25ºC prior to measurement. Triplicate measurements were performed for the formulation and data are reported as mean ± S.D.

2.2.7 Thermal Analysis by Differential Scanning Calorimetry (DSC)

The EC10 polymer particles that had been dried overnight at 60°C before analysis, and the C2E5 non-aqueous gel samples were analyzed using a TA Instruments DSC Model Q200 (Newcastle, DE, USA) under a nitrogen flow of 50 mL/min. Samples (5-10 mg) were heated in a sealed aluminum pan at a ramp rate of 10°C/min, cooled at a rate of 5°C/min, and subsequently heated at 10°C/min in heat/cool/heat mode from -10°C to 160°C. The glass transition (T*g*), and melting (T*m*) temperatures in the third heating cycle were determined using TA Universal Software.

2.2.8 Scanning Electron Microscope (SEM) Imaging

The pre-dried EC10 polymer particles and C2E5 non-aqueous gel samples were observed and recorded using a Hitachi S-4700 scanning electron microscope at an

accelerated voltage of 15kV. All images were taken at a scan rate of 100 millisec per line. The EC10 polymer particles and C2E5 non-aqueous gel samples were deposited directly over double-sided carbon tape and imaged without further treatment. The C2E5 non-aqueous gel samples were imaged on the stub which was tilted 45º toward the lower scanning election detector for better imaging results.

2.2.9 Americium Decorporation in a Rodent Wound Model of Contamination

All animal studies were conducted according to a protocol approved by the University of North Carolina at Chapel Hill Institutional Animal Care and Use Committee (IACUC). Adult female SD rats weighing from 200 to 400 g were used in these studies (Charles River Labs, Raleigh, NC). Food and water were given ad libitum. The animal room was kept at a controlled temperature (23°C) and light cycle (light exposure from 8 AM to 8 PM). For the duration of the study, the rats were individually housed in metabolic cages.

To evaluate the efficacy of transdermal delivery of the C2E5 non-aqueous gel, a proof of principle radionuclide decorporation efficacy study was conducted in rats contaminated with ^{241}Am. Adult female SD rats were anesthetized with 2-3% isoflurane. Dorsal skin between the cervical vertebrae and anterior thoracic vertebrae was clipped with caution before all animals were contaminated with [^{241}Am]-Americium nitrate solution (250 nCi, 0.1 mL) via an i.m. injection in the anterior thigh muscle. Freshly prepared C2E5 non-aqueous gel formulations containing 30% C2E5, 63% Miglyol 840 and 7% of EC7, EC10 or EC100 (formulations N-1, N-5 and N-9 – see Table 2) were applied at a dose of 200 mg C2E5/kg (375 µmol C2E5/kg) using a cotton swab to approximately 6-8 cm^2 of the clipped dorsal region immediately after contamination. The mass of C2E5 gel applied was recorded for each animal to permit the actual dose determination. Negative control included animals without any treatment. The animals were observed once daily and their body weights

recorded at pre-dose and prior to necropsy. Urine and feces were collected daily until the animals were euthanized on day 7 at which time the cage washes were collected. As ~35% of the decay of ^{241}Am is associated with photon emissions of 59.7 keV, ^{241}Am in samples was quantified using a gamma counter (2470 Wizard 2, Perkin Elmer, Waltham, MA, USA). The samples were counted for one minute using a 40-80 keV energy detection window and were background-corrected. Additionally, ^{241}Am activity was quantified in 2 x 0.1 mL aliquots of the dosing solution to determine the initial administered dose of ^{241}Am. For all samples, ^{241}Am content was expressed as a percentage of the initial injected dose. The percent of enhanced decorporation for animals treated with transdermal C2E5 non-aqueous gels compared to the no treatment control animals were calculated from Equation 2-1 (90).

$$\text{Percentage Enhanced Decorporation} = \frac{\%\ \text{ID (Treatment)} - \%\ \text{ID (No Treatment)}}{\%\ \text{ID (No Treatment)}} * 100 \quad (\text{Eq. } 2-1)$$

In this equation, % ID represents the percent of the initial injected dose.

2.2.10 Statistical Analysis

Comparisons between non-aqueous gel formulations were made using one-way analysis of variance (one-way ANOVA). Having determined by one-way ANOVA that gel formulation was not a significant effect, two-tailed t-tests were used to compare decorporation efficacy between C2E5 treated and untreated animals. All measurements are expressed as mean ± standard deviation (S.D.). The level of significance was set at $p < 0.05$.

2.3 RESULTS

2.3.1 Stability of C2E5 Cream and Ointment Formulations

The composition and stability testing results of C2E5 cream formulations are presented in Table 2.1. The base cream is white and the C2E5 containing cream became more yellow with increasing C2E5 content. No phase separation was observed for the C2E5 cream formulations for the 2 month stability testing period at 25 ± 2°C/60 ± 5% relative humidity. Because of the high concentrations of C2E5 in these formulations and the fact that C2E5 is self-buffering, the final pH of all of the cream formulations was in the range of pH 5 to 6. Based on the stability testing results of the C2E5 oil-in-water cream-based formulations, it indicated that higher C2E5 content in the creams resulted in a better stability profile, ranging from 52.6% to 61.6% C2E5 remaining for 1% C2E5 cream formulations, to 77.1% to 90.6% C2E5 remaining for 16.7% C2E5 cream formulations. The major degradants of C2E5 in the cream formulations were partially hydrolyzed products of C2E5, such as the tri- and tetra-ethyl esters of DTPA. Although the cream formulations with higher C2E5 content showed improved C2E5 stability over lower C2E5 containing cream formulations, they failed to deliver an acceptable C2E5 stability profile for a reasonable product shelf life.

The C2E5 ointment formulations showed a similar trend in terms of physical appearance as C2E5 containing cream formulations. The ointment formulation containing 20% C2E5 underwent phase separation within the first month after storage at 25 ± 2°C/60 ± 5% relative humidity; the C2E5 ointment formulation with 5% and 10% C2E5 contents experiencing phase separation within 3 months under the same storage conditions.

2.3.2 Stability of C2E5 Non-aqueous Gels

The composition and stability data of C2E5 non-aqueous gel formulations after 3 months storage at 25 ± 2°C/60 ± 5% relative humidity are presented in Table 2.2. The C2E5 non-aqueous gel formulations appeared to be yellow and opaque. During the 3 month storage period, no phase separation was observed for the non-aqueous gel formulations. The improved C2E5 stability in the non-aqueous gel matrix was achieved over the C2E5 cream formulations with greater than 93% of the original C2E5 remaining for most of the non-aqueous gel formulations stored at the same storage condition for 3 months. Clumps were observed for formulations associated with C2E5 non-aqueous gel using EC100 as the gelling agent possibly due to EC100's longer polymer chain and higher molecular weight, which make the solubilization of EC100 in C2E5 and Miglyol 840 inadequate. Lack of content uniformity in these gels may explain the higher than expected C2E5 concentration observed in the formulation of N-10.

2.3.3 Viscosity of C2E5 Non-aqueous Gels

The apparent viscosity measurements of C2E5 non-aqueous gel formulations are reported in Table 2.2. An increase in concentration of the ethyl cellulose, the gelling agent, resulted in the increase in the apparent viscosity of the non-aqueous gel formed, as well as the same trend in the ethyl celluloses with higher molecular weight and polymeric chain length, an indication of a stronger gel structure as a result of stronger interaction between the ethyl cellulose chains and between the ethyl cellulose chain and the dispersion media molecules. This observation is consistent with the result reported by Heng (126). The non-aqueous gels containing 10% and 12% EC100 failed to yield a stable reading at this shear year due to the breakup of the gel samples.

2.3.4 Thermal Analysis by Differential Scanning Calorimetry (DSC)

The DSC spectra of pre-dried EC10, C2E5 non-aqueous gel formulation comprised of 10% EC10, 30% C2E5 and 60% Miglyol 840 (Formulation N-7) are presented in Figure 2.2. The DSC spectrum of pre-dried EC10 (Figure 2.2A) showed one minor endothermic peak appearing at 63°C and one major endothermic peak at 120°C. The latter peak was determined to be the EC10 glass transition temperature (128). The endothermic peak at 63°C appeared to be glyoxal, which is a major impurity in ethyl cellulose (129), or reaction products associated with glyoxal. However, further investigation is necessary for confirmation of this peak. The DSC spectrum of the C2E5 non-aqueous gel formulation N-7 (Figure 2.2B) showed one major endothermic peak appearing at 106°C and one minor endothermic peak at 120°C. The presence of a minor EC10 glass transition endothermic peak at 120°C indicated that there was nearly complete solubilization of EC10 particles in Miglyol 840 and C2E5 and a minuscule amount of partially solubilized EC10 particles present in the gel sample was expected. The endothermic peaks at 106°C might be due to water trapped in the EC10 material, which could be a result of use of the EC10 that was not dried before incorporated in the gel preparation.

2.3.5 Scanning Electron Microscope (SEM) Imaging

Figure 2.3 shows the SEM images of pre-dried EC10 particles and the C2E5 non-aqueous gel (formulation N-7). In Figures 2.3A and 2.3B, the SEM images showed tightly clumped EC10 particles with a relatively uniform size distribution averaging 1 to 5 μm in length. The SEM images of the C2E5 non-aqueous gel (Figure 2.3C and 2.3D) displayed a relatively smooth gel surface that was embedded with small particles. The small particles

were determined to be residual EC10 material that failed to be completely solubilized by Miglyol 840 and C2E5 during the gel preparation process. This assessment is supported by the DSC spectrum of the C2E5 non-aqueous gel in which a minor EC10 glass transition endothermic peak appeared at 120°C.

2.3.6 Radionuclide Decorporation

The excretion of ^{241}Am in urine and feces after seven days in untreated rats and in rats treated with a single 200 mg/kg dose of C2E5 applied topically in different non-aqueous gel formulations immediately after radionuclide contamination are summarized in Table 2.3. The mean total decorporation observed following treatment with C2E5 non-aqueous gels formulated with EC7, EC10 and EC100 was not significantly different ($F_{Formulations(2,3)} = 0.15$, $p = 0.87$) and clearance in the urine and feces were consistent across all formulations ($F_{Urine(2,3)} = 0.41$, $p = 0.70$ and $F_{Feces(2,3)} = 0.72$, $p = 0.56$), indicating that the type of the ethyl cellulose polymers used in formulating C2E5 non-aqueous gels did not affect decorporation efficacy in a statistical manner. Therefore, the C2E5 treatment groups were combined into one C2E5 treated animal group and compared with untreated animals. The daily excretion of ^{241}Am in contaminated animals treated with the C2E5 gel and untreated control animals is presented in Figure 2.4. Application of a single dose of the C2E5 gel immediately after contamination resulted in enhanced excretion of ^{241}Am for a period of at least 3 days compared to untreated animals. Treatment with C2E5 transdermal gels enhanced total decorporation compared with untreated controls. The enhanced decorporation was primarily due to urinary, but significantly increased fecal decorporation was also observed. The enhanced decorporation over no treatment control on total decorporation, decorporation by urine, and decorporation by feces was 142%, 181% and 86%, respectively.

2.4 DISCUSSION

In the present study, by testing the stability and compatibility of C2E5 in different transdermal drug delivery vehicles, we demonstrate that a non-aqueous gel matrix comprised of ethyl cellulose/Miglyol 840 can be used to protect a hydrolysis prone compound while retaining the drug's efficacy for transdermal delivery. DSC and SEM results confirmed the nearly complete solubilization of ethyl cellulose in the dispersion media.

As the largest organ of the integumentary system in humans, skin has a surface area of about 2 m^2 and is involved in many biological functions. One major function of the skin is to serve as a protective barrier for xenogenous substances. A highly stratified "brick and mortar" lipophilic stratum corneum greatly limits the compounds that can effectively penetrate this layer, and only allows absorption of compounds possessing suitable physicochemical properties, such as molecular weight generally less than 500 Dalton, partition coefficient (log P) between 1 to 3, and melting point below 200ºC (72, 73). Furthermore, to be a successful transdermal drug delivery candidate, a balance of lipophilicity and hydrophilicity is highly desirable because the drug needs to reabsorbed into an aqueous environment after it penetrates through the stratum corneum (75). Consequently, many topical and transdermal drugs possess ester or other functional groups that increase the lipophilicity of the drug molecules and as a result, render them moisture-sensitive and prone to a variety of degradation reactions (130, 131). Although C2E5 possesses suitable physicochemical properties for transdermal delivery, which include a log P of 3.3 and a melting point well below 200ºC (44), it suffers from a poor stability profile due to hydrolysis and other potential secondary degradation pathways. The pH of the water phase for the cream formulations was set at 3.5, 4.5 and 5.5 based on C2E5 pre-formulation data which demonstrated that C2E5 degradation in buffered aqueous solution follows a pseudo-first order kinetics and C2E5 is most stable at approximately pH 4.2 (44). From the

C2E5 cream stability testing results, it suggests that the C2E5 content in the cream plays a more important role for the stability of the C2E5 incorporated in the cream matrix than the pH of the water phase, with a much higher percent of C2E5 remaining intact in the cream formulation with higher C2E5 content. However, the cream formulation failed to stabilize the C2E5 incorporated in the cream matrix for sufficient storage stability at 25°C.

As a consequence of poor stability of the cream formulations, ointment formulations comprising white petrolatum, Miglyol 812 and Capmul MCM was developed. The C2E5 ointment formulations were physically unstable and underwent phase separation within 3 months after storage at 25 ± 2°C/60 ± 5% relative humidity, which demonstrates the instability of C2E5 ointment formulations as a result of incompatibility and lack of interaction between the white petrolatum, the main component of the ointment matrix, and the C2E5. White petrolatum consists of saturated hydrocarbons with carbon numbers mainly greater than 25 (132). In order to maintain the physical stability of ointment structure, interactions between petrolatum molecules and dispersion medium molecules are necessary. Because the major force existing between petrolatum molecules are hydrophobic-hydrophobic interaction, and considerable interactions of this type exist between the C-8 and C-10 chains of Miglyol 812 and Capmul MCM, and the petrolatum molecules, addition of the C2E5 molecules that lack hydrophobic-hydrophobic interaction potential would destabilize the ointment matrix, with the expectation that the higher the C2E5 content in the ointment formulation, the faster the ointment formulation would undergo phase separation. The limited physical stability of the C2E5 ointment formulations could be well explained by these observations.

Due to the high hydrolytic tendency of the C2E5 ester bonds and incompatibility of C2E5 with the hydrocarbon base ointment matrix, the focus of the C2E5 formulation development was shifted to select a semisolid dosage form that contains a dispersion medium lacking functional groups such as hydroxyl and carboxylic groups that facilitate the

hydrolysis of the C2E5 ester bonds and a gelling agent that is compatible with C2E5. Furthermore, the process to make this semisolid dosage form should not expose C2E5 to harsh conditions that accelerate its degradation. Non-aqueous gel formulations were pursued as a viable dosage form candidate to stabilize C2E5 in the delivery vehicles. In contrast to extensive research on traditional semisolid dosage forms such as creams, ointments and hydrogels, there are far fewer reports on the development of non-aqueous gel matrices intended for topical and transdermal drug delivery (126, 133-136). Advantages of non-aqueous gel dosage form include matrix components that stabilize the moisture sensitive drug substance and candidate non-aqueous gel matrices that possess the suitable rheological and mechanical properties for topical and transdermal drug delivery. The Heng group reported on non-aqueous gel matrices containing ethyl cellulose and Miglyol 840 by directly mixing the ethyl cellulose and Miglyol 840 at 60°C (126). ETHOCEL, an ethyl cellulose polymer suitable for pharmaceutical application, contains ~50% hydroxyl content on the polymer chain which is not readily available to interact with other molecules compared to hydroxyl groups in a small molecule due to steric and rotational hindrance. Miglyol 840, a neutral oil mixture of propylene glycol dicaprylate and dicaprate, has excellent penetration-promoting, emollient and skin-smoothing properties as well as a high stability against oxidation (137). The C2E5 stability profile in the non-aqueous gel formulations demonstrated pronounced improvement compared to that of neat C2E5 containing 0.6% α-tocopherol in which less than 70% of C2E5 remained intact after three months of storage under similar conditions (46), as well as that of C2E5 incorporated in the cream formulations. The improved stability profile of C2E5 in this ethyl cellulose/Miglyol 840 matrix may be attributed to steric and rotational hindrance of the hydroxyl groups on the ethyl cellulose polymer backbone resulting in decreased interactions with C2E5 molecules. In addition, Miglyol 840 neutral oil is non-hygroscopic, possesses high stability against oxidation and contains no free hydroxyl groups. No phase separation observed in the 3

month storage period for the C2E5 containing non-aqueous gel formulations indicated that a stable and extensive three-dimensional reversible physical crosslinks were formed within the gel structures (126). Based on the initial report on the viscosity of the prepared C2E5 non-aqueous gels and previous studies on an ethyl cellulose/Miglyol 840 non-aqueous gel matrix (126, 138, 139), further investigation may focus on the relationship between the viscosity and the ratios of the ethyl cellulose, Miglyol 840 and C2E5 could yield the ideal C2E5 non-aqueous formulations with suitable rheological and mechanical properties for the transdermal delivery of C2E5.

Contrary to the transdermal patches which are viewed as a medical device and normally demand highly specialized expertise and multi-step manufacturing process, the C2E5 non-aqueous gel is readily prepared by directly mixing the ethyl cellulose with the mixture of C2E5 and Miglyol 840. In contrast to the DSC spectrum of the EC10 polymers, the DCS spectrum of an EC10 based gel (Figure 2.2B) indicated nearly complete solubilization of EC10 by Miglyol 840 and C2E5. The SEM images of the same EC10 based gel (Figures 2.3C and 2.3D) confirmed the DSC result in that a relatively smooth EC10 gel surface was embedded with residual EC10 particles. To improve the quality of the C2E5 non-aqueous formulations, procedures such as pre-drying the ethyl cellulose before use to remove water and volatile impurities and milling the ethyl cellulose particles before use to improve EC10 solubilization were applied. To reduce the potential C2E5 degradation in the gel preparation stage, addition of C2E5 after ethyl cellulose/Miglyol 840 gel formation and filling the head space of the gel preparation vessel with nitrogen could retard C2E5 degradation.

C2E5, applied topically to contaminated rats, in non-aqueous gel formulations at 200 mg/kg was able to enhance ^{241}Am decorporation. A preliminary pharmacokinetic study conducted by this research group on SD rats using a C2E5 non-aqueous gel at a dose of 200 mg C2E5/kg demonstrated that C2E5 was converted into DTPA *in vivo* (47), confirming

that C2E5 is indeed a prodrug of DTPA. We had previously reported on the enhanced decorporation of ^{241}Am after oral delivery of C2E5 (45); decorporation efficacy achieved by transdermal delivery of C2E5 at the same dose level is comparable. Analysis of the *in vivo* data showed that changing the ethyl cellulose polymer chain length in the non-aqueous gel matrix did not alter C2E5 efficacy. Together, these data suggest that ethyl cellulose based non-aqueous gels can be readily optimized to provide effective delivery of C2E5 in a stable vehicle. As the first report using ethyl cellulose/Miglyol 840 gel matrix developed by the Heng group to incorporate a hydrolytically sensitive drug, we believe this non-aqueous delivery vehicle may find useful applications for moisture and hydrolysis sensitive compounds intended for topical and transdermal drug delivery.

2.5 CONCLUSION

In summary, C2E5, a DTPA prodrug for transdermal delivery, was formulated in cream, ointment and non-aqueous gel delivery vehicles. Due to the hydrolysis labile nature of C2E5, it rapidly degraded in a cream matrix comprised of an aqueous phase. Incompatibility between hydrophobic petrolatum and C2E5 resulted in the phase separation of C2E5 containing ointment formulations. C2E5 was shown to be stable in a non-aqueous gel comprised of ethyl cellulose and Miglyol 840. This non-aqueous gel matrix has the potential for use with current and future moisture-sensitive drug molecules intended for topical and transdermal delivery. Enhanced ^{241}Am decorporation in a wound contamination animal model was demonstrated following topical application of C2E5 non-aqueous gels. Future studies including pharmacokinetic and dose-dependent decorporation studies are being conducted to evaluate this novel treatment option for internal radionuclide contamination by transuranic elements.

Table 2.1 C2E5 Cream Formulation Composition, Physical Appearance and Stability Results after Storage at 25 ± 2°C and 60 ± 5% Relative Humidity for 2 Months

Formulation	pH of Base Cream	C2E5 (%)	C2E5 cream Appearance	% C2E5 Remaining
C-1	3.5	1.0	White	61.6
C-2	3.5	4.8	Off-white	72.2
C-3	3.5	9.1	Pale yellow	77.0
C-4	3.5	16.7	Yellow	77.1
C-5	4.5	1.0	White	53.0
C-6	4.5	4.8	Off-white	71.4
C-7	4.5	9.1	Pale yellow	80.5
C-8	4.5	16.7	Yellow	87.3
C-9	5.6	1.0	White	52.3
C-10	5.6	4.8	Off-white	76.9
C-11	5.6	9.1	Pale yellow	81.7
C-12	5.6	16.7	Yellow	90.6

Table 2.2 Ethyl Cellulose-containing C2E5 Non-aqueous Gel Formulation Composition, Related Physical Characterization Data and Stability Results after Storage at 25 ± 2°C and 60 ± 5% Relative Humidity for 3 Months

Formulation	EC Type (%)	C2E5 (%)	Miglyol 840 (%)	Gel Appearance	% C2E5 Remaining	Apparent Viscosity (Pa s)*
N-1	EC7 7%	30	63	yellow and opaque	94.0 ± 2.6	0.51 ± 0.01
N-2	EC7 8%	20	72	yellow and opaque	97.7 ± 7.6	0.55 ± 0.00
N-3	EC7 14%	30	56	yellow and opaque	94.8 ± 8.3	3.82 ± 0.04
N-4	EC7 16%	20	64	yellow and opaque	84.0 ± 1.1	4.74 ± 0.08
N-5	EC10 7%	30	63	yellow and opaque	93.9 ± 7.1	0.72 ± 0.01
N-6	EC10 8%	20	72	yellow and opaque	96.7 ± 6.6	0.73 ± 0.01
N-7	EC10 10%	30	60	yellow and opaque	92.9 ± 3.4	2.56 ± 0.02
N-8	EC10 12%	20	68	yellow and opaque	97.4 ± 5.4	3.26 ± 0.05
N-9	EC100 7%	30	63	yellow and opaque	101.0 ± 5.9	2.38 ± 0.02
N-10	EC100 8%	20	72	yellow and opaque	106.2 ± 5.1	2.89 ± 0.03
N-11	EC100 10%	30	60	yellow and opaque	99.0 ± 7.8	N/A
N-12	EC100 12%	20	68	yellow and opaque	102.7 ± 11.1	N/A

* Apparent viscosity at a shear rate of 1000 s^{-1}; N/A: No stable viscosity reading available.

Table 2.3 Distribution of Americium-241 in Excreta 7 Days after Different Treatments Immediate Post Contamination at a Dose of 200 mg C2E5/kg

Treatment groups	Cumulative excretion (% of ID, mean ± S.D.)					
	In urine	Enhanced decorp.	In feces	Enhanced decorp.	Total eliminated	Enhanced decorp.
Untreated* (n = 4)	4.2 ± 0.6		2.9 ± 1.0		7.1 ± 1.4	
Transdermal C2E5 non-aqueous gels (n = 6)	11.8 ± 2.3***	181%	5.4 ± 1.7*	86%	17.2 ± 3.5***	142%

Significant difference by t-test comparison of means, *$p < 0.05$, **$p < 0.01$, and ***$p < 0.001$ against no treatment control; *From previously published results (45).

Figure 2.1 Structures of DTPA (A) and its prodrug C2E5 (B).

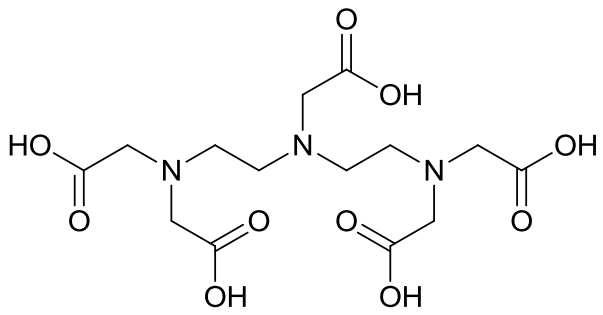

A. DTPA

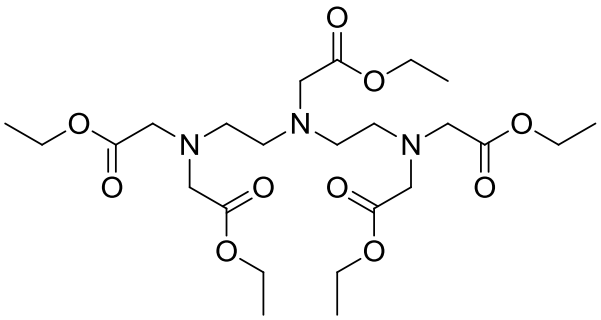

B. C2E5

Figure 2.2 DSC traces of pre-dried EC10 (A) and a C2E5 non-aqueous gel formulation consisting of 10% EC10, 30% C2E5 and 60% Miglyol 840 (B) from -10°C to 160°C at a scanning rate of 10°C min^{-1}.

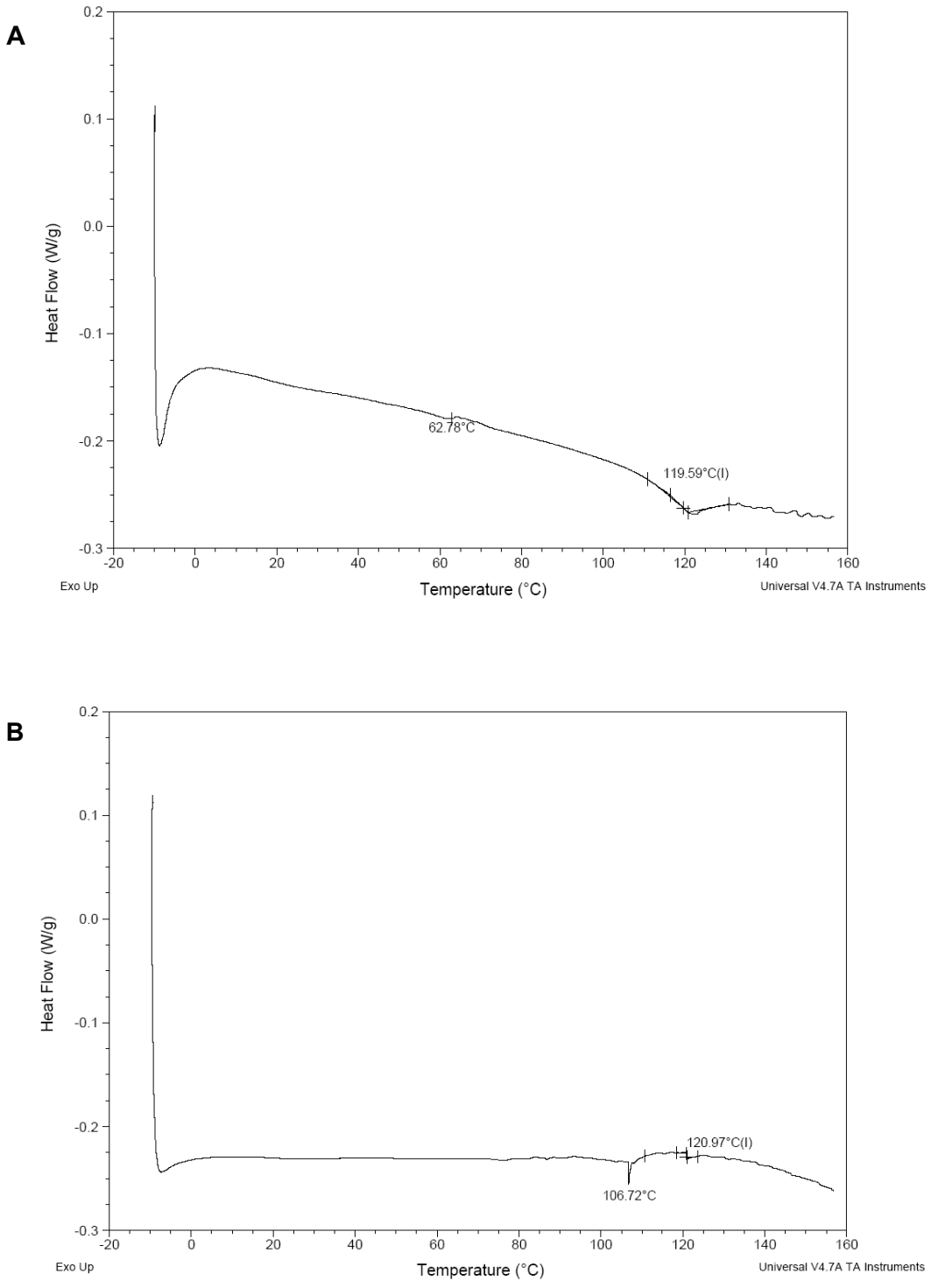

Figure 2.3 SEM images of EC10 particles (A and B) and a C2E5 non-aqueous gel formulation consisting of 10% EC10, 30% C2E5 and 60% Miglyol 840 (C and D) at magnifications of ~500 X and 3,000 X.

A

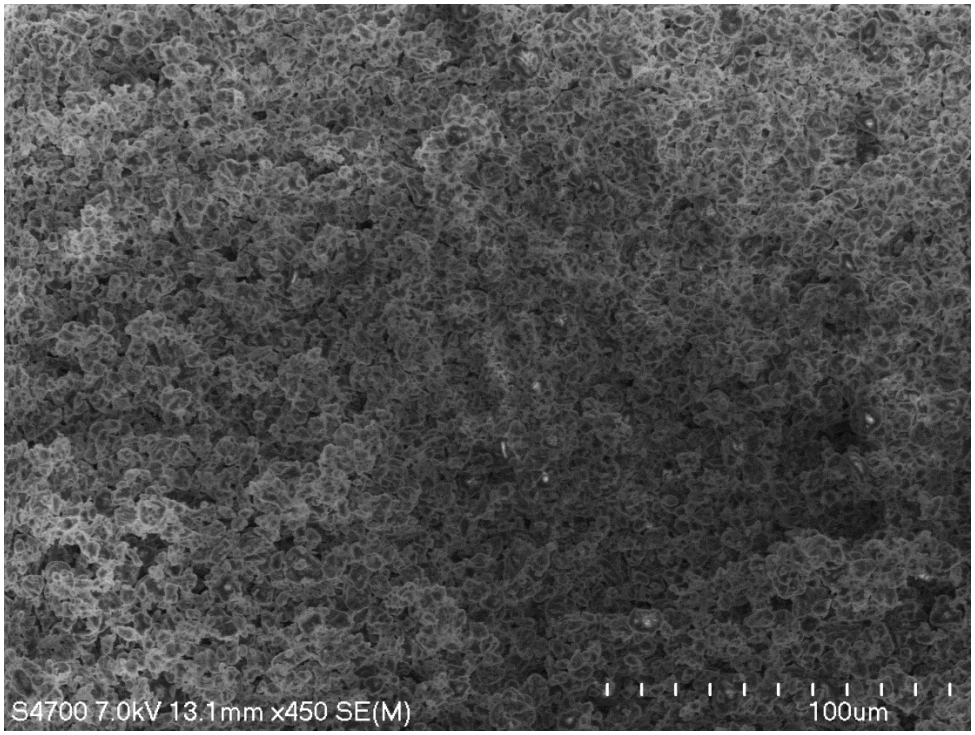

B

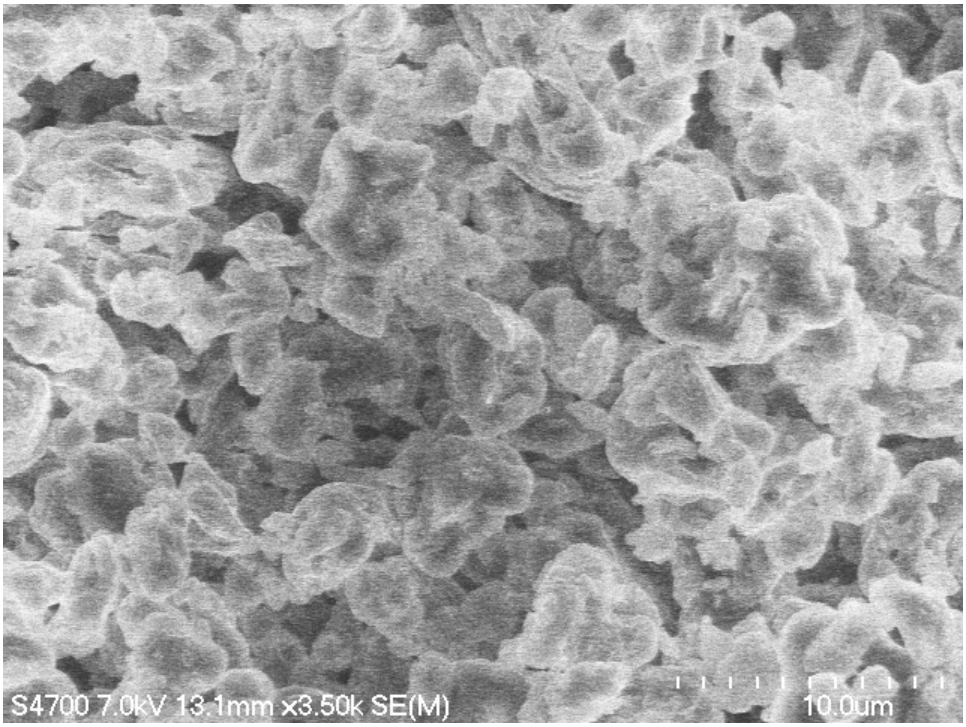

C

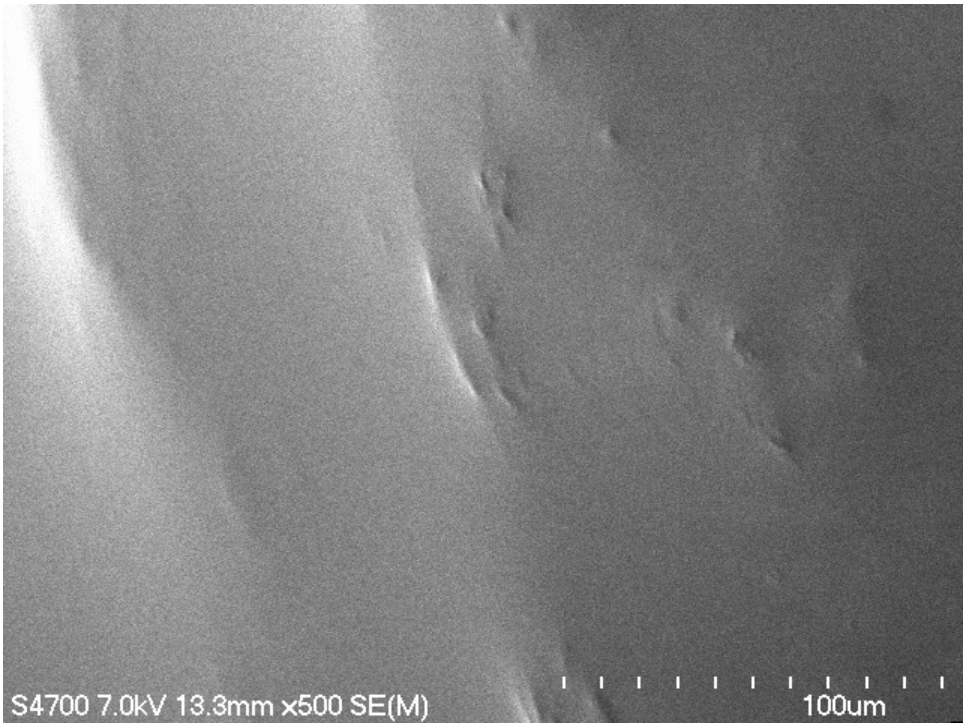
S4700 7.0kV 13.3mm x500 SE(M)
100um

D

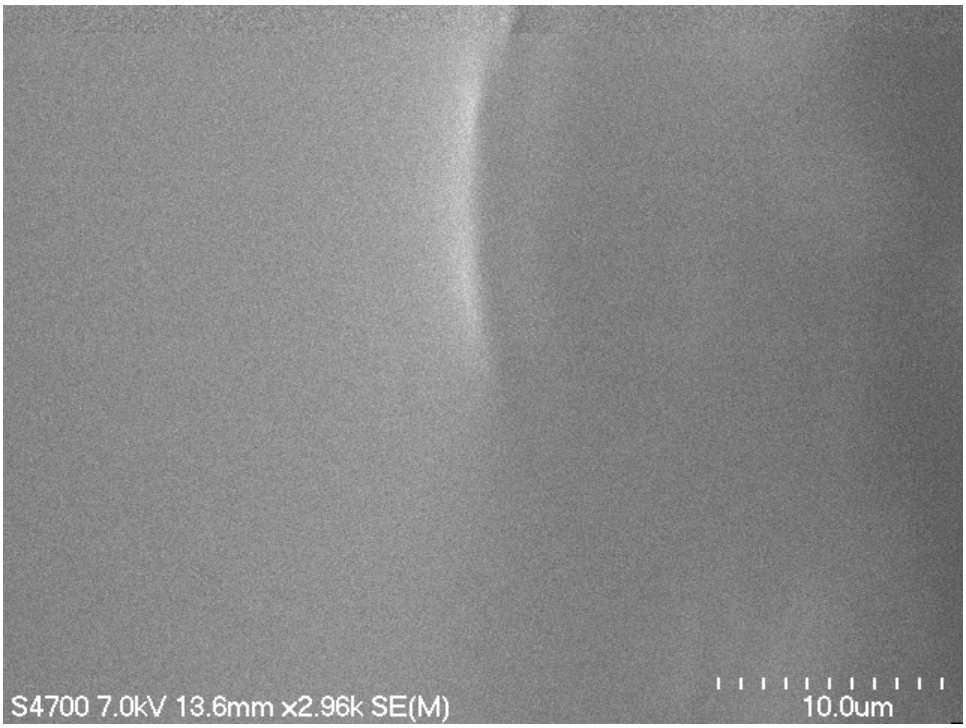
S4700 7.0kV 13.6mm x2.96k SE(M)
10.0um

Figure 2.4 Daily excretion of ^{241}Am in excreta after a single dose of topical application of 40% C2E5 non-aqueous gels (n=6) versus untreated control (n=4) (Data are means ± S.D.). (C2E5 gel group, –●–; untreated control, –■–)

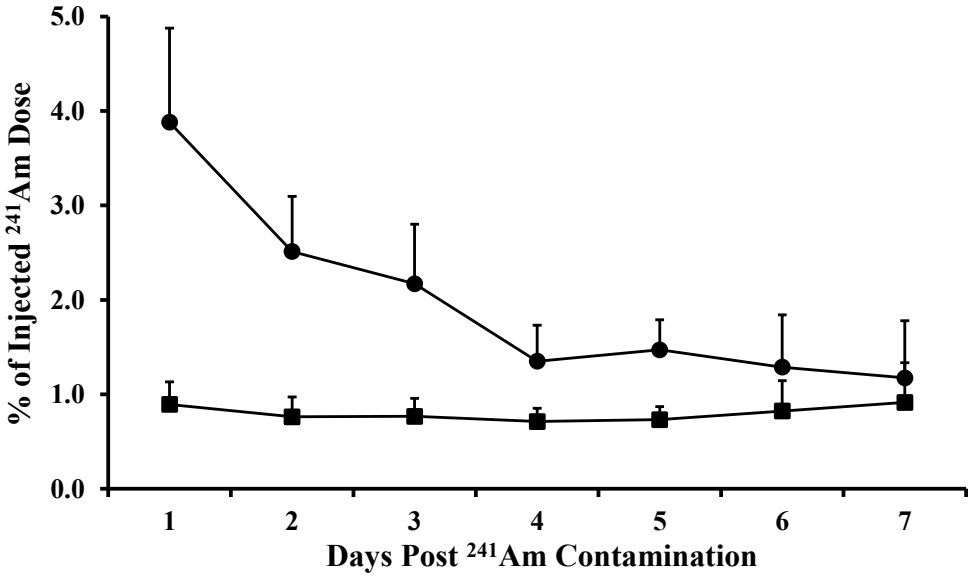

CHAPTER 3: NON-AQUEOUS GEL FOR TRANSDERMAL DELIVERY OF PENTA-ETHYL ESTER OF DTPA

Diethylenetriamine pentaacetic acid (DTPA) penta-ethyl ester, designated as C2E5, was successfully incorporated into a non-aqueous gel for transdermal delivery. The thermal and rheological properties of a formulation containing 40% C2E5, 20% ethyl cellulose and 40% Miglyol 840® prepared using the solvent evaporation method demonstrated that the gel had acceptable content uniformity and flow properties. *In vitro* studies showed that C2E5 was steadily released from the gel at a rate suitable for transdermal delivery. Topical application of the gel at a 200 mg C2E5/kg dose level in rats achieved significantly higher plasma exposures of several active metabolites compared with neat C2E5 oil at the same dose level. The results suggest that transdermal delivery of a chelator prodrug is an effective radionuclide decorporation strategy by delivering chelators to the circulation with a pharmacokinetic profile that is more consistent with the biokinetic profile of transuranic elements in contaminated individuals.

3.1 INTRODUCTION

The Fukushima Daiichi nuclear incident in March 2011 attracted world attention to currently available radiological countermeasures for such disasters. In addition, the threat of nuclear terrorism resulting from detonation of a radiological dispersion device (RDD, “dirty bomb”) calls for effective medical countermeasures designed for use in mass casualty scenarios. In both of these events, significant release of transuranic radionuclides into the

environment could result in human exposure via inhalation, ingestion, or absorption at a wound site. The injuries and risks associated with internal deposition of the transuranic elements americium (Am), curium (Cm), and plutonium (Pu) can be mitigated by administration of radionuclide decorporation agents such as the calcium (Ca) and zinc (Zn) trisodium salts of diethylenetriamine pentaacetic acid (DTPA), which are the only agents approved by the US Food and Drug Administration (FDA) to treat internal contamination by transuranics. DTPA is a synthetic polyamino carboxylic acid with eight coordinate bond forming sites that can sequester metal ions and form highly stable DTPA-metal ion complexes. DTPA has wide industrial and medical applications including control of water hardness, medical imaging and decorporation of internally deposited radionuclides (34). Ca- and Zn-DTPA achieve therapeutic efficacy by exchanging the Ca and Zn cations with transuranic radionuclides in vivo to form higher-affinity complexes and promoting their elimination from contaminated individuals (140). The high aqueous solubility and low permeability of these compounds result in poor bioavailability after oral administration (124, 141, 142). Therefore, these compounds must be administered by slow intravenous (i.v.) push, i.v. infusion, or inhalation using a nebulizer (35). The administration of DTPA by i.v. or inhalation to those contaminated with transuranic isotopes requires skilled medical professionals, which imposes a logistical challenge in a mass casualty setting. As a consequence, there is an urgent need for new decorporation treatments that allow patients to self-administer in a timely manner after a nuclear disaster.

Contamination by radioactive Am, Pu and Cm can occur by inhalation, skin adsorption, or by entrance through a wound. The transfer of these radioactive elements from experimental deep puncture wounds to the systemic circulation is generally a slow, steady process and transfer rates ranging from 0.052 to 6.3% of the injected dose per day have been observed, depending on the radio-contaminants and the animal species (80). In contrast, the total body clearance of ^{14}C-labeled DTPA from rats 24 h after i.v. administration

has been reported to range from 94-100% with the half-life ranging from 18.5 to 31.8 min (79, 94). Comparison of the short half-life and rapid elimination of DTPA after i.v. injection to the slow introduction of radioactive actinide species into the bloodstream reveals a mismatch between the pharmacokinetics of DTPA and the biokinetic profiles of the actinides, which may limit the effectiveness of the currently available DTPA treatments.

Transdermal delivery of therapeutic agents provides many advantages over parenteral and oral routes such as more uniform plasma drug levels, a longer duration of action with a reduced dosing frequency, and improved patient compliance and comfort with ease of self-administration (72-74, 102). It is highly desirable to deliver decorporation agents including DTPA to the circulation at a zero-order rate to better match actinide biokinetic profiles and thus achieve optimal radionuclide decorporation over an extended duration. Due to its low partition coefficient (log P = -4.90) and high melting point (219-220ºC), DTPA is not a good candidate for transdermal delivery (73, 96). However, the penta-ethyl ester of DTPA, designated as C2E5, was designed and synthesized as a new radionuclide decorporation prodrug to overcome the limitations of the current DTPA treatments (31, 43). The structures of C2E5 as well as its potential degradation products and metabolites including DTPA tetra-ethyl ester (C2E4), DTPA tri-ethyl ester (C2E3), DTPA di-ethyl ester (C2E2), DTPA mono-ethyl ester (C2E1), and the fully de-esterified DTPA are shown in Figure 1. C2E5 possesses physicochemical properties suitable for transdermal delivery. It has a log P value of 3.3, a log D value of 2.4 at pH 7.0, its aqueous solubility is 3.0 mg/mL at pH 7.0, and it is a Newtonian liquid with a viscosity of 175 cP at 25ºC (44).

The aim of these studies was to develop C2E5 transdermal formulations and evaluate them for sustained delivery of DTPA and other active metabolites in vivo. Cream and ointment formulations were initially screened as potential C2E5 delivery vehicles, but the results showed that either C2E5 proved to be unstable in the matrices due to degradation or the C2E5 formulations underwent phase separation. C2E5 degradation in

buffered aqueous solution follows pseudo-first order kinetics and C2E5 is most stable at a pH of approximately 4.2 (44). Due to the high hydrolytic tendency of the C2E5 ester bonds in aqueous media, non-aqueous gel formulations were pursued to stabilize the moisture-labile C2E5 in the delivery vehicles. Many drugs for topical and transdermal drug delivery are moisture-sensitive and undergo degradation reactions with water (131). The major degradation pathway involved with moisture-sensitive drugs is hydrolysis followed by secondary degradation reactions such as polymerization and isomerization (129). In contrast to extensive research on traditional semisolid dosage forms such as creams, ointments and hydrogels, there are far fewer reports on the development of non-aqueous gel matrices intended for topical and transdermal drug delivery (126, 133-136). Ethyl cellulose is frequently used as a gelling agent for non-aqueous gel vehicles. A series of non-aqueous gels with 15 and 20% (% w/w) ethyl cellulose were prepared as topical formulations of naproxen (134). Lee and colleagues developed a non-aqueous gel with 3% to 10% (% w/w) ethyl cellulose dispersed in an ethanol/tricaprylin (40/60, w/w) mixture (135). Lisazo and coworkers heated ethyl cellulose and phthalate ester derivative mixtures to 180°C and formed a non-aqueous gel during the cooling process (136). The Heng group reported on non-aqueous gel matrices containing ethyl cellulose and Miglyol 840®, which is a mixture of propylene glycol dicaprylate and dicaprate, obtained by directly mixing the ethyl cellulose and Miglyol 840 at 60°C (23). The rheological, mechanical, wettability and spreadability properties of the ethyl cellulose/Miglyol 840 non-aqueous gels indicate that these matrices possess favorable attributes for transdermal and topical delivery (126, 138, 139). Here we report on the preparation and characterization of C2E5 non-aqueous gels including their physical and rheological properties, determination of the stability of C2E5 in the gel, in vitro release properties, and preliminary in vivo pharmacokinetics of the lead C2E5 non-aqueous gel formulation.

3.2 MATERIALS AND METHODS

3.2.1 Materials

Miglyol 840 was purchased from Sasol (Hamburg, Germany). Ethyl cellulose polymers, including ETHOCEL Std 7 FP Premium (EC7), ETHOCEL Std 10 FP Premium (EC10), and ETHOCEL Std 100 FP Premium (EC100) with an ethoxyl content of 48.0-49.5%, were gifts from Dow Chemical (Midland, MI, USA). C2E5 was prepared based on the Fischer esterification method by reacting DTPA with ethanol under reflux in the presence of a hydrochloric acid catalyst (44). Acetonitrile, trifluoroacetic acid, anhydrous ethanol, methanol, isopropyl alcohol, formic acid, iron (III) chloride hexahydrate, ammonium formate, tributylamine and acetic acid were purchased from VWR International (Radnor, PA) or Fisher Scientific (Fairlawn, NJ). Double-distilled water was obtained from a Milli-Q system (Millipore, Billerica, MA, USA).

3.2.2 Preparation of C2E5 Non-aqueous Gels

The C2E5 non-aqueous gels were prepared using the solvent evaporation method. The EC10 material was dried at 60°C for ~24 h before use in gel preparations. Pre-dried EC10 particles were initially dissolved in anhydrous ethanol (10% w/v of EC10 to ethanol) to form an EC10 stock solution. The C2E5 non-aqueous gel was prepared by mixing the EC10 stock solution, Miglyol 840 and C2E5 to form a homogenous solution, followed by removing ethanol under vacuum. When the gel was less than 102% of the theoretical weight, the C2E5 non-aqueous gels were transferred to a storage container under nitrogen and sealed with an airtight cap, covered with aluminum foil to protect from light, and stored at 4°C for later use.

The C2E5 concentration in these gel formulations was determined using a Shimadzu Prominence High Pressure Liquid Chromatography (HPLC) system equipped with an Alltech 3300 Evaporative Light Scattering Detector (ELSD). A reverse-phase gradient separation was performed using an Alltima C18 column (250 × 2.1 mm I.D., 5 µm) at 40°C and a flow rate of 0.25 mL/min. The solvents that comprised the mobile phase were water with 0.1% trifluoroacetic acid (A), acetonitrile (B), and isopropyl alcohol (C). The linear gradient for the mobile phase mixture (A:B:C) was from 94:4:2 to 25:50:25 over 35 min, followed by a change to 0:0:100 in 0.5 min and an equilibration phase of 0:0:100 for 9.5 min, and ending with a reversal to 94:4:2 in 0.5 min and an equilibration phase of 94:4:2 for 9.5 min. The ELSD was operated at 40°C with 1.9 L/min nitrogen gas flow. Triplicate injections for each sample of C2E5 non-aqueous gel dissolved in anhydrous ethanol were performed with a volume of 10 µL per injection, and the retention time of C2E5 was 26 min. Samples were held at ambient temperature during analysis and analyzed using a standard curve over a concentration range of 0.02–2.00 mg/mL which had a power regression fit of R^2 = 0.999. C2E5 non-aqueous gel samples stored at 4°C for 6 months were monitored for C2E5 degradation using this HPLC method.

Physical characterization, *in vitro* release testing and pharmacokinetic studies were performed with a formulation comprised of 20% EC10, 40% C2E5 and 40% Miglyol 840 prepared using the solvent evaporation method.

3.2.3 Differential Scanning Calorimetry (DSC)

The EC10 polymer particles and the C2E5 non-aqueous gel samples were analyzed using a TA Instruments DSC Model Q200 (Newcastle, DE, USA) under a nitrogen flow of 50 mL/min. Approximately 5 to 10 mg samples were heated in a sealed aluminum pan at a ramp rate of 10°C/min, cooled at a rate of 5°C/min, and subsequently heated at 10°C/min in

heat/cool/heat mode from -10°C to 160°C. The glass transition (T*g*), and melting (T*m*) temperatures in the third heating cycle were determined using TA Universal Software.

3.2.4 Scanning Electron Microscope (SEM) Imaging

The pre-dried EC10 polymer particles and C2E5 non-aqueous gel samples prepared by solvent evaporation method were observed and recorded using a Hitachi S-4700 scanning electron microscope at an accelerated voltage of 15kV. All images were taken at a scan rate of 100 millisec per line. The EC10 polymer particles and C2E5 non-aqueous gel samples were deposited directly over double-sided carbon tape and imaged without further treatment. The C2E5 non-aqueous gel samples were imaged on the stub which was tilted 45º toward the lower scanning election detector for better imaging results.

3.2.5 Rheological Measurements

A stress-controlled cone-and-plate rheometer (TA Instruments, Model AR-G2, Newcastle, DE, USA) with a cone of 40 mm in diameter and 1° cone angle at controlled temperatures of 25 ± 0.5°C and 32 ± 0.5°C was utilized to measure continuous shear rheometry of the non-aqueous gels with a formulation comprised of 20% EC10, 40% C2E5 and 40% Miglyol 840 prepared using the solvent evaporation method. The gel samples were carefully loaded to the lower plate to reduce shearing effects and equilibrated for 5 min at the designated temperatures prior to measurement. Fresh samples were used for each individual measurement, and triplicate measurements were performed for the formulation. Data are reported as mean ± S.D.

Continuous shear rheometry was obtained by changing the shear rate from 0.1 s^{-1} to 40 s^{-1} over a period of 300 s. The power law equation for simple steady shear (Equation 3-1) was used to fit the data obtained from the upward flow curves (27):

$$\tau = m\dot{\gamma}^n \quad \text{(Eq. 3-1)}$$

where τ = shear stress; $\dot{\gamma}$ = shear rate; m = consistency index; and n = flow behavior index. The estimated yield stress was derived by fitting the data using the Casson model described in Equation 3-2 (143):

$$\tau^{1/2} = \tau_y{}^{1/2} + (\eta\dot{\gamma})^{1/2} \qquad \text{for } \tau \geq \tau_y \quad \text{(Eq. 3-2)}$$

where τ_y = yield stress and η = creep viscosity. The square root of yield stress τ_y was obtained from the plot as the y-axis intercept when $\dot{\gamma}$ = 0.

3.2.6 *In Vitro* Release of C2E5 Non-aqueous Gel

An *in vitro* release study was carried out using a vertical diffusion cell system equipped with an autosampler (Hanson Microette Autosampling System, Hanson Research Co., USA) to evaluate the non-aqueous gel formulations comprised of 20% EC10, 40% C2E5 and 40% Miglyol 840 prepared using the solvent evaporation method. The area for permeation was 1.767 cm^2, and the receiver compartment volume was 7 mL. The receiver medium was 0.1 M phosphate buffer (pH 7.4) maintained at 32°C and continuously stirred at 400 rpm. A cellulose acetate membrane (25 mm in diameter, with a 0.45 µm pore diameter, Whatman®) was first treated by soaking in the receiving medium and then mounted and clamped between the receiver and donor compartments of the diffusion cells. Approximately 300 mg of C2E5 non-aqueous gel was loaded evenly on the surface of the cellulose acetate

membrane (n = 5) and covered with a glass disk to exclude air. One mL samples were removed from the receiver compartment at 0.5 h, 1 h, 2 h, 4 h, and 6 h which were replaced with an equal volume of fresh media.

The C2E5 content in the collected samples was determined by the HPLC method described above. The cumulative amount of C2E5 released per unit membrane area from the tested non-aqueous gel was plotted as a function of the square root of time and as a function of time. The Higuchi equation (Equation 3-3) dictates the drug release from semisolid dosage forms including creams, gels and ointments, and holds true when the released drug from the vehicle is below 30% (144, 145):

$$Q = 2C_{veh}\sqrt{\frac{Dt}{\pi}} \qquad (Eq. 3-3)$$

where Q = amount of drug released per unit area (mg/cm^2); C_{veh} = initial drug concentration (mg/cm^3) in the vehicle; D = apparent diffusion coefficient (cm^2/h); t = time (h); π = constant. The release rate constant k of C2E5 from the non-aqueous gel formulation was determined using a simplified form of the Higuchi equation (Equation 3-4):

$$Q = k\sqrt{t} \qquad (Eq. 3-4)$$

where k is the release rate constant which is determined from the slope of the cumulative amount of C2E5 released per unit membrane area from the non-aqueous gel versus the square root of time.

Fick's law (Equation 3-5) has been used as a simple model to describe the steady-state diffusion of drug through synthetic membranes and skin:

$$J_{ss} = \left(\frac{D * K_p}{h}\right) * A * C_{veh} \qquad (Eq.3-5)$$

where J_{ss} = steady-state flux (mg/h); D = drug diffusivity (cm^2/h); h= membrane thickness (cm); K_p = drug's membrane-vehicle partition coefficient; C_{veh} = initial drug concentration (mg/cm^3) in the vehicle; and A = surface area (cm^2). J_{ss} can be determined from the slope of the linear plot in the steady-state region of the cumulative amount of C2E5 permeated (mg) per unit diffusion surface (cm^2) versus a function of time.

Throughout the experiment the C2E5 concentration in the receptor compartment was kept below 30% of the solubility of C2E5 at pH 7.4, which is about 2.2 mg/mL at room temperature (44). Therefore, steady-state flux condition and sink condition were maintained for the duration of the experiment.

3.2.7 Absorption of C2E5 Administered as a Neat Oil or as a Non-aqueous Gel

All animal studies were conducted according to a protocol approved by the University of North Carolina at Chapel Hill Institutional Animal Care and Use Committee (IACUC). Ten-week-old adult female Sprague-Dawley (SD) rats weighing 200-300 g were used in these studies (Charles River Labs, Raleigh, NC). Food and water were provided ad libitum. The animal room was kept at a controlled temperature on a 12 h/12 h light/dark cycle (light exposure from 7 AM to 7 PM). For the duration of the study, the rats were individually housed in metabolic cages until euthanasia at 24 h after neat C2E5 oil or C2E5 gel application.

In all animals the dorsal skin between the cervical vertebrae and anterior thoracic vertebrae of SD rats was carefully clipped prior to drug application to remove hair. C2E5 non-aqueous gel was applied at a C2E5 dose of 200 mg/kg to a 2 cm x 3 cm region using a

cotton swab. For comparison, neat C2E5 oil (200 mg/kg) was applied using a 1 mL syringe to the same size area on a control group of rats. For each rat, the mass of the drug and applicator was recorded before and after application with the difference being the delivered dose. Finally, a jacket with a dermal insert (VWR International, Radnor, PA) was placed on the rats to protect the applied treatments. Blood samples (0.4 mL) were collected from the tail vein using SurFlash® polyurethane i.v. catheters (Terumo, Somerset, NJ) at either before or 0.5 h after treatment, and then at 1 h, 2 h, 4 h, 8 h, 12 h and 24 h after treatment. The collected samples were immediately transferred from the syringes into pre-chilled sampling tubes containing 5 mg sodium fluoride and 4 mg potassium oxalate (BD Vacutainer Product # 367921). The tubes were inverted 8 times per manufacturer's recommendation, and centrifuged (1300 x g for 10 min at 4°C). Plasma samples were then portioned into two 1.7 mL Eppendorf tubes, which contained an equal amount of a 20% formic acid aqueous solution. These tubes were immediately vortexed and placed on dry ice until transfer to storage at -80°C until analysis. The animals were transferred to individual housing in metabolic cages after C2E5 treatment. Animals were euthanized 24 h after C2E5 gel or neat C2E5 oil application. The animals were observed during the study period and the body weight of each animal was recorded at pre-dose and prior to necropsy.

An LC/MS/MS method was developed for the analysis of C2E5 and metabolites except for the fully de-esterified metabolite, DTPA, in these samples. Acidified plasma samples (100 µL) were first treated with 25 µL of 13C-C2E5 stable-label internal standard (1000 ng/mL), followed by precipitation with acetonitrile (400 µL). The supernatant (400 µL) was removed, evaporated to dryness and the residue was reconstituted with 500 µL of 85/15/0.1% water/acetonitrile/formic acid. A 10 µL injection was used for LC/MS/MS analysis. Reverse-phase chromatography was performed at 0.3 mL/min on a YMC® ODS-AM C18 (100 x 2 mm, 3 µm) column with mobile phases A (0.1% formic acid in water) and B (0.1% formic acid in acetonitrile) using a 10 min gradient (isocratic at 13% mobile phase B

for 1 min, linear gradient to 50% mobile phase B at 6 min, linear gradient to 60% mobile phase A at 6.5 min, linear gradient to 90% mobile phase B at 8 min, return to initial 13% mobile phase B at 8.1 min, and equilibrate at 13% mobile phase B until 10 min). After separation by liquid chromatography, the analytes and internal standard were detected on a triple quadrupole mass spectrometer using Heated Electrospray Ionization (HESI-II) (Thermo Scientific) in the positive-ion mode. Suitable reference standard material was available to provide reliable results for C2E5, C2E4, and C2E2. Although reference standard material was not available for C2E3 and C2E1, these analytes were present as trace impurities in the reference standards for C2E5, C2E4, and C2E2. The assumption of response factors for C2E3 and C2E1 equal to those of the reference standards afforded an estimate of the concentrations of C2E3 and C2E1 in calibration standards; this allowed the generation of calibration curves for C2E3 and C2E1 that were used to estimate the levels of these analytes in samples. Due to lack of pure internal standards for C2E3 and C2E1, the plasma concentrations of C2E3 and C2E1 in the samples were considered as estimates. The lower limit of quantification (LLQ) for C2E5, C2E4, C2E3, C2E2 and C2E1 were determined to be 5.0 ng/mL, 10.0 ng/mL, 1.0 ng/mL, 10.0 ng/mL and 5.0 ng/mL, respectively.

For detection of DTPA, acidified plasma samples (100 µL) were first treated with 50 µL of 2 mM iron (III) chloride hexahydrate, followed by addition of 400 µL of 13C-DTPA stable-label internal standard (100 ng/mL in 0.1% acetic acid in acetonitrile). This solution was vortexed for 5 min and then centrifuged at 3,000 rpm for 10 min. The supernatant (350 µL) was removed, evaporated to dryness and reconstituted with 100 µL of 0.1% aqueous acetic acid. A 10 µL aliquot of the reconstituted sample was used for LC/MS/MS analysis. The highly polar nature of DTPA required the incorporation of ion-pairing chromatography to produce acceptable LC peak shape and retention. Mobile phase A was 90:10 water:methanol with 1 mM ammonium formate and 1 mM tributylamine and mobile phase B

was 50:50 acetonitrile:(5:95 water:methanol) with 1 mM acetic acid and 1 mM tributylamine. A 10 min gradient was used to afford separation (isocratic at 5% mobile phase B for 1 min, linear gradient to 80% mobile phase B at 7 min, linear gradient to 90% mobile phase B at 7.1 min, maintaining at 90% mobile phase B through 8 min, return to initial 5% mobile phase B at 8.1 min, and equilibrate at 5% mobile phase B until 10 min). Reverse-phase chromatography was performed at 0.3 mL/min on an Advanced Materials Technology HALO® Phenyl-Hexyl column (50 x 2.1 mm, 2.7 µm). The analyte and internal standard were detected on a triple quadrupole mass spectrometer using HESI-II in the negative-ion mode. The LLQ for DTPA was determined to be 10.0 ng/mL.

For C2E5 and its metabolites in the pharmacokinetic samples, plasma concentrations below the limit of quantification were labeled as not detected (ND) and assigned a value of zero for the area under the curve (AUC) analysis. The AUCs were calculated using the trapezoidal method.

3.2.8 Statistical Analyses

The concentrations of C2E2 and C2E3 in plasma samples collected at different times from the two C2E5 dosage forms (neat oil and non-aqueous gel) were compared by unbalanced two-way analysis of variance (two-way ANOVA). Analysis of the calculated exposure to C2E3 and C2E2 was by two-tailed t-test. All measurements are expressed as mean ± standard deviation (S.D.). The level of significance was set at $p < 0.05$.

3.3 RESULTS

3.3.1 Preparation of C2E5 Non-aqueous Gels

The solvent evaporation method was used to prepare the C2E5 non-aqueous gel formulations. To maximize C2E5 loading in the gel and achieve desirable rheological and mechanical properties, a formulation that contained 40% C2E5, 20% EC10 and 40% Miglyol 840 was prepared and yielded a slightly yellow translucent gel which was determined to have a density of 1.02 g/cm^3. Based on the HPLC analysis, the C2E5 content in non-aqueous gel samples stored at 4°C for 6 months contained 98.2% of the C2E5 content in a freshly prepared C2E5 non-aqueous gel, with C2E4 being as the main degradant.

3.3.2 Thermal Analysis by DSC

The DSC thermogram of pre-dried EC10 (Fig. 2.2A) showed one minor endothermic peak appearing at 63°C and one major endothermic peak at 120°C. The endothermic peak at 120°C is the EC10 glass transition temperature (128). The endothermic peak at 63°C can be assigned to glyoxal, an impurity in ethyl cellulose (129). However, further investigation is necessary for confirmation of this peak. The DSC thermogram of the C2E5 non-aqueous gel (Fig. 3.2) containing 20% EC10, 40% C2E5 and 40% Miglyol 840 prepared using the solvent evaporation method showed no prominent endothermic peaks in the range from -10°C to 160°C. Complete dissolution of the EC10 in ethanol prior to gel formation eliminated the EC10 glass transition endothermic peak at 120°C. The impurity in EC10 which showed the endothermic peak at 63°C on the DSC thermogram of pre-dried EC10 could possibly have been dissolved in ethanol and later removed during the solvent evaporation process, either through direct evaporation (the boiling point of glyoxal is 51°C) or by formation of an

azeotrope with ethanol. The residual water content in the gel components could also have been effectively removed during the solvent evaporation process by formation of an azeotrope with ethanol.

3.3.3 Scanning Electron Microscope (SEM) Imaging

Figure 2.3 shows the SEM images of pre-dried EC10 particles and the C2E5 non-aqueous gel prepared by direct mixing method (formulation N-7 in Chapter 2). In Figures 2.3A and 2.3B, the SEM images showed tightly clumped EC10 particles with a relatively uniform size distribution averaging 1 to 5 μm in length. The SEM images of the C2E5 non-aqueous gel (Figure 2.3C and 2.3D) displayed a relatively smooth gel surface that was embedded with small particles. The small particles were determined to be residual EC10 material that failed to be completely solubilized by Miglyol 840 and C2E5 during the gel preparation process. This assessment is supported by the DSC spectrum of the C2E5 non-aqueous gel in which a minor EC10 glass transition endothermic peak appeared at 120°C. The C2E5 non-aqueous gel comprised of 20% EC10, 40% C2E5 and 40% PGD prepared by the solvent evaporation method exhibited a much smoother gel surface in SEM images (Figures 3.3A and 3.3B) which indicated that there were no particle present on the gel surface. This was also consistent with the absence of an ethyl cellulose glass transition endothermic peak at 120°C on the DSC thermogram.

3.3.4 Rheological Measurement Results

Rheograms derived from continuous shear rheometry (Figure 3.4) demonstrated that the C2E5 non-aqueous gel is a typical shear-thinning system at both 25°C and 32°C. The shear stress vs. shear rate rheogram exhibits a convex shape and a hysteresis loop. The

rheological properties of the 40% C2E5 non-aqueous gel at different temperatures are summarized in Table 3.1. The flow behavior index values (n) were below 1 for both the 25°C and 32°C measurements, indicating a shear-thinning gel structure under each of these temperature conditions (146). Yield stress and hysteresis area are parameters representing the rigidity and cohesion between the molecules forming a three-dimensional gel structure and the extensiveness of this three-dimensional gel structure (147, 148).

3.3.5 *In Vitro* Release of C2E5 Non-aqueous Gel

A plot of the cumulative amount of C2E5 released per unit membrane area versus the square root of time, for the lead non-aqueous gel (20% EC10, 40% C2E5 and 40% Miglyol 840), is presented in Figure 3.5. The cumulative amount of C2E5 released per unit membrane area from the lead non-aqueous gel versus the square root of time yielded a linear plot with $y = 1.57x - 0.78$ and $R^2 = 0.996$. The amounts of C2E5 released after 6 h from the 5 individual *in vitro* release runs ranged from 2.89 mg/cm^2 to 3.33 mg/cm^2, with an average value of 3.11 ± 0.17 mg/cm^2 (coefficient of variance = 5.5%). The average release rate constant k and average steady-state flux J_{ss} per unit area of the 40% C2E5 non-aqueous gel were determined to be 1.57 ± 0.09 mg/cm^2/h$^{0.5}$ and 0.556 ± 0.031 mg/cm^2/h, respectively, with both having a coefficient of variance of 5.6%. For each individual run, an acceptable linear regression fit was achieved for the release rate constant k per unit area ($R^2 \geq 0.994$) and the steady-state flux J_{ss} per unit area ($R^2 \geq 0.969$).

3.3.6 Absorption of C2E5 Administered as a Neat Oil or as a Non-aqueous Gel

Following topical application of either the neat C2E5 oil or the 40% C2E5 non-aqueous gel, the principal circulating metabolites detected in plasma were C2E3 and C2E2.

The concentrations of C2E3 and C2E2 detected in the rat plasma samples plotted versus time for the neat C2E5 oil and the 40% C2E5 non-aqueous gel groups are presented in Figure 3.6 and Figure 3.7. Two-way ANOVA showed that C2E5 dosage form had a significant effect on the plasma concentration of both C2E2 ($F_{(1,36)}$ = 13.33, $p < 0.001$) and C2E3 ($F_{(1,36)}$ = 6.91, $p < 0.05$), the time the plasma was sampled was not a significant effect for either metabolite (C2E2, $F_{(7,36)}$ = 1.06, p = 0.41 and C2E3, $F_{(7,36)}$ = 0.84, p = 0.56), and no interaction between dosage form and time was observed (C2E2, $F_{(7,36)}$ = 0.84, p = 0.56 and C2E3, $F_{(7,36)}$ = 1.04, p = 0.42). The pharmacokinetic parameters of C2E3 and C2E2 after application of neat C2E5 oil or 40% C2E5 non-aqueous gel at 200 mg/kg dose (n=4) are shown in Table II. We observed a trend for increased exposure to the metabolites C2E3 and C2E2 following C2E5 application as a non-aqueous gel compared with application as the neat oil; however, this trend did not reach statistical significance for either metabolite alone (AUC_{C2E2}, p = 0.073 and AUC_{C2E3}, p = 0.087; both two-tailed t-test). Enhancement ratios based on the AUCs for C2E3 and C2E2 were determined to compare the AUC obtained from the 40% C2E5 non-aqueous gel group to the neat C2E5 oil group.

There was only two plasma samples in which C2E5 was detected with a concentration above the LLQ among the 56 samples, one from the neat C2E5 oil group (28.4 ng/mL at 2 h) and one from the C2E5 non-aqueous gel group (7.2 ng/mL at 24 h). There were five plasma samples in which C2E4 was detected with a concentration above the LLQ among 56 samples, three from the neat C2E5 oil group (13.5 ng/mL at 0.5 h, 52.7 ng/mL at 2 h and 45.1 ng/mL at 24 h) and two from the C2E5 non-aqueous gel group (59.9 ng/mL at 1 h and 83.8 ng/mL at 2 h).

C2E3 and C2E2 species were consistently detected in the plasma samples from both groups throughout the experimental period with the C_{max} values ranging from 85.3 ng/mL to 485.4 ng/mL for C2E3, and from 17.4 ng/mL to 412.6 ng/mL for C2E2, indicating that C2E3 and C2E2 are stable C2E5 metabolites *in vivo*. The concentrations of C2E3 and

C2E2 reported in the rat plasma samples versus time figures showed a sustained release profile from transdermal neat C2E5 oil and C2E5 non-aqueous gel formulations. Average steady-state concentrations (C_{ss}) for both C2E3 and C2E2 were between 100 ng/mL and 200 ng/mL for the C2E5 non-aqueous gel group and between 20 ng/mL and 80 ng/mL for the neat C2E5 oil group. Overall systemic exposures to C2E3 and C2E2 were approximately 2.9-fold and 4.2-fold (based on $AUC_{0\text{-}24h}$) higher for the C2E5 non-aqueous gel group compared to the neat C2E5 oil group.

There was no C2E1 detected above the quantification limit in any rat plasma samples for either the neat C2E5 oil group or the C2E5 non-aqueous gel group during the experimental period. DTPA was frequently detected in the plasma samples at time points after 4 h post-dosing for both the neat C2E5 oil group and the C2E5 non-aqueous gel group. Most of the detected DTPA plasma concentrations were in the range of 10 ng/mL to 30 ng/mL, which is just above the LLQ of DTPA (10 ng/mL). The maximum DTPA concentration detected in plasma in the neat C2E5 oil group was 61.4 ng/mL, compared with 692.9 ng/mL in the C2E5 non-aqueous gel group.

3.4 DISCUSSION

Non-aqueous gel formulations have been a useful vehicle for moisture-sensitive drugs for topical and transdermal application (126, 133-136). Critical components for the successful development of a semisolid product for topical and transdermal applications include the stability of the active pharmaceutical ingredient (API) in the delivery matrix, product uniformity and the release profile of API from the delivery matrix. In this study, we report on the development and characterization of a non-aqueous gel formulation that stabilizes the hydrolysis-prone API, enhances its percutaneous permeation flux and improves its pharmacokinetic profile following topical application to rats.

Candidate non-aqueous gel formulations showed improved stability of C2E5 under various storage conditions when compared with the neat API and other tested delivery vehicles, such as creams and ointments (149, 150), suggesting a clear benefit of the ethyl cellulose based non-aqueous gel for this moisture-sensitive compound. The enhanced stability profile of C2E5 in the non-aqueous gel matrix is probably due to decreased interactions with the hydroxyl groups on the ethyl cellulose polymer chains. These hydroxyl groups are not readily available to interact with other molecules compared to the hydroxyl groups in small molecule due to steric and rotational hindrance. The use of Miglyol 840 neutral oil as a dispersion medium also contributes to the enhanced stability of C2E5 in the gel matrix because Miglyol 840 is non-hygroscopic, possesses high stability against oxidation and contains no free hydroxyl groups (23).

Modification of the published direct mixing method for gel preparation (23), by using anhydrous ethanol to dissolve the ethyl cellulose before forming the gel and then evaporating the ethanol from the gel mixture, resulted in a significant improvement in gel uniformity. Although the solvent evaporation method is a commonly used technique for making films, microspheres and solid dispersions (151-153), to our knowledge this method has not been reported previously for preparation of ethyl cellulose based non-aqueous gels. To minimize the amount of solvent used in the gel preparation, EC7 and EC10 were selected because much more ethanol is needed to dissolve EC100 than for equal amounts of EC7 or EC10. Our method of gel preparation requires simple evaporation of the solvent and is suitable for scale up, with ethanol content in the gels readily reduced to below 2% of gel weight. The solvent evaporation method was successfully scaled up to prepare 400 g of C2E5 non-aqueous gels in one batch. Any residual ethanol present in the gel system would not interact with the C2E5 molecules and might possibly retard its hydrolysis. Ethanol is approved for human use in commercial topical and transdermal products at relatively high concentrations as a basic component and can act as a permeation enhancer by changing

the characteristics of the skin (126, 154). A C2E5 formulation screening study was carried out and phase separation was observed in gels with low EC content (< 10%) and particularly in gels with lower molecular weight EC chains. This phase separation may be due to a decrease in the interactions between the gel matrix and the C2E5 dissolved in it (data not shown). A C2E5 non-aqueous gel formulation comprised of 20% EC10, 40% C2E5 and 40% Miglyol 840 was chosen as a candidate formulation for further physical characterization and *in vivo* pharmacokinetic evaluation.

The stability study with the 40% C2E5 non-aqueous gel showed that less than 2% of C2E5 had degraded after being stored at 4°C for 6 months, suggesting an acceptable stability profile of this formulation. As demonstrated by the DSC thermograms, the slightly yellow translucent C2E5 non-aqueous gel possessed acceptable uniformity. This was a result of EC10 being completely solubilized in ethanol before incorporation into the gel matrix and thus eliminating the problems related to residual EC particulates encountered when using the direct mixing method.

The rheological and mechanical properties of the non-aqueous gel matrices containing ethyl cellulose and Miglyol 840 were investigated in detail by the Heng group (23). The rheological properties of the C2E5 non-aqueous gel comprised of 20% EC10, 40% C2E5 and 40% Miglyol 840 (Table I) exhibited characteristics and flow patterns similar to non-aqueous gels comprised of ethyl cellulose and Miglyol 840, suggesting that an adequate adhesion force to the skin surface for prolonged periods could be maintained, a critical property for the sustained delivery of drug substance from the gel (155). Other characteristics, such as a 36.6% decrease in viscosity from 176.6 (Pa s) to 129.3 (Pa s) and a 116.8% decrease in hysteresis area with a temperature increase from 25°C to 32°C, are good indicators that the gel is suitable for application on human skin with a surface temperature of 32-34°C. The *in vivo* pharmacokinetic studies using this gel formulation confirmed the predictions based on these physical measurements; the gel spread easily

during application and remained at the application site for the entire study. In contrast, neat C2E5 oil presented a challenge for application to the skin and retention at the application site due to its lower viscosity.

In vitro release testing is widely used to assess content uniformity and drug release from semisolid products, and can also be used to compare performance across different batches and after storage or changes in the manufacturing process (156, 157). Although transdermal delivery of C2E5 to the systemic circulation is a multistep process, *in vitro* release results suggest that C2E5 is readily released from the non-aqueous gel matrix and the steady state flux (0.556 ± 0.031 mg/cm^2/h) associated with this release is expected provide the required sustained concentration of drug in plasma. The narrow distribution of the release rate constant (1.57 ± 0.09, coefficient of variance = 5.6%) confirmed the optimal content uniformity of the 40% C2E5 non-aqueous gel prepared by solvent evaporation method.

Pharmacokinetic data obtained from *in vivo* studies confirmed our observations from the *in vitro* release testing, with metabolites of C2E5 detected in plasma throughout the collection period. Additionally, an improved plasma pharmacokinetic profile for drug released from the C2E5 non-aqueous gel compared with the neat C2E5 oil suggests that Miglyol 840, a major component of the gel, perhaps along with residual ethanol in the gel, are working as permeation enhancers (126, 137, 154). The enhanced ratios of systemic exposure to major C2E5 metabolites (C2E3 and C2E2) with C2E5 non-aqueous gel were greater than those observed with neat C2E5 oil. The pharmacokinetic data also support our hypothesis that the mismatch between the biokinetics of transuranic contaminants and the pharmacokinetics of DTPA used to treat contamination could be overcome using a transdermal prodrug strategy.

C2E5 and C2E4 were only detected in concentrations above their respective LLQs in less than 10% of all samples; detection of C2E4 suggests that it is a direct metabolite of C2E5 *in vivo*, generated by a stepwise de-esterification process involving esterases in the

rat skin and plasma (116, 117). C2E2 and C2E3 were observed as the principal metabolites detected in circulation throughout the 24 hour study period, matching the findings of the C2E5 *in vitro* metabolism study (116, 117). C2E1 was not detected above the LLQ in any plasma samples throughout the study, but is likely present transiently resulting from the stepwise de-esterification of C2E5 to DTPA. Detection of DTPA at low concentrations, close to the 10 ng/mL LLQ, was not unexpected as DTPA has a short half-life ranging from 18.5 to 31.8 min (79, 94).

In addition to DTPA, other metabolites, such as C2E3, C2E2 and C2E1, may effectively sequester transuranic radionuclides and form stable complexes. For example, ^{241}Am, an abundant transuranic radionuclide, forms complexes with various chelators, including DTPA and other molecules structurally similar to C2E3 and C2E2, with stability constants ranging from 10.7 M^{-1} to 24.0 M^{-1} (119). Although stability constants for americium binding to C2E5 metabolites are not known, the binding of Gd^{3+} with DTPA mono-propyl ester and DTPA di-propyl ester (compounds analogous to C2E1 and C2E2) are reported to be 18.91 M^{-1} and 16.30 M^{-1} (118). Because gadolinium is viewed as a biochemical analogue of americium and Gd^{3+} ion is structurally very similar to $^{241}Am^{3+}$ (158, 159), comparable binding constants and thermodynamic stability can be expected for the binding of $^{241}Am^{3+}$ with C2E1 and C2E2 *in vivo*. Furthermore, studies in americium-contaminated rats demonstrated that C2E5 administered orally enhanced ^{241}Am decorporation (44, 45).

3.5 CONCLUSIONS

The penta-ethyl ester of DTPA (C2E5) was incorporated into a non-aqueous gel comprised of ethyl cellulose and Miglyol 840 using the solvent evaporation method, and was characterized by thermal and rheological analysis and in vitro release. A superior pharmacokinetic profile of C2E5 metabolites, including DTPA, was achieved when C2E5

was administered as a non-aqueous gel as opposed to a neat oil, perhaps as a result of permeation enhancement by Miglyol 840 and ethanol. These findings demonstrate that transdermal delivery of a chelator prodrug is a viable approach for delivering DTPA and other chelating agents to the circulation as a potential treatment of transuranic radionuclide contamination, and provide additional understanding of the properties of non-aqueous gel formulations as well as their utility in applications requiring transdermal and topical delivery of moisture-sensitive drugs.

Table 3.1 Rheological properties of a 40% C2E5 non-aqueous gel at different temperatures.

Temperature (ºC)	Flow behavior index, *n* (mean ± SD)	Consistency index, *m* (Pa s^n) (mean ± SD)	Apparent viscosity* (Pa s) (mean ± SD)	Yield stress (Pa) (mean ± SD)	Hysteresis area (Pa s^{-1}) (mean ± SD)
25	0.407 ± 0.013	691 ± 17	177 ± 1	663 ± 18	16.7 ± 0.7
32	0.462 ± 0.005	446 ± 13	129 ± 3	381 ± 14	7.71 ± 0.28

* Apparent viscosity at a shear rate of 10 s^{-1}.

Table 3.2 Pharmacokinetic parameters of C2E3 and C2E2 after application of neat C2E5 oil or 40% C2E5 non-aqueous gel at a C2E5 dose of 200 mg/kg (n=4) and the enhancement ratio of C2E3 and C2E2 based on the formula $AUC_{0\text{-}24h\ (C2E5\ gel)}/AUC_{0\text{-}24h\ (Neat\ C2E5)}$.

Treatment	C2E3				C2E2			
	C_{max} (mean ± SD, μg/mL)	T_{max} (mean ± SD, h)	$AUC_{0\text{-}24h}$ (mean ± SD, h*μg/mL)	Enhancement ratio ($AUC_{0\text{-}24h\ (C2E5\ gel)}$ / $AUC_{0\text{-}24h\ (Neat\ C2E5)}$)	C_{max} (mean ± SD, μg/mL)	T_{max} (mean ± SD, h)	$AUC_{0\text{-}24h}$ (mean ± SD, h*μg/mL)	Enhancement ratio ($AUC_{0\text{-}24h\ (C2E5\ gel)}$ / $AUC_{0\text{-}24h\ (Neat\ C2E5)}$)
Neat C2E5 oil at 200 mg/kg	0.181 ± 0.097	9.6 ± 10.9	1.21 ± 0.16		0.059 ± 0.041	17.0 ± 8.2	0.660 ± 0.351	
				2.9				4.2
40% C2E5 non-aqueous gel at 200 mg/kg	0.281 ± 0.159	4.5 ± 4.0	3.52 ± 2.26		0.203 ± 0.161	4.5 ± 2.5	2.75 ± 1.89	

C_{max}: maximum plasma concentration during 0 to 24 h period; T_{max}: time of maximum plasma concentration during 0 to 24 h period; $AUC_{0\text{-}24h}$: area under the curve during 0 to 24 h period.

Fig. 3.1 Structures of DTPA, the prodrug C2E5 and its metabolites.

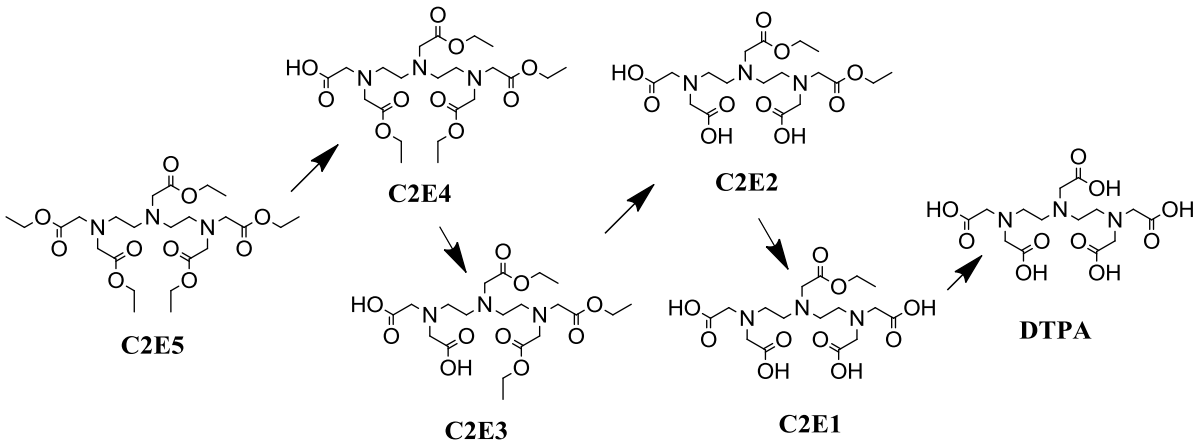

Fig. 3.2 DSC spectrum of C2E5 non-aqueous gel comprised of 20% EC10, 40% C2E5 and 40% Miglyol 840 by solvent evaporation method from -10°C to 160°C at a scanning rate of 10°C min^{-1}.

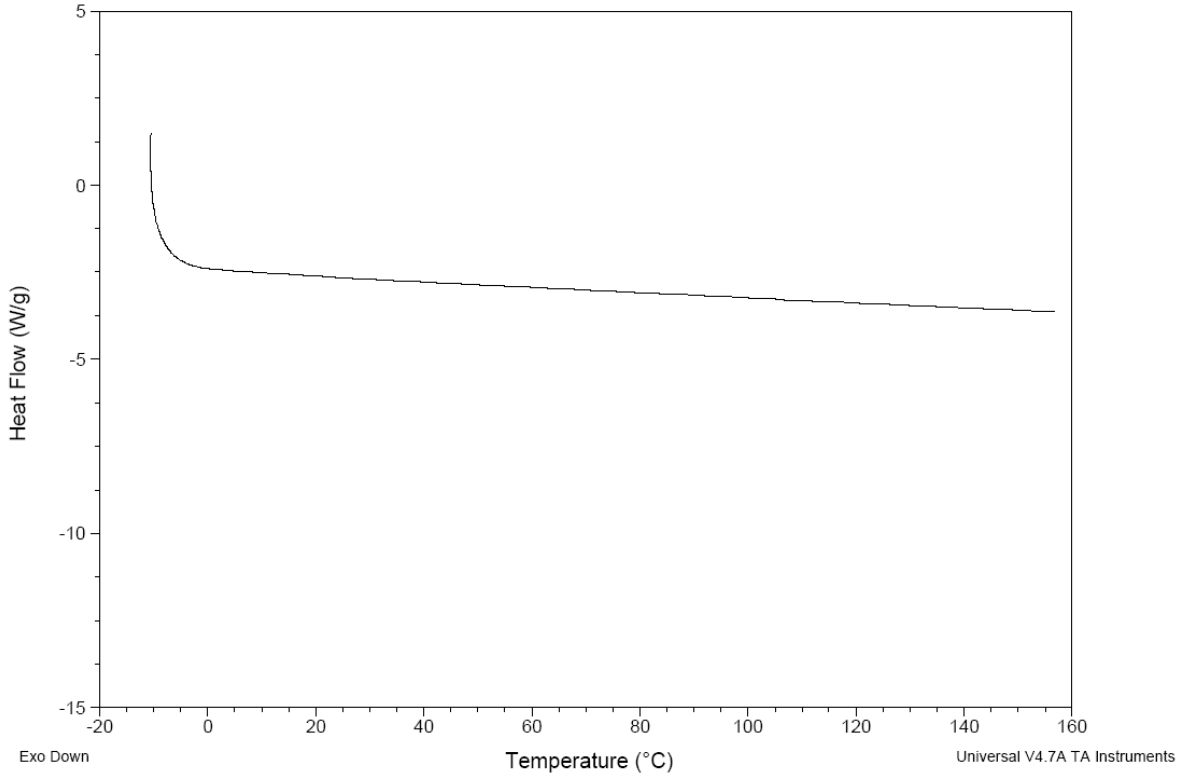

Fig. 3.3 SEM images of (A–B) C2E5 non-aqueous gel comprised of 20% EC10, 40% C2E5 and 40% Miglyol 840 by solvent evaporation method at three magnifications (~500 X and 3,000 X).

A

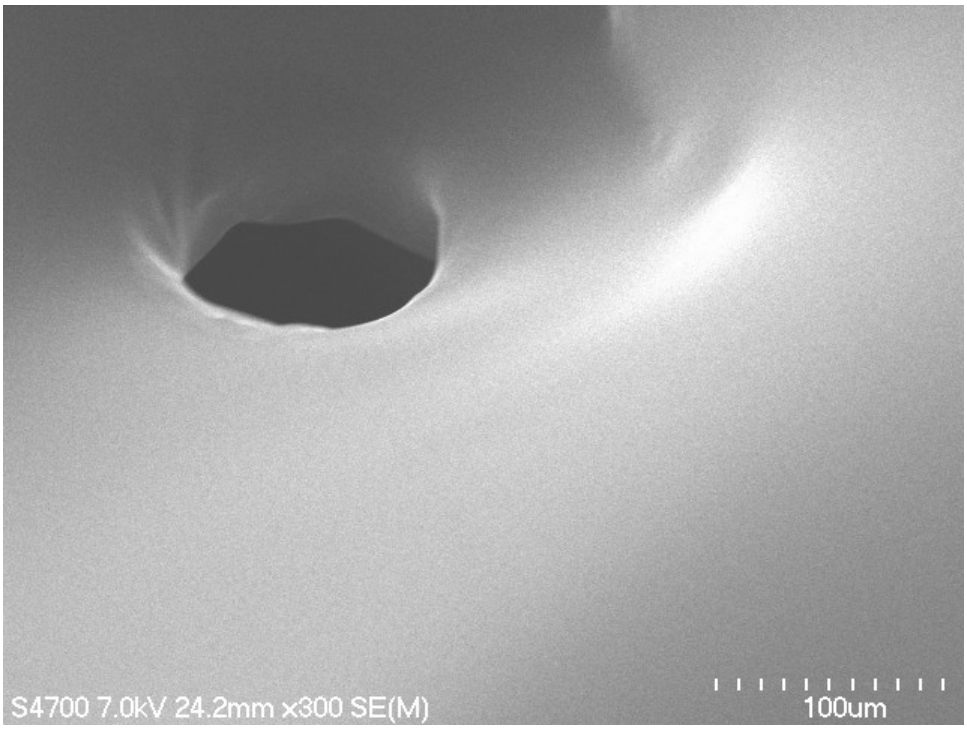

B

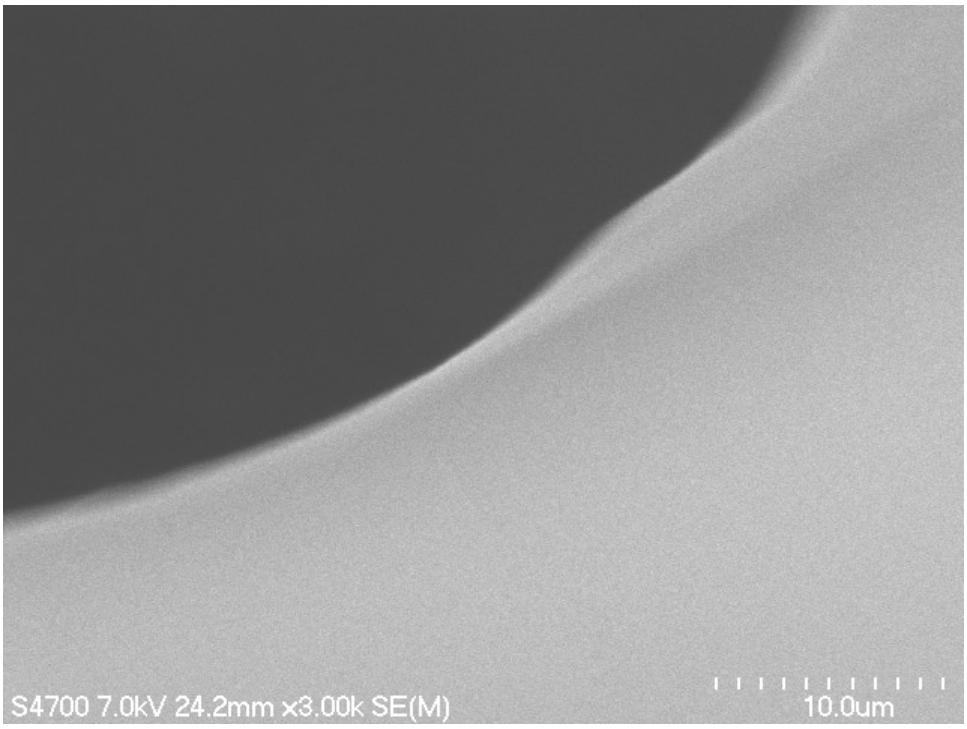

Fig. 3.4 Continuous shear rheogram showing shear rate vs. shear stress at 25 °C and 32 °C of C2E5 non-aqueous gel comprised of 20% EC10, 40% C2E5 and 40% Miglyol 840 prepared using the solvent evaporation method.

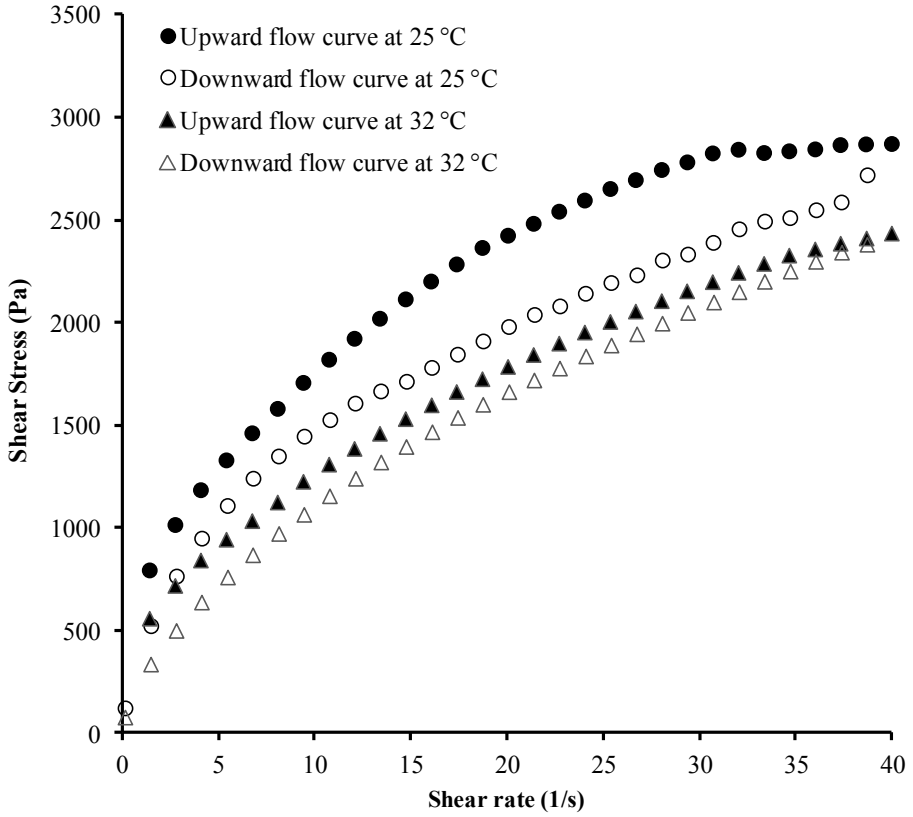

Fig. 3.5 Relationship between square root of time and cumulative amount of C2E5 released through a cellulose membrane into 0.1 M phosphate buffer after application of C2E5 non-aqueous gel (n=5). The C2E5 non-aqueous gel consisted of 20% EC10, 40% C2E5 and 40% Miglyol 840. The release rate constant k is determined from the slope of the cumulative amount of C2E5 released per unit membrane area from the tested non-aqueous gel versus square root of time defined in Eq. 3-4.

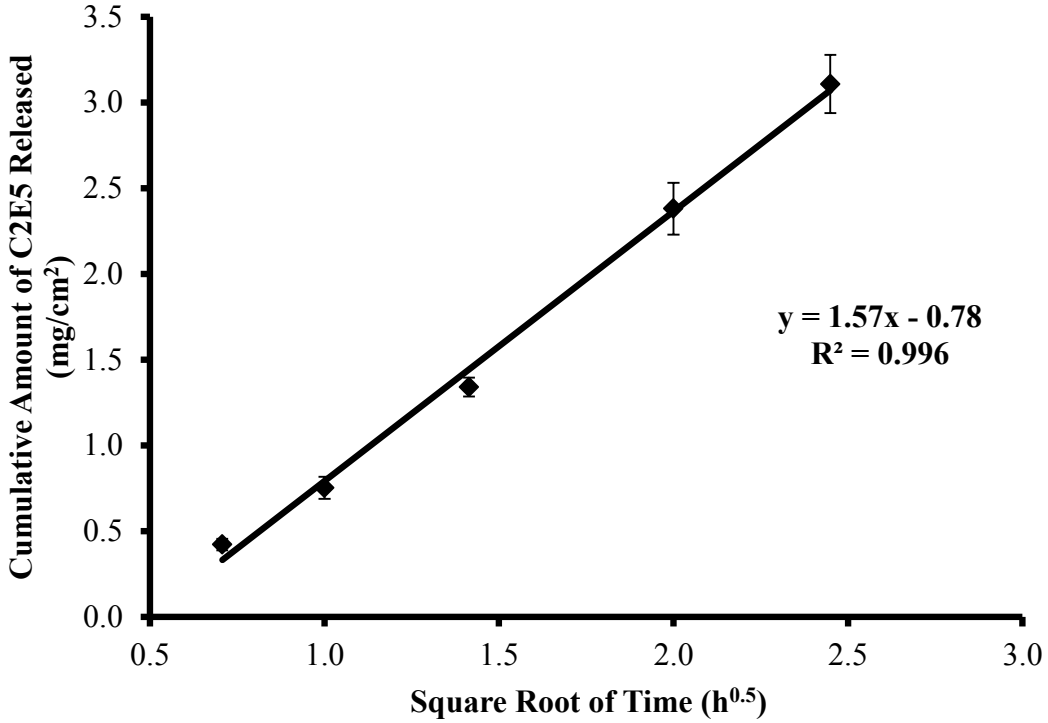

Fig. 3.6 Concentration of C2E3 detected in rat plasma *versus* time after topical administration of the neat C2E5 oil and the 40% C2E5 non-aqueous gel (mean ± SD) (n=4).

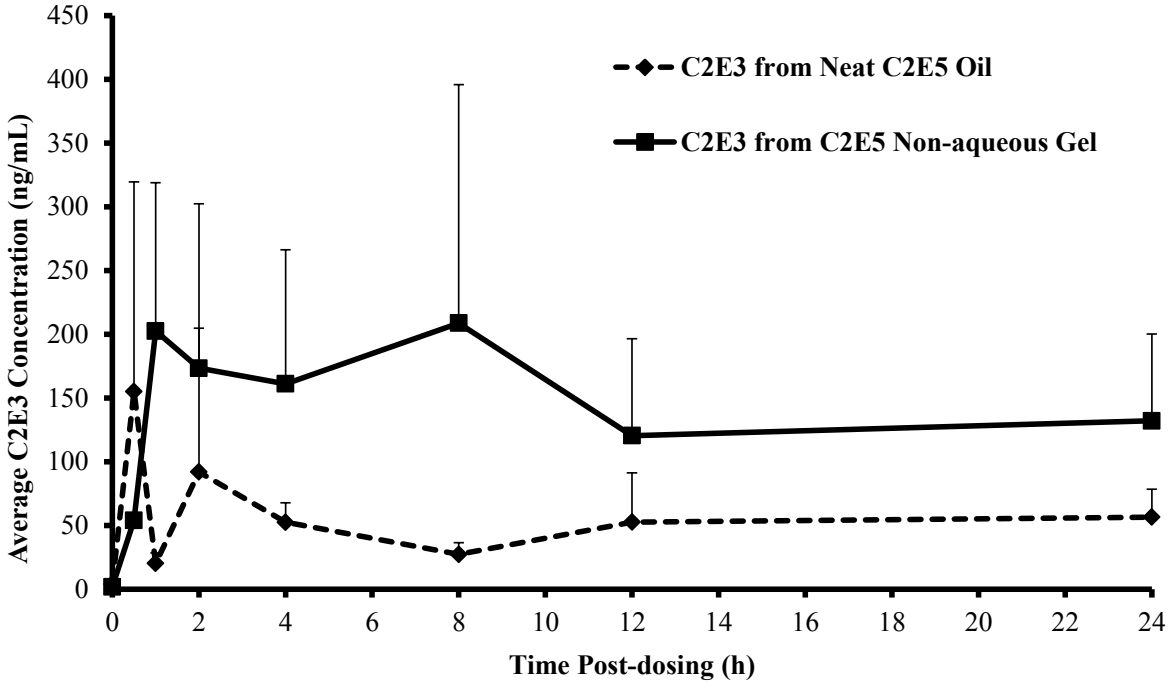

Fig. 3.7 Concentration of C2E2 detected in rat plasma *versus* time after topical administration of the neat C2E5 oil and the 40% C2E5 non-aqueous gel (mean ± SD) (n=4).

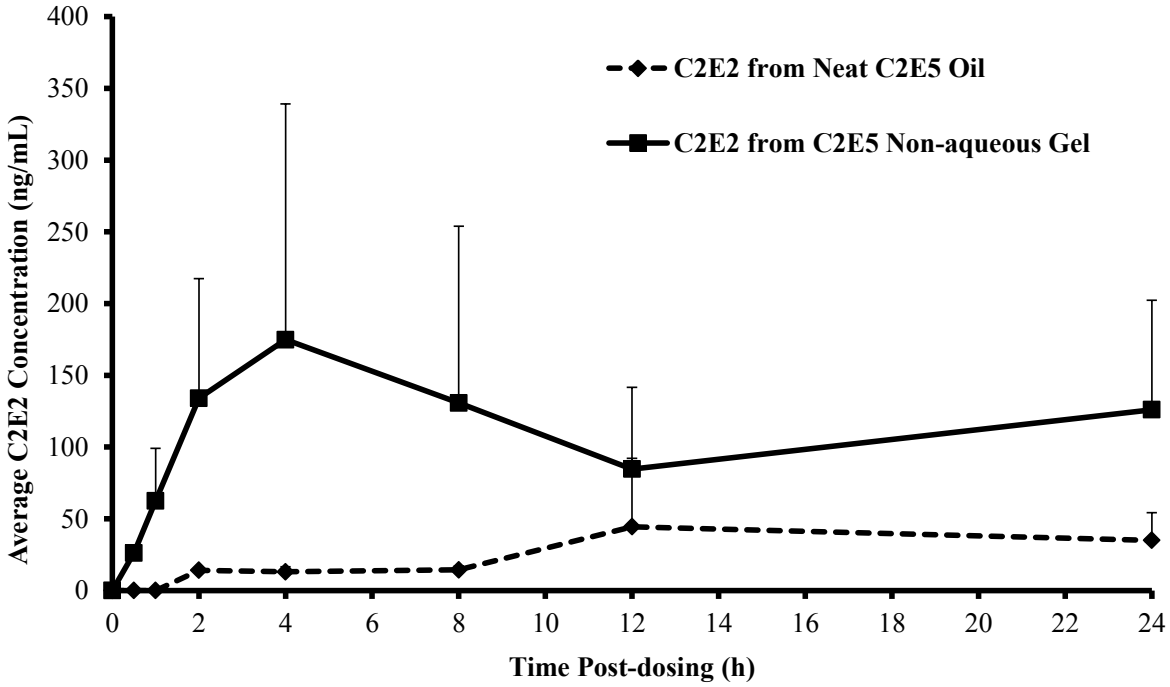

CHAPTER 4: RADIONUCLIDE DECORPORATION: MATCHING THE BIOKINETICS OF ACTINIDES BY TRANSDERMAL DELIVERY OF PRO-CHELATORS

The threat of nuclear terrorism by the deliberate detonation of a nuclear weapon or radiological dispersion device ('dirty bomb') has made emergency response planning a priority. The only FDA-approved treatments for contamination with isotopes of the transuranic elements Am, Pu and Cm are the Ca and Zn-salts of diethylenetriamine pentaacetic acid **(**DTPA). These injectable products are not well suited for use in a mass contamination scenario as they require skilled professionals for their administration and are rapidly cleared from the circulation. To overcome the mismatch in the pharmacokinetics of DTPA and the biokinetics of these transuranic elements, which are slowly-released from contamination sites, the penta-ethyl ester of DTPA (C2E5) was prepared and formulated in a non-aqueous gel for transdermal administration. When gels comprised of 40% C2E5, 40-45% Miglyol® 840 and 15-20% ethyl cellulose were spiked with [^{14}C]-C2E5 and applied to rat skin, over 60% of the applied dose was absorbed within a 24 h period. Radioactivity was observed in urinary and fecal excretions for over three days after removal of the gel. Using an ^{241}Am wound contamination model, transdermal C2E5 gels were able to enhance total body elimination and reduce the liver and skeletal burden of ^{241}Am in a dose-dependent manner. The efficacy achieved by a single 1000 mg/kg dose to contaminated rats was statistically comparable to the intravenous Ca-DTPA treatment. The effectiveness of this treatment, favorable sustained release profile of pro-chelators and ease of administration support its use following radiological emergencies and for its inclusion in the Strategic National Stockpile.

4.1 INTRODUCTION

The increasing threat of nuclear terrorism as well as incidents that involved the release of radioactive materials into the environment, such as the accident at the Fukushima Daiichi power plant in March 2011, has heightened the awareness that many nations need to be prepared for such cataclysmic events (32). Detonation of a nuclear weapon or a radiological dispersion device (RDD, “dirty bomb”) near densely populated areas could result in a large number of individuals being contaminated by radionuclides via inhalation, ingestion or through wounds. Internalization of radioactive materials may result in acute radiation sickness or chronic injuries including an increased risk of developing cancers (160-163). Due to their abundance and availability, isotopes of the transuranic elements americium (Am), curium (Cm), and plutonium (Pu) are among the radionuclides of greatest concern with respect to accidental or deliberate contamination. The injuries and risks associated with contamination by these radionuclides can be mitigated by the intravenous (i.v.) administration of radionuclide decorporation agents such as the calcium (Ca) and zinc (Zn) trisodium salts of diethylenetriamine pentaacetic acid (DTPA). Ca-DTPA and Zn-DTPA exert their pharmacological effect by sequestering these radionuclides with high affinity and promoting the elimination of the resulting chelate complexes from contaminated individuals. DTPA is administered via slow i.v. push, i.v. infusion, or inhalation with a nebulizer (39); treatment is most effective when administered shortly after contamination before the transuranic radionuclides become fixed in tissues such as liver and bone (90). The efficacy of Ca/Zn-DTPA injections has been demonstrated for decades in workers injured in accidents in the nuclear power industry (140, 161, 164, 165).

Mass contamination scenarios call for effective and prompt medical countermeasures for the affected populations. Current DTPA treatment options do not meet

the challenge imposed by a mass casualty setting in that skilled medical professionals are required to administer Ca/Zn-DTPA by i.v. injection; multiple injections may be required due to the short circulating half-life of DTPA. Stevens and colleagues studied the clearance of DTPA in man and observed that intravenously administered ^{14}C-labeled DTPA was quantitatively excreted intact in urine in 24 hours (125). The total body clearance of ^{14}C-labeled DTPA in rats 24 h after i.v. injection has been reported to range from 94% to 100% with half-lives from 0.28 to 0.53 h and with no metabolic degradation (79, 94). In contrast, the release rates of internalized Am, Pu and Cm contaminants from wound sites to the systemic circulation in various animal species range from 0.052 to 6.3% of the administered radionuclides per day, a relatively slow and steady transfer process (Figure 4.1) (80). It has been suggested that a chelating agent must be maintained at a concentration of at least 10 to 25 μM in both extracellular and intercellular fluids for a sustained duration to ensure an optimal chelation effect of transuranic radionuclides (88). In comparing the short half-life and rapid clearance of DTPA after i.v. administration to the slow and sustained introduction of radio-actinides into the systemic circulation (80), there is a mismatch between the pharmacokinetic profile of intravenously administered DTPA and the biokinetic profile of transuranic radionuclides. This mismatch leads to a period where DTPA plasma concentrations are below the effective concentration required to chelate radionuclides in the systemic circulation and, thus, may limit the effectiveness of the current parenteral DTPA treatments. Previous efforts have addressed this mismatch and produced encouraging results. Guilmette and Muggenburg implanted subcutaneous osmotic pumps to continuously deliver Zn-DTPA to dogs that had been contaminated with $^{241}AmO_2$ by inhalation, and achieved enhanced decorporation of ^{241}Am (92). DTPA has been entrapped in various liposome formulations for prolonged circulation after i.v. administration, and improved decorporation of ^{238}Pu was achieved (94, 95). However, these approaches involve parenteral administration, thus making them unsuitable for mass casualty scenarios after a

major nuclear/radiological emergency. As a result, a non-parenteral delivery system which can provide sustained levels of chelators in the circulation that match the biokinetic profile of actinides after inhalation or wound contamination is highly desirable.

There are several efforts underway to improve the oral bioavailability of Ca/Zn DTPA and other actinide decorporation agents (31). DTPA is a synthetic polyamino carboxylic acid with eight coordinate bond forming sites for complexing metal ions. Due to the presence of five carboxylic acid groups and three nitrogen atoms, DTPA is highly ionic. Thus, Ca-DTPA and Zn-DTPA are hydrophilic and are considered Class III compounds (high solubility, low permeability) according to the Biopharmaceutical Classification System. While oral formulations may provide for sustained blood concentrations of DTPA, a zero-order release profile can be achieved via transdermal drug delivery. Because DTPA is hydrophilic (log P = -4.90) with a high melting point (219-220ºC), it is not a good candidate for transdermal delivery (72, 73). However, esterification of the 5 carboxylic groups on DTPA produces lipophilic compounds which possess desirable physicochemical properties for transdermal delivery (43, 44). We have prepared the penta-ethyl ester of DTPA, designated as C2E5, and successfully incorporated it into a non-aqueous gel formulation comprised of ethyl cellulose (EC) and Miglyol 840® with acceptable stability and rheological properties (47). The selected 40% C2E5 non-aqueous gel was applied to Sprague-Dawley (SD) rats at a dose of 200 mg C2E5/kg and achieved sustained release of C2E5 metabolites *in vivo* for an extended duration (47).

The aim of the current studies was to evaluate the radionuclide decorporation efficacy of transdermal C2E5 non-aqueous gels at different dose levels when applied 24 hours after contamination using an ^{241}Am wound contamination model. To our knowledge, this is the first report of the use of a transdermal formulation for the systemic delivery of a radionuclide decorporation agent with the goal of providing a sustained release

pharmacokinetic profile of a chelator in order to match the biokinetic profile of internalized actinides.

4.2 MATERIALS AND METHOD

4.2.1 Materials

Miglyol 840 was purchased from Sasol (Hamburg, Germany). EC (ethyl cellulose, Ethocel Std 10 FP Premium polymer) with an ethoxyl content of 48.0-49.5% was a gift from Dow Chemical (Midland, MI, USA). C2E5 was prepared using the Fischer esterification method by reacting DTPA with ethanol under reflux in the presence of a hydrochloric acid catalyst (44). [^{14}C]-diethylenetriaminepentaacetic acid penta-ethyl ester ([^{14}C]-C2E5; 50 mCi/mmol) labeled at carbon-1 (carbonyl carbon) was purchased from American Radiolabeled Chemicals, Inc. (St. Louis, MO). [^{241}Am]-americium nitrate solution for intramuscular (i.m.) contamination of adult female SD rats was prepared from [^{241}Am]-Americium chloride (Eckert & Ziegler Isotope Products, Valencia, CA) by dilution with a solution of concentrated nitric acid. Anhydrous ethanol, isopropyl alcohol, 30% hydrogen peroxide solution were purchased from VWR International (Radnor, PA) and/or Fisher Scientific (Fairlawn, NJ). Liquid scintillation cocktails Ultima GoldTM and an aqueous based tissue solubilizer SolvableTM were purchased from PerkinElmer Life and Analytical Sciences (Waltham, MA).

4.2.2 Preparation of C2E5 Non-aqueous Gel

C2E5 non-aqueous gels comprised of 40% C2E5, 15-20% EC, and 40- 45% Miglyol 840 were prepared using the solvent evaporation method described previously [23]. Briefly,

pre-dried EC particles were first dissolved in anhydrous ethanol (10% w/v of EC in ethanol) to form a clear solution. This was followed by addition of Miglyol 840 and C2E5 to form a homogenous solution under stirring and subsequently removing ethanol under vacuum to yield the C2E5 non-aqueous gel.

[^{14}C]-Labeled C2E5 non-aqueous gel was prepared by adding [^{14}C]-C2E5 (50 mCi/mmol) into the C2E5 non-aqueous gels followed by mixing. The [^{14}C] content of the non-aqueous gel was quantified by adding a fixed quantity of the gel with 10 mL of Ultima Gold™ scintillation cocktail and counting directly for radioactivity by liquid scintillation counting (LSC) using a Packard TriCarb 3100TR (PerkinElmer Life and Analytical Sciences, Waltham, MA) with automatic quench correction. Samples were counted for 10 min or until a 5% confidence level was achieved. The specific activity of [^{14}C]-labeled C2E5 non-aqueous gel was calculated by dividing sample radioactivity by total sample mass.

4.2.3 *In vivo* Studies

4.2.3.1 Animals

All animal studies were conducted according to a protocol approved by the University of North Carolina at Chapel Hill Institutional Animal Care and Use Committee (IACUC). Ten-week-old adult female SD rats weighing from 200 to 300 g were used in these studies (Charles River Labs, Raleigh, NC). Food and water were given ad libitum. The animal room was kept at a controlled temperature on a 12 h/12 h light/dark cycle (light exposure from 7 AM to 7 PM). For the duration of the study, the rats were housed in metabolic cages individually with daily urine and feces collection until euthanasia on Day 6 for mass balance study and on Day 7 for radionuclide decorporation study.

4.2.3.2 Absorption and Mass Balance Study with [^{14}C]-Labeled C2E5 Non-aqueous Gels

To evaluate the absorption and mass balance of transdermal delivery of the C2E5 non-aqueous gel, the [^{14}C]-labeled C2E5 non-aqueous gel was applied to rats at a 200 mg C2E5/kg dose level. Six adult female SD rats were anesthetized with 2-3% isoflurane before the dorsal skin between the cervical vertebrae and anterior thoracic vertebrae was clipped with caution. The [^{14}C]-labeled gel was applied to a 2 cm x 3 cm region using a cotton swap. The mass of the gel applied was recorded for each rat to permit actual dose determination, and a jacket with a dermal insert (VWR International, Radnor, PA) was placed on the rats to protect the area on which the gel was applied. Twenty-four hours after application, the remaining gel at the application site and the jacket with the dermal inserts were carefully removed, and the recovered C2E5 content was assayed by LSC. The animals were housed in metabolic cages individually and were euthanized 6 days after application of the gel. The animals were observed once daily and their body weights recorded at pre-dose and prior to necropsy. Urine and feces were collected daily until euthanasia on Day 6, when the liver and the skin from the application site and surrounding area were also collected. Cage washes were collected at the end of each experiment.

Collected urine samples were added to Ultima Gold™ scintillation cocktail at a ratio of 100 µL:10 mL and assayed directly for radioactivity by LSC. For feces samples, the fecal pellets were mixed and vortexed with 20 mL of a mixture of acetonitrile and water (1:1 ratio) for 10 min followed by a 30 min sonication and subsequently centrifugation at 1,000 x g at 4°C for 10 min. The supernatant was transferred to a scintillation vial for analysis by LSC (100 µL of feces extraction supernatant sample directly dispersed into 10 mL of scintillation cocktail). The extraction process was repeated until the sample count was less than 1000 disintegrations per minute (DPM) per 100 µL of feces extraction supernatant sample. The

liquid cage wash samples were processed in a manner similar to the urine samples and assayed by LSC; the solid cage wastes were processed as fecal pellets and assayed by LSC. For skin and liver samples, tissues were mixed with tissue solubilizer (10% w/v of tissue to Solvable) and incubated at 50°C until the tissues became totally solubilized. One mL of the solubilized tissue solution was transferred to a vial, decolorized by incubation with 0.1 mL of 30% hydrogen peroxide solution for 1 h at 50°C, and then added to 10 mL of scintillation cocktail for LSC analysis.

4.2.3.3 Radionuclide Decorporation of Contaminated Rats

To evaluate the efficacy of transdermal delivery of C2E5 in a non-aqueous gel, a radionuclide decorporation efficacy study was conducted in rats contaminated with ^{241}Am. Adult female SD rats were anesthetized with 2-3% isoflurane. All animals were contaminated with [^{241}Am]-Americium nitrate solution (250 nCi, 0.1 mL) via an i.m. injection in the anterior thigh muscle. Dorsal skin between the cervical vertebrae and anterior thoracic vertebrae was clipped with caution before application of the gel. C2E5 doses of 200 mg/kg, 600 mg/kg, and 1000 mg/kg were applied 24 h post ^{241}Am contamination to a 6 cm^2 (2 cm x 3 cm) area of the clipped dorsal region using cotton swab. Fick's law (Equation 4-1) dictates the steady-state diffusion of drug through skin:

$$J_{ss} = \left(\frac{D * K_p}{h}\right) * A * C_{veh} \qquad (Eq. 4-1)$$

where J_{ss} = steady-state flux (mg/h); D = drug diffusivity (cm^2/h); h= membrane thickness (cm); K_p = drug's membrane-vehicle partition coefficient; C_{veh} = initial drug concentration (mg/cm^3) in the vehicle; and A = surface area (cm^2). Keeping all other parameters constant,

the flux of the drug (J_{ss}) is proportional to the surface area of drug application. To assess the effect of application area, the C2E5 non-aqueous gel was applied at a dose of 600 mg/kg dose 24 h post ^{241}Am contamination using cotton swab to an 18 cm^2 (3 cm x 6 cm) area of the clipped dorsal region. A jacket with plastic dorsal insert was placed on the rats to protect the gel application region. The mass of C2E5 gel applied was recorded for each animal to permit the actual dose determination. Twenty-four hours after application of the C2E5 gel, the remaining gel at the application site and the jacket with the dermal insert were carefully removed. The animals were housed in metabolic cages individually and were euthanized 7 days after contamination. Positive and negative controls included animals administered Ca-DTPA intravenously at a dose of 14 mg/kg 24 h after contamination, and untreated animals. Daily observations and body weights were recorded at pre-dose and prior to necropsy. Urine and feces were collected daily until euthanasia, when the liver, kidneys, both femurs, the muscle tissue around the femurs, and the pelt around the ^{241}Am injection site were also collected. Cage washes were collected at the end of each experiment. As ~35% of the decay of ^{241}Am is associated with photon emissions of 59.7 keV, ^{241}Am present in samples was quantified using a gamma counter (2470 Wizard 2, Perkin Elmer, Waltham, MA). The samples were counted for one minute using a 40-80 keV energy detection window and were background-corrected. Additionally, ^{241}Am activity was quantified in 2 x 0.1 mL aliquots of the dosing solution. For all samples, ^{241}Am content was expressed as a percentage of the injected dose (ID). An estimate of the total skeletal burden was made using the method of Volf that was determined by the ^{241}Am burden in the contra-lateral femur multiplied by 20 (166). The ^{241}Am retained at the wound site was quantified by measuring the ^{241}Am content of the muscle surrounding the injection site plus the ^{241}Am content in the femur. An estimate of muscle burden was calculated based on the assumption that it represents 45% of the body weight (166). The ^{241}Am content of the muscle from the opposite hind leg and animal body weight at sacrifice were used to determine the estimated ^{241}Am burden in muscle.

Total recovery = Total decorporation + liver ^{241}Am content + kidney ^{241}Am content + (Skeleton ^{241}Am content - ^{241}Am in contra-lateral femur) + ^{241}Am content at the wound site + muscle ^{241}Am content + ^{241}Am content at the pelt around the ^{241}Am injection site.

4.2.4 Statistical Analysis

All data reported are mean ± standard deviation (S.D.) from a given number of observations. Statistical analysis was performed on the data from the efficacy study. To assess treatment and dose induced changes in endpoint ^{241}Am data i.e., liver, skeleton, and wound site burden as well as total decorporation, one-way ANOVA with Tukey's posttest was performed among three C2E5 transdermal treatment groups at 200, 600 and 1000 mg/kg doses applied to a 6 cm^2 application site, an untreated negative control group, and a positive control group that received i.v. Ca-DTPA. A second one-way ANOVA with Tukey's posttest was performed among all the four C2E5 gel treatment groups, negative untreated and positive i.v. DTPA treatment groups. To assess the sustained efficacy of transdermal C2E5 treatment, daily ^{241}Am decorporation in the urine and feces was analyzed by repeated measures one-way ANOVA with Dunnett's posttest to compare each C2E5 treatment group with the untreated control group. For all statistical analysis $p < 0.05$ was considered significant. Statistical analyses were performed using the SAS analysis system (v. 9.3; SAS Institute, Inc., Cary, NC).

4.3 RESULTS

4.3.1 Preparation of C2E5 Non-aqueous Gels

The structures of C2E5, its potential metabolites, including DTPA tetra-ethyl ester (C2E4), DTPA tri-ethyl ester (C2E3), DTPA di-ethyl ester (C2E2), DTPA mono-ethyl ester (C2E1), and the fully de-esterified metabolite (DTPA) are depicted in Figure 4.2. C2E5 is a clear, light yellow, slightly viscous Newtonian liquid with a viscosity of ~175 cP (44).

C2E5 non-aqueous gels comprised of 40% C2E5, 15-20% EC, and 40-45% Miglyol 840 were prepared using the solvent evaporation method described previously (47). The C2E5 gels were slightly yellow translucent semisolids with a density of 1.02 g/cm3. C2E5 non-aqueous gels comprised of 40% C2E5, 15-20% EC, and 40-45% Miglyol 840 were radiolabeled with [^{14}C]-C2E5 (specific activity = 0.10 µCi/mg) for a mass balance study. All gels were stored at 4°C until applied to experimental animals.

4.3.2 Absorption and Mass Balance of [^{14}C]-Labeled C2E5 Non-aqueous Gels

Significant C2E5 transdermal absorption was achieved after topical application of the gels; approximately 31% of the 200 mg/kg C2E5 applied dose was recovered from the skin as unabsorbed dose 24 hours after application (Table 4.1). Six days after application, a ^{14}C-C2E5 mass balance of over 90% was obtained, with approximately 90% of the absorbed dose recovered in the excreta and tissues (Table 4.1). Low retention of C2E5 and its metabolites was observed at the application site; only 1.5% of the applied dose was present in the skin taken from the application site six days after application (Table 4.1). There was no significant [^{14}C] radioactivity remaining in the liver 6 days after application of the

radiolabeled gel suggesting that C2E5 and its metabolites had relatively short half-lives in plasma and were rapidly metabolized.

As demonstrated in Figure 4.3, the urinary elimination of [^{14}C] radioactivity peaked one day after application and gradually declined to the baseline level by the sixth day; the fecal elimination of [14C] radioactivity peaked two days after administration and gradually declined after the third day until it reached background levels by the sixth day.

4.3.3 *In vivo* Radionuclide Decorporation

When C2E5 was applied transdermally one day after animals were contaminated with ^{241}Am using the wound contamination model (i.m. injection), the total ^{241}Am decorporation over a seven day period was significantly enhanced when compared with untreated control animals (Table 4.2). The enhanced decorporation showed a dose dependent trend, with a non-significant increase in decorporation between 0 and 200 mg/kg dose, followed by significant increases in decorporation between the 200 mg/kg dose and the 600 mg/kg dose ($p < 0.05$) and between the 600 mg/kg dose and the 1000 mg/kg dose ($p < 0.001$). The 1000 mg/kg C2E2 dose achieved decorporation that was comparable to the current standard of care, i.v. DTPA. No statistically significant differences were found in the ^{241}Am contents recovered from the wound sites among all the experimental groups.

The observed increase in ^{241}Am decorporation was in part due to significant reductions in the ^{241}Am burden in the tissues of greatest concern, the liver and skeleton. C2E5 significantly reduced liver burden compared with untreated animals at all the doses tested. A dose dependent effect of C2E5 treatment was observed, with a decrease in mean liver ^{241}Am burden as the applied C2E5 dose increased; this effect was statistically significant when the 1000 mg/kg dose was compared with the 200 and the 600 mg/kg doses ($p < 0.001$ and $p < 0.05$, respectively). The same trend was observed for the mean skeletal

burden, with a significant reduction compared with untreated control animals at the 1000 mg/kg dose. In all tissues examined, the effect of the highest transdermal C2E5 dose on ^{241}Am reduction was comparable with i.v. DTPA (Table 4.2). The daily excretion of ^{241}Am in the urine (Figure 4.4A) and feces (Figure 4.4B) of untreated animals and animals treated with different doses of C2E5 further illustrated dose dependent efficacy. Additionally, although the residual gel was removed from the skin 24 h after application (the same time that the day 2 urine and feces samples were collected), significantly enhanced decorporation was detected in the urine and feces at least three days after the gel was removed.

As transdermal drug flux is dependent on the drug application area, the decorporation efficacy of a C2E5 dose of 33.3 mg/kg/cm^2 applied to a 6 cm^2 vs. an 18 cm^2 application area was determined. This threefold increase in application area resulted in significantly enhanced decorporation and a significantly reduced liver ^{241}Am burden compared with the untreated control ($p < 0.001$ and $p < 0.001$, respectively) and 200 mg/kg dose treatment groups ($p < 0.001$ and $p < 0.05$, respectively) (Table 4.2). The daily excretion of ^{241}Am in the urine (Figure 4.4A) and feces (Figure 4.4B) demonstrated that elevated ^{241}Am levels in the urine and feces were consistently achieved when the gel was applied to an 18 cm^2 area compared to untreated controls as well as to animals that were treated with C2E5 doses of 200 mg/kg and 600 mg/kg applied over a 6 cm^2 area.

4.4. DISCUSSION

Transdermal drug delivery possesses many advantages over other drug delivery routes such as parenteral and oral routes. These include the delivery of a steady-state profile that reduces side effects related to fluctuations in plasma drug concentration, reduced dosing frequency, avoidance of first-pass metabolism, and improved patient

compliance due to its convenient and non-invasive means of self-administration (72-74). It may also offer benefits to special populations such as patients with needle phobia, those who are unconscious or too nauseated to take oral medications, pediatric patients and the elderly. The latter two populations are specific areas of concern to the FDA related to the development of radionuclide decorporation agents (29). The stringent physicochemical requirements for potential transdermal drug candidates have limited the number of commercial transdermal drug products on the market (72, 73). The DTPA prodrug, C2E5, was synthesized, determined to possess suitable physicochemical properties for transdermal delivery (43, 44), and achieved sustained release of C2E5 metabolites when applied topically to rats in a non-aqueous gel formulation (47).

In the present study, the elimination profile for C2E5 was obtained, and dose- and area-dependent radionuclide decorporation efficacy profiles following transdermal application were demonstrated. The mass balance study using [^{14}C]-labeled C2E5 non-aqueous gels showed that approximately 62% of the applied C2E5 dose was absorbed in 24 h and that about half of the absorbed dose was eliminated in the urine. The overall [^{14}C] recovery for the study was 93%, a satisfactory end point for a mass balance study using rats where at least 90% recovery is defined as acceptable [27]. The small amount of [^{14}C] recovered from the skin application site indicated that C2E5 did not reside there for an extended period after administration, thus avoiding potential skin irritation and inflammation issues associated with drug retention at the application site. The fact that no signs of irritation were evident on visual inspection of the application site further confirmed the suitability of C2E5 for transdermal delivery. The daily excretion of [^{14}C] radioactivity in urine and feces (Figure 4.2) showed sustained excretion of C2E5 and metabolites over 72 h following the removal of C2E5 gels from the application site. In addition, the recovery of most of the absorbed radioactivity in the excreta and the low residual radioactivity in the liver suggests that C2E5 and its metabolites were not retained in tissues.

We observed that about half of the absorbed C2E5 dose was eliminated in the urine over six days after topical administration. In contrast, i.v. DTPA results in ≥ 90% renal clearance within 24 h of administration (79, 94). C2E5 is metabolized by esterases in the skin and plasma in a step-wise manner, yielding metabolites such as DTPA, C2E1 and C2E2 (47); compounds that are more lipophilic than DTPA are known to shift elimination of actinides from a predominantly renal pattern to a pattern with increased fecal excretion (71, 167). It is anticipated that these partially hydrolyzed C2E5 metabolites (C2E2 and C2E1) can form relatively stable chelating complexes with transuranic elements, such as ^{241}Am, with log stability constants in the range 16.3 M^{-1} to 24.0 M^{-1} (118, 119). Even though such complexes are less stable than the ^{241}Am-DTPA complex, they may result in increased ^{241}Am decorporation consistent with the results observed in the C2E5 gel decorporation study. A strong temporal relationship was observed when the daily excretion of [^{14}C] in the urine is compared with the urinary fraction of the ^{241}Am decorporation (Figure 4.5A). The relationship between fecal ^{241}Am decorporation and the content of [^{14}C] in the feces (Figure 4.5B) was less clear possibly due to delayed biliary excretion of the chelation complex and intestinal transit time. These observations are consistent with earlier reports, where delayed excretion of transuranic radionuclides, such as ^{238}Pu, ^{239}Pu and ^{241}Am, after chelation with DTPA or other decorporation agents was observed in dogs and rodents (95, 167, 168).

Animal models have been developed to facilitate the understanding of the biokinetic profiles that are observed following contamination by transuranic elements (80). For the model used in this study, a simulated wound contamination with [^{241}Am]-Americium nitrate, the ^{241}Am at the intramuscular contamination site initially enters the bloodstream as the stable trivalent $^{241}Am^{3+}$ form. Once in the circulation, approximately 95% of the $^{241}Am^{3+}$ is cleared from the plasma in less than 1 h with the majority accumulating in the liver and skeleton (91, 169, 170). An adequate concentration of a chelator in the blood can sequester the $^{241}Am^{3+}$ as a stable chelation complex, reducing the translocation and deposition of

radionuclides into the adjacent bone and other tissues. In addition to promote the excretion of $^{241}Am^{3+}$, Markley reported that intraperitoneally administered DTPA penta-ethyl ester successfully reduced the ^{239}Pu content in mouse liver (171). Guilmette et al demonstrated that i.v. administration of a series of mono- and dialkyl esters of DTPA (including a form of C2E1 and C2E2, respectively) effectively reduced the plutonium burden in the skeleton of contaminated rodents (120). Because the biokinetics of ^{242}Cm and ^{244}Cm is very similar to that for ^{241}Am (91), the effective decorporation treatment for ^{241}Am would also likely be effective in treating individuals contaminated with ^{242}Cm and ^{244}Cm. Thus, the previous reports suggest that this C2E5 gel treatment may promote the excretion of several transuranic elements.

In the studies reported here, a well-defined C2E5 dose-dependent increase in excretion of ^{241}Am in the urine and feces was observed for animals treated with the C2E5 gels 24 h post contamination; total body decorporation of ^{241}Am increased by approximately 2% for every 100 mg/kg of administered C2E5. A similar trend was observed for the reduction in the liver ^{241}Am burden; each 100 mg/kg increment of C2E5 dose reduced the liver ^{241}Am burden by approximately 1%. Although the reduction in skeleton burden for 24 h post contamination C2E5 gel groups did not appear to be dose-dependent, a lower skeletal burden was observed in contaminated animals treated with C2E5 gels at all dose levels compared to untreated animals. As the liver and bone tissues are key target organs for the chronic damage caused by radionuclide contamination (172, 173), this improved ability for C2E5 metabolites to remove actinides fixed in liver and bone tissues may result in a therapeutic benefit. In addition to demonstrating a dose dependent response to C2E5 treatment when applied to the same area, we also demonstrated increased efficacy when the application area was increased from 6 cm^2 to 18 cm^2. Based on Fick's law, the drug flux across the skin is directly proportional to the drug application area when all other parameters are kept constant. For animals treated with the C2E5 gel at a 1000 mg/kg dose

spread over 6 cm^2 or at 600 mg/kg dose applied over 18 cm^2, the overall efficacy in terms of enhancement in decorporation as well as reduction in liver and skeletal burden was comparable to that observed for animals intravenously administered Ca-DTPA at the standard recommended dose of 14 mg/kg.

All animals were examined daily during the experimental period for indications of disease or abnormalities including morbidity, mortality, and signs of toxicity (no radio-toxicity was anticipated due to the low amounts of ^{241}Am employed in these studies). In C2E5 treated animals, no elevated skin reddening or local skin inflammation was observed at the locus where the dose was applied, and gel treatment did not significantly alter animal body weights compared with untreated control animals. These preliminary results suggest that the C2E5 gel was well tolerated by the animals. The ^{241}Am content at the wound site for all the experimental groups was consistent with literature reports (80), and no statistical significance was observed in the retained ^{241}Am at wound sites among the different treatment groups. The radionuclide decorporation results confirmed the validity of maintaining chelator concentrations for an adequate duration to ensure optimal in vivo chelation of transuranic radionuclides (88).

Unlike most new drug candidates, the efficacy of radionuclide decorporation therapies has not been systemically evaluated in human clinical trials due to ethical concerns involving the contamination of healthy human subjects with radionuclides. The “Animal Rule” (21 CFR 314.600) has been implemented by the FDA as a paradigm for the approval of drugs that treat radiological, chemical, and biological threats (174, 175). The ^{241}Am decorporation results in the rodent wound contamination model presented here demonstrate that this treatment option can be as effective as the current FDA approved i.v. DTPA treatment when administered one day after radionuclide contamination, a realistic response timeframe for victims in a mass casualty scenario after a nuclear/radiological event.

In order to predict an appropriate human dosing regimen for this transdermal gel treatment based on rodent efficacy data, interspecies differences in the drug's pharmacokinetics need to be considered. Based on allometric scaling (176), the 6 cm^2 application area used on the ~250 g rats would translate to a gel application area of approximately 300 cm^2 (a circle with a radius of ~10 cm) for a 70 kg human; this application area is within the range of current topical products (177). The renal clearance of chelators like DTPA is slower in humans (1.3 mL/min/kg) than in the rat (5.9 mL/min/kg) (178), which, for a given dose, would result in a higher steady-state plasma concentration in humans. It has also been demonstrated that the DTPA plasma concentration required to quantitatively bind ^{241}Am in rat plasma is approximately 3-fold greater than in human plasma (179). These two factors may result in a lower dose being required for human efficacy. The dose may be further lowered by increasing the frequency of dosing.

4.5 CONCLUSIONS

To our knowledge, this is the first report which demonstrates that the transdermal delivery of a pro-chelator is a viable strategy for delivering chelating agents to the systemic circulation, resulting in an effective, mass-casualty-ready treatment option for radionuclide contamination. Efficacy was demonstrated by enhancing total body decorporation and reducing the liver and skeletal burden of ^{241}Am with a single topical administration of the C2E5 gel 24 h after contamination. Enhanced ^{241}Am elimination for at least three days after application indicated that the C2E5 non-aqueous gels provided sustained delivery of metabolites capable of chelating ^{241}Am. No skin abnormalities or signs of skin irritation were observed after administration of the C2E5 non-aqueous gel throughout the entire study period. The effectiveness of this treatment option, favorable sustained release profile of pro-chelators and ease of administration support the use of C2E5 non-aqueous gels following

nuclear/radiological emergencies and for its inclusion in the Strategic National Stockpile. We expect that this work will be of great interest to the general scientific community and especially to researchers in medical countermeasures field, as well as to the government agencies in emergency response and preparation.

Table 4.1 Percent of administered dose in various tissues 6 days after administration of [^{14}C]-labeled C2E5 non-aqueous gels at a dose of 200 mg C2E5/kg (n=6).

Sample	Mean	S.D.
Urine*	29.9	3.2
Feces	30.6	2.5
Skin at the application site	1.57	0.28
Liver	0.11	0.30
Recovered gel from the application site	30.8	6.6
Mass Balance	93.0	3.9

* Include [^{14}C] recovered from cage washes.

Table 4.2 ^{241}Am recovered in samples seven days following single dose treatments 24 h post i.m. contamination of rats with ^{241}Am nitrate (% of ID of ^{241}Am).

Treatment	Application Area	Total Excretion (Urine + Feces)	Liver	Skeleton	Wound Site	Total Recovery
Untreated control (n=4)	N/A	13.73 ± 2.59	23.58 ± 1.38	16.34 ± 1.33	30.20 ± 4.86	86.34 ± 3.38
i.v. Ca-DTPA 14 mg/kg (n=8)	N/A	37.65 ± 4.03***	12.13 ± 1.59***	11.65 ± 2.18*	24.73 ± 6.10	88.62 ± 2.10
C2E5 gel 200 mg/kg (n=7)	6 cm^2	18.79 ± 3.10$^{\#\#\#}$	19.22 ± 2.40*$^{\#\#\#}$	13.97 ± 3.06	31.71 ± 7.45	87.94 ± 2.05
C2E5 gel 600 mg/kg (n=8)	6 cm^2	24.50 ± 3.21***$^{\#\#\#}$	16.24 ± 3.10***$^{\#\#}$	13.49 ± 1.82	30.43 ± 5.29	87.50 ± 1.65
C2E5 gel 1000 mg/kg (n=8)	6 cm^2	33.27 ± 3.73***	13.05 ± 1.33***	12.46 ± 2.02*	23.02 ± 6.09	86.84 ± 2.09
C2E5 gel 600 mg/kg (n=4)	18 cm^2	32.69 ± 5.64***	14.63 ± 2.14***	12.86 ± 1.34	24.89 ± 7.51	88.54 ± 1.29

Significant difference by one-way ANOVA with Tukey's post hoc comparison of means, *$p < 0.05$, **$p < 0.01$, and ***$p < 0.001$ against untreated control; Significant difference by one-way ANOVA with Tukey's post hoc comparison of means, $^{\#}p < 0.05$, $^{\#\#}p < 0.01$, and $^{\#\#\#}p < 0.001$ against i.v. Ca-DTPA treatment. N/A: Not Applicable.

Figure 4.1 Release-time profile of soluble, colloidal and particulate radionuclides (including actinides such as ^{238}Pu, ^{239}Pu, ^{241}Am and $^{242,244}Cm$) following i.m. injected in rats. (CIS: Colloid & Intermediate State; PABS: Particles, Aggregates & Bound State.). Reprinted with permission of the National Council on Radiation Protection and Measurements, http://NCRPpublications.org.

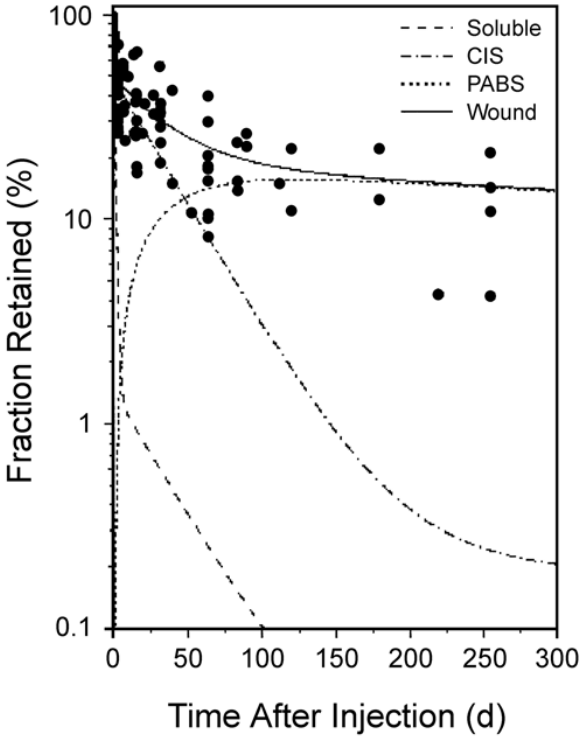

Figure 4.2 Structures of C2E5 and its metabolites.

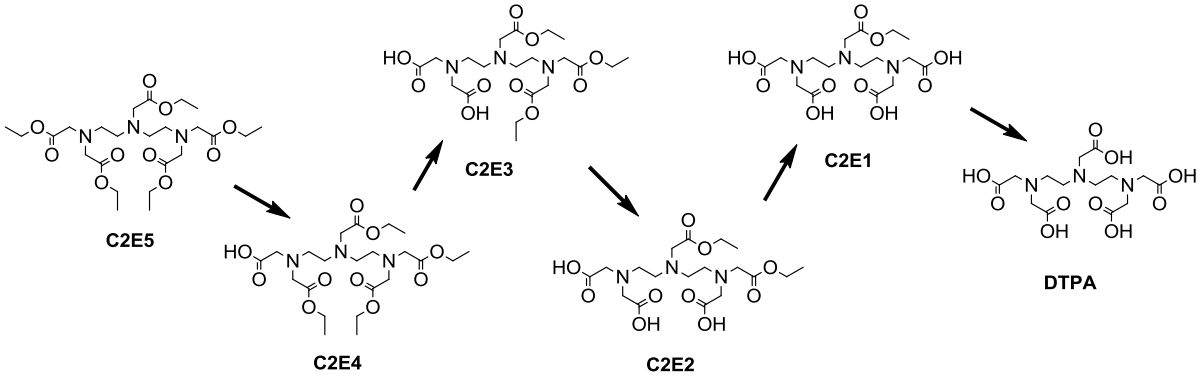

Figure 4.3 Daily excretion of radioactivity in urine and feces after topical application of [^{14}C]-labeled 40% C2E5 non-aqueous gels (Data are means ± SD) (n=6). (Urinary excretion, -■-; fecal excretion, -●-)

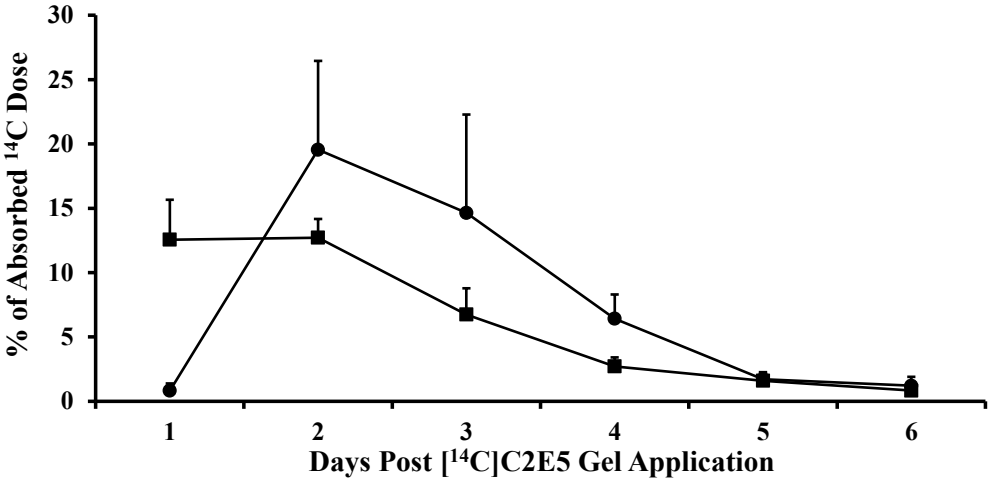

Figure 4.4 Daily excretion of ^{241}Am in urine (A) or in feces (B) after a single dose of the decorporation agents at different dose levels and application areas 24 h post contamination. Significant (*p < 0.05, **p < 0.01, and ***p < 0.001) by Dunnett's test. (Untreated control, ■; 200 mg/kg applied to 6 cm^2, ●; 600 mg/kg applied to 6 cm^2, ♦; 1,000 mg/kg to 6 cm^2, ▲; 600 mg/kg to 18 cm^2, ■)

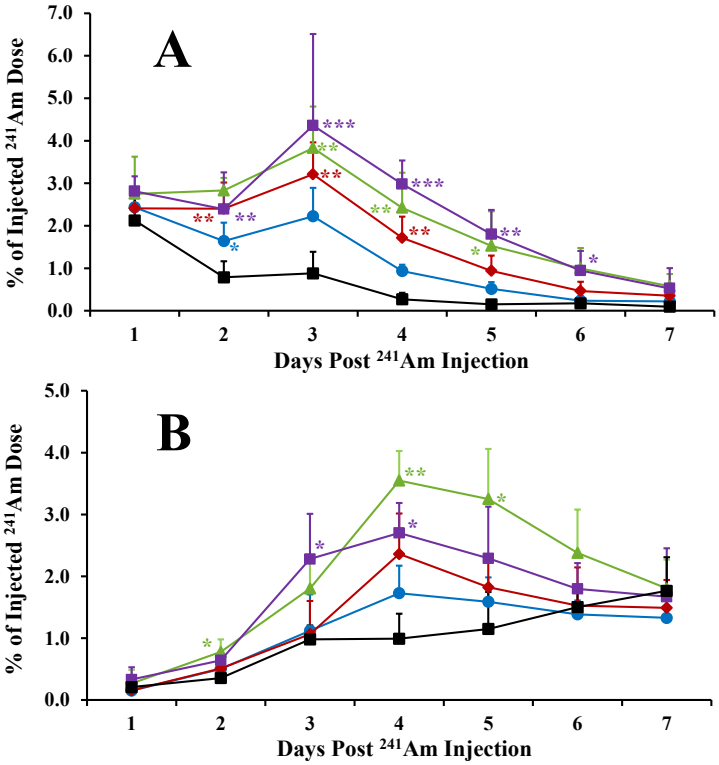

Figure 4.5 Daily ^{14}C excretion and ^{241}Am decorporation via urine (A) and feces (B) by C2E5 gel formulations at 200 mg/kg dose applied 24 h post contamination. (Urinary excretion of ^{14}C, -■-; fecal excretion of ^{14}C, -●-; Urinary excretion of ^{241}Am, -■-; fecal excretion of ^{241}Am, -●-)

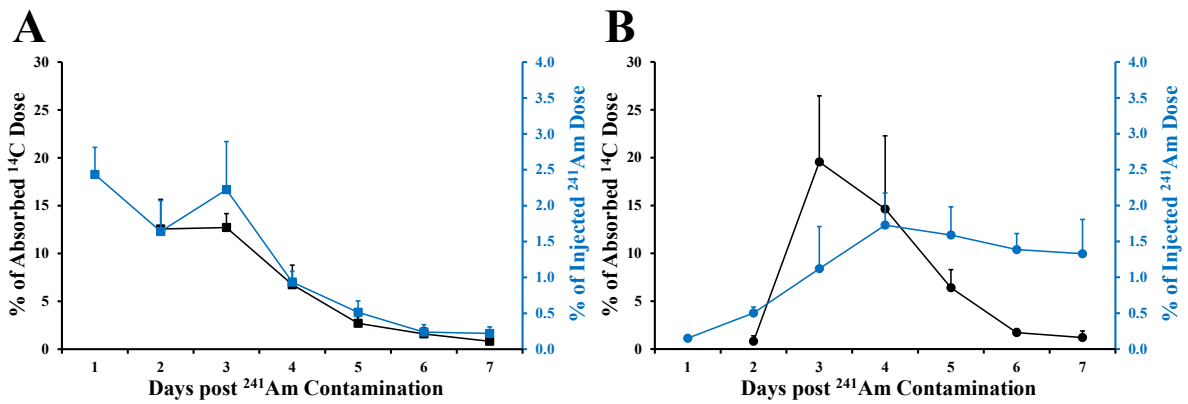

CHAPTER 5: GENERAL CONCLUSIONS AND FUTURE DIRECTION

5.1 GENERAL CONCLUSIONS

The first goal of this research project was to screen the various semisolid dosage forms to identify a formulation matrix that can stabilize the C2E5. A non-aqueous gel comprised of ethyl cellulose and Miglyol 840 was selected based on its ability to stabilize the hydrolysis prone C2E2 molecules over an oil-in-water cream and hydrocarbon based ointment matrices.

The second goal of the study was to characterize the C2E5 non-aqueous gel formulations. Thermal analysis by DSC and SEM imaging results showed unsolubilized ethyl cellulose particles present in the gel that was prepared by directly mixing ethyl cellulose particles with Miglyol 840 and C2E5. Improved gel uniformity was achieved for the C2E5 non-aqueous gels prepared using solvent evaporation method. Rheograms derived from continuous shear rheometry of C2E5 non-aqueous gel comprised of 40% C2E5, 20% EC10 and 40% Miglyol 840demonstrated that the C2E5 non-aqueous gel is a typical shear-thinning system rheological properties. The *in vitro* release testing of this gel formulation revealed that C2E5 was readily released from the gel matrix.

The pharmacokinetic and absorption and mass balance demonstrated that C2E5 was able to successfully permeate through the skin, to be converted into partially or fully hydrolyzed metabolites, and to enter systemic circulation en mass. Decorporation efficacy studies proved the validity of the working hypothesis. The efficacy achieved by a single 1000

mg/kg dose to contaminated rats was statistically comparable to the intravenous Ca-DTPA treatment, currently FDA approved treatment option. The effectiveness of this treatment, favorable sustained release profile of pro-chelators and ease of administration support its use following radiological emergencies and for its inclusion in the Strategic National Stockpile.

5.2 FUTURE WORK

The future work of this project include aspects on decorporation studies with different transuranic radionuclides and different contamination models, irritation study and skin sensitization study of the gel formulations, and PK/PD model of the C2E5 transdermal delivery and radionuclide decorporation.

It's important to evaluate the C2E5 non-aqueous gel formulations using the same wound contamination model with ^{238}Pu and $^{242/244}$Cm species and prove to be efficacious in decorporating all the major transuranic elements. Furthermore, C2E5 non-aqueous gel formulations will be evaluated using an inhalation contamination model with ^{241}Am, ^{238}Pu and $^{242/244}$Cm in rats.

Major side effects of topical and transdermal treatments are associated with irritation and skin sensitization reactions. Irritation study in rats will be conducted using selected C2E5 non-aqueous gel formulations, a vehicle control and a placebo, followed by a skin sensitization study in Guinea pigs.

A PK/PD model of the C2E5 transdermal delivery and radionuclide decorporation needs to be established to understand of the interactions between the chelating agents and radionuclides *in vivo*. A detailed analysis of pharmacokinetic and efficacy study results will shed light and provide insight for the PK/PD model.

APPENDICES

APPENDIX A DTPA Derivatives Synthesized for the Dissertation Research

APPENDIX B Non-aqueous Gel for the Transdermal Delivery of a DTPA Penta-ethyl Ester Prodrug

APPENDIX C Transdermal Prodrug Delivery for RadionuclideDecorporation: Non-aqueous Gel Formulation Development and In Vitro and In Vivo Assessment

APPENDIX A DTPA Derivatives Synthesized for the Dissertation Research

(A) An isomer of tetra-ethyl ester of DTPA

(B) An isomer of di-ethyl ester of DTPA

(C) Penta-amide of DTPA

A

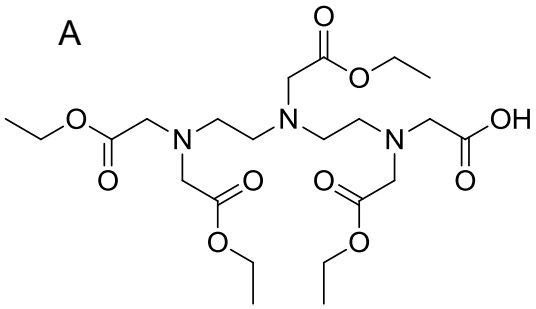

B

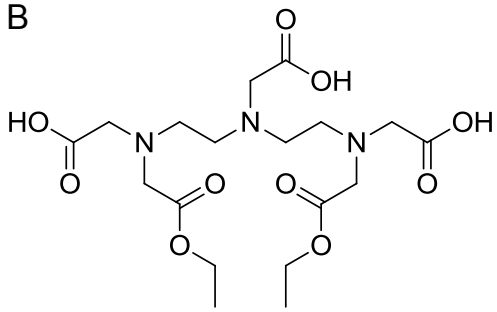

C

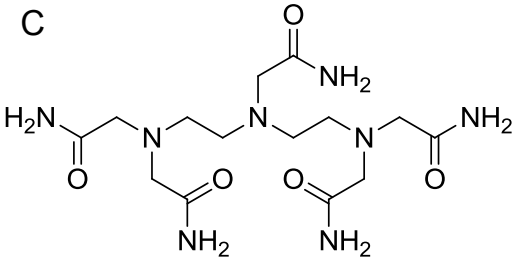

APPENDIX B Non-aqueous Gel for the Transdermal Delivery of a DTPA Penta-ethyl Ester Prodrug

The AAPS Journal, Vol. 15, No. 2, April 2013 (© 2013)
DOI: 10.1208/s12248-013-9459-5

Research Article

Nonaqueous Gel for the Transdermal Delivery of a DTPA Penta-ethyl Ester Prodrug

Yong Zhang,[1] Matthew P. Sadgrove,[1] Katsuhiko Sueda,[1] Yu-Tsai Yang,[1] Erik K. Pacyniak,[1] John R. Kagel,[2] Brenda A. Braun,[2] William C. Zamboni,[2,3] Russell J. Mumper,[1] and Michael Jay[1,4]

Received 6 November 2012; accepted 17 January 2013; published online 7 February 2013

Abstract. Diethylenetriamine pentaacetic acid penta-ethyl ester, designated as C2E5, was successfully incorporated into a nonaqueous gel for transdermal delivery. The thermal and rheological properties of a formulation containing 40% C2E5, 20% ethyl cellulose, and 40% Miglyol 840® prepared using the solvent evaporation method demonstrated that the gel had acceptable content uniformity and flow properties. *In vitro* studies showed that C2E5 was steadily released from the gel at a rate suitable for transdermal delivery. Topical application of the gel at a 200 mg C2E5/kg dose level in rats achieved significantly higher plasma exposures of several active metabolites compared with neat C2E5 oil at the same dose level. The results suggest that transdermal delivery of a chelator prodrug is an effective radionuclide decorporation strategy by delivering chelators to the circulation with a pharmacokinetic profile that is more consistent with the biokinetic profile of transuranic elements in contaminated individuals.

KEYWORDS: nonaqueous gel; pharmacokinetics; radionuclide decorporation; transdermal drug delivery.

INTRODUCTION

The Fukushima Daiichi nuclear incident in March 2011 attracted world attention to currently available radiological countermeasures for such disasters. In addition, the threat of nuclear terrorism resulting from detonation of a radiological dispersion device ("dirty bomb") calls for effective medical countermeasures designed for use in mass casualty scenarios. In both of these events, significant release of transuranic radionuclides into the environment could result in human exposure via inhalation, ingestion, or absorption at a wound site. The injuries and risks associated with internal deposition of the transuranic elements americium (Am), curium (Cm), and plutonium (Pu) can be mitigated by administration of radionuclide decorporation agents such as the calcium (Ca) and zinc (Zn) trisodium salts of diethylenetriamine pentaacetic acid (DTPA), which are the only agents approved by the US Food and Drug Administration to treat internal contamination by transuranics. DTPA is a synthetic polyamino carboxylic acid with eight coordinate bond forming sites that can sequester metal ions and form highly stable DTPA–metal ion complexes. DTPA has wide industrial and medical applications including control of water hardness, medical imaging, and decorporation of internally deposited radionuclides (1). Ca- and Zn-DTPA achieve therapeutic efficacy by exchanging the Ca and Zn cations with transuranic radionuclides *in vivo* to form higher-affinity complexes and promoting their elimination from contaminated individuals (2). The high aqueous solubility and low permeability of these compounds result in poor bioavailability after oral administration (3–5). Therefore, these compounds must be administered by slow intravenous (i.v.) push, i.v. infusion, or inhalation using a nebulizer (6). The administration of DTPA by i.v. or inhalation to those contaminated with transuranic isotopes requires skilled medical professionals, which imposes a logistical challenge in a mass casualty setting. As a consequence, there is an urgent need for new decorporation treatments that allow patients to self-administer in a timely manner after a nuclear disaster.

Contamination by radioactive Am, Pu, and Cm can occur by inhalation, skin adsorption, or by entrance through a wound. The transfer of these radioactive elements from experimental deep puncture wounds to the systemic circulation is generally a slow, steady process and transfer rates ranging from 0.052% to 6.3% of the injected dose per day

[1] Division of Molecular Pharmaceutics, UNC Eshelman School of Pharmacy, University of North Carolina at Chapel Hill, CB# 7362, 120 Mason Farm Rd, Chapel Hill, North Carolina 27599-7362, USA.
[2] UNC Lineberger Comprehensive Cancer Center, Carolina Center for Cancer Nanotechnology Excellence, UNC Institute for Pharmacogenomics and Individualized Therapy, University of North Carolina at Chapel Hill, Chapel Hill, North Carolina 27599-7295, USA.
[3] Division of Pharmacotherapy and Experimental Therapeutics, UNC Eshelman School of Pharmacy, University of North Carolina at Chapel Hill, Chapel Hill, North Carolina 27599-7569, USA.
[4] To whom correspondence should be addressed. (e-mail: mjay@unc.edu)

1550-7416/13/0200-0523/0 © 2013 American Association of Pharmaceutical Scientists

have been observed, depending on the radio-contaminants and the animal species (7). In contrast, the total body clearance of ^{14}C-labeled DTPA from rats 24 h after i.v. administration has been reported to range from 94% to 100% with the half-life ranging from 18.5 to 31.8 min (8,9). Comparison of the short half-life and rapid elimination of DTPA after i.v. injection to the slow introduction of radioactive actinide species into the bloodstream reveals a mismatch between the pharmacokinetics of DTPA and the biokinetic profiles of the actinides, which may limit the effectiveness of the currently available DTPA treatments.

Transdermal delivery of therapeutic agents provides many advantages over parenteral and oral routes such as more uniform plasma drug levels, a longer duration of action with a reduced dosing frequency, and improved patient compliance and comfort with ease of self-administration (10–13). It is highly desirable to deliver decorporation agents including DTPA to the circulation at a zero-order rate to better match actinide biokinetic profiles and thus achieve optimal radionuclide decorporation over an extended duration. Due to its low partition coefficient (log P=−4.90) and high melting point (219–220°C), DTPA is not a good candidate for transdermal delivery (12,14). However, the penta-ethyl ester of DTPA, designated as C2E5, was designed and synthesized as a new radionuclide decorporation prodrug to overcome the limitations of the current DTPA treatments (15,16). The structures of C2E5 as well as its potential degradation products and metabolites including DTPA tetra-ethyl ester (C2E4), DTPA tri-ethyl ester (C2E3), DTPA di-ethyl ester (C2E2), DTPA mono-ethyl ester (C2E1), and the fully de-esterified DTPA are shown in Fig. 1. C2E5 possesses physicochemical properties suitable for transdermal delivery. It has a log P value of 3.3, a log D value of 2.4 at pH7.0, its aqueous solubility is 3.0 mg/mL at pH7.0, and it is a Newtonian liquid with a viscosity of 175 cP at 25°C (16,17).

The aim of these studies was to develop C2E5 transdermal formulations and evaluate them for sustained delivery of DTPA and other active metabolites *in vivo*. Cream and ointment formulations were initially screened as potential C2E5 delivery vehicles, but the results showed that either C2E5 proved to be unstable in the matrices due to degradation or the C2E5 formulations underwent phase separation. C2E5 degradation in buffered aqueous solution follows pseudo-first order kinetics and C2E5 is most stable at a pH of approximately 4.2 (17). Due to the high hydrolytic tendency of the C2E5 ester bonds in aqueous media, nonaqueous gel formulations were pursued to stabilize the moisture-labile C2E5 in the delivery vehicles. Many drugs for topical and transdermal drug delivery are moisture-sensitive and undergo degradation reactions with water (18). The major degradation pathway involved with moisture-sensitive drugs is hydrolysis followed by secondary degradation reactions such as polymerization and isomerization (19). In contrast to extensive research on traditional semisolid dosage forms such as creams, ointments, and hydrogels, there are far fewer reports on the development of nonaqueous gel matrices intended for topical and transdermal drug delivery (20–24). Ethyl cellulose is frequently used as a gelling agent for nonaqueous gel vehicles. A series of nonaqueous gels with 15 and 20% (% *w*/*w*) ethyl cellulose were prepared as topical formulations of naproxen (20). Lee and colleagues developed a nonaqueous gel with 3–10% (% *w*/*w*) ethyl cellulose dispersed in an ethanol/tricaprylin (40:60, *w*/*w*) mixture (21). Lizaso and coworkers heated ethyl cellulose and phthalate ester derivative mixtures to 180°C and formed a nonaqueous gel during the cooling process (22). The Heng group reported on nonaqueous gel matrices containing ethyl cellulose and Miglyol 840®, which is a mixture of propylene glycol dicaprylate and dicaprate, obtained by directly mixing the ethyl cellulose and Miglyol 840 at 60°C (23). The rheological, mechanical, wettability, and spreadability properties of the ethyl cellulose/Miglyol 840 nonaqueous gels indicate that these matrices possess favorable attributes for transdermal and topical delivery (23,25,26). Here, we report on the preparation and characterization of C2E5 nonaqueous gels including their physical and rheological properties, determination of the stability of C2E5 in the gel, *in vitro* release properties, and preliminary *in vivo* pharmacokinetics of the lead C2E5 nonaqueous gel formulation.

MATERIALS AND METHODS

Materials

Miglyol 840 was purchased from Sasol (Hamburg, Germany). Ethyl cellulose polymers, including ETHOCEL Std 7 FP Premium (EC7), ETHOCEL Std 10 FP Premium (EC10), and ETHOCEL Std 100 FP Premium (EC100) with an ethoxyl content of 48.0–49.5%, were gifts from Dow Chemical (Midland, MI, USA). C2E5 was prepared based on the Fischer esterification method by reacting DTPA with ethanol under reflux in the presence of a hydrochloric acid catalyst (17). Acetonitrile, trifluoroacetic acid, anhydrous ethanol, methanol, isopropyl alcohol, formic acid, iron (III)

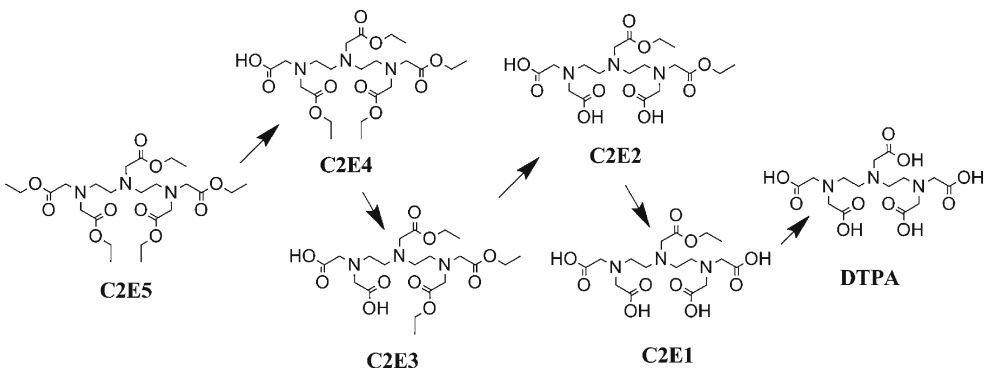

Fig. 1. Structures of DTPA, the prodrug C2E5, and its metabolites

chloride hexahydrate, ammonium formate, tributylamine, and acetic acid were purchased from VWR International (Radnor, PA, USA) or Fisher Scientific (Fairlawn, NJ, USA). Double-distilled water was obtained from a Milli-Q system (Millipore, Billerica, MA, USA).

Preparation of the C2E5 Nonaqueous Gels

The C2E5 nonaqueous gels were prepared using the solvent evaporation method. The EC10 material was dried at 60°C for ~24 h before use in gel preparations. Predried EC10 particles were initially dissolved in anhydrous ethanol (10% *w/v* of EC10 to ethanol) to form an EC10 stock solution. The C2E5 nonaqueous gel was prepared by mixing the EC10 stock solution, Miglyol 840 and C2E5 to form a homogenous solution, followed by removing ethanol under vacuum. When the gel was <102% of the theoretical weight, the C2E5 nonaqueous gels were transferred to a storage container under nitrogen and sealed with an airtight cap, covered with aluminum foil to protect from light, and stored at 4°C for later use.

The C2E5 concentration in these gel formulations was determined using a Shimadzu Prominence high pressure liquid chromatography (HPLC) system equipped with an Alltech 3300 evaporative light scattering detector (ELSD). A reverse-phase gradient separation was performed using an Alltima C18 column (250×2.1 mm I.D., 5 μm) at 40°C and a flow rate of 0.25 mL/min. The solvents that comprised the mobile phase were water with 0.1% trifluoroacetic acid (A), acetonitrile (B), and isopropyl alcohol (C). The linear gradient for the mobile phase mixture (A/B/C) was from 94:4:2 to 25:50:25 over 35 min, followed by a change to 0:0:100 in 0.5 min and an equilibration phase of 0:0:100 for 9.5 min, and ending with a reversal to 94:4:2 in 0.5 min and an equilibration phase of 94:4:2 for 9.5 min. The ELSD was operated at 40°C with 1.9 L/min nitrogen gas flow. Triplicate injections for each sample of C2E5 nonaqueous gel dissolved in anhydrous ethanol were performed with a volume of 10 μL per injection, and the retention time of C2E5 was 26 min. Samples were held at ambient temperature during analysis and analyzed using a standard curve over a concentration range of 0.02–2.00 mg/mL, which had a power regression fit of R^2=0.999. C2E5 nonaqueous gel samples stored at 4°C for 6 months were monitored for C2E5 degradation using this HPLC method.

Physical characterization, *in vitro* release testing and pharmacokinetic studies were performed with a formulation comprised of 20% EC10, 40% C2E5, and 40% Miglyol 840 prepared using the solvent evaporation method.

Differential Scanning Calorimetry

The EC10 polymer particles and the C2E5 nonaqueous gel samples were analyzed using a TA Instruments differential scanning calorimetry (DSC) Model Q200 under a nitrogen flow of 50 mL/min. Approximately 5–10 mg samples were heated in a sealed aluminum pan at a ramp rate of 10°C/min, cooled at a rate of 5°C/min, and subsequently heated at 10°C/min in heat/cool/heat mode from −10 to 160°C. The glass transition (T_g) and melting (T_m) temperatures in the third heating cycle were determined using TA Universal Software.

Rheological Measurements

A stress-controlled cone-and-plate rheometer (TA Instruments, Model AR-G2) with a cone of 40 mm in diameter and 1° cone angle at controlled temperatures of 25 ±0.5°C and 32±0.5°C was utilized to measure continuous shear rheometry of the nonaqueous gels with a formulation comprised of 20% EC10, 40% C2E5, and 40% Miglyol 840 prepared using the solvent evaporation method. The gel samples were carefully loaded to the lower plate to reduce shearing effects and equilibrated for 5 min at the designated temperatures prior to measurement. Fresh samples were used for each individual measurement, and triplicate measurements were performed for the formulation. Data are reported as mean±SD.

Continuous shear rheometry was obtained by changing the shear rate from 0.1 to 40 s^{-1} over a period of 300 s. The power law equation for simple steady shear (Eq. 1) was used to fit the data obtained from the upward flow curves (27):

$$\tau = m\dot{\gamma}^{n} \tag{1}$$

where τ=shear stress, $\dot{\gamma}$ = shear rate , m=consistency index, and n=flow behavior index.

The estimated yield stress was derived by fitting the data using the Casson model described in Eq. 2 (27):

$$\tau^{1/2} = \tau_y^{1/2} + \left(\eta\dot{\gamma}\right)^{1/2} \quad \text{for } \tau \geq \tau_y \tag{2}$$

where τ_y=yield stress and η=creep viscosity. The square root of yield stress τ_y was obtained from the plot as the y-axis intercept when $\dot{\gamma} = 0$.

In Vitro Release of C2E5 Nonaqueous Gel

An *in vitro* release study was carried out using a vertical diffusion cell system equipped with an autosampler (Hanson Microette Autosampling System, Hanson Research Co., USA) to evaluate the nonaqueous gel formulations comprised of 20% EC10, 40% C2E5, and 40% Miglyol 840 prepared using the solvent evaporation method. The area for permeation was 1.767 cm^2, and the receiver compartment volume was 7 mL. The receiver medium was 0.1 M phosphate buffer (pH7.4) maintained at 32°C and continuously stirred at 400 rpm. A cellulose acetate membrane (25 mm in diameter, with a 0.45 μm pore diameter, Whatman®) was first treated by soaking in the receiving medium and then mounted and clamped between the receiver and donor compartments of the diffusion cells. Approximately 300 mg of C2E5 nonaqueous gel was loaded evenly on the surface of the cellulose acetate membrane (n=5) and covered with a glass disk to exclude air. One-milliliter samples were removed from the receiver compartment at 0.5, 1, 2, 4, and 6 h, which were replaced with an equal volume of fresh media.

The C2E5 content in the collected samples was determined by the HPLC method described above. The cumulative amount of C2E5 released per unit membrane area from the tested nonaqueous gel was plotted as a function of the

square root of time and as a function of time. The Higuchi equation (Eq. 3) dictates the drug release from semisolid dosage forms including creams, gels, and ointments, and holds true when the released drug from the vehicle is below 30% (28,29):

$$Q = 2C_{veh}\sqrt{\frac{Dt}{\pi}} \quad (3)$$

where Q=amount of drug released per unit area (mg/cm^2), C_{veh}=initial drug concentration (mg/cm^3) in the vehicle, D=apparent diffusion coefficient (cm^2/h), t=time (h), and π=constant. The release rate constant k of C2E5 from the nonaqueous gel formulation was determined using a simplified form of the Higuchi equation (Eq. 4):

$$Q = k\sqrt{t} \quad (4)$$

where k is the release rate constant, which is determined from the slope of the cumulative amount of C2E5 released per unit membrane area from the nonaqueous gel *versus* the square root of time.

Fick's law (Eq. 5) has been used as a simple model to describe the steady-state diffusion of drug through synthetic membranes and skin:

$$J_{ss} = \left(\frac{D \times K_p}{h}\right) \times A \times C_{veh} \quad (5)$$

where J_{ss}=steady-state flux (mg/h), D=drug diffusivity (cm^2/h), h=membrane thickness (cm), K_p=drug's membrane-vehicle partition coefficient, C_{veh}=initial drug concentration (mg/cm^3) in the vehicle, and A=surface area (cm^2). J_{ss} can be determined from the slope of the linear plot in the steady-state region of the cumulative amount of C2E5 permeated (mg) per unit diffusion surface (cm^2) *versus* a function of time.

Throughout the experiment the C2E5 concentration in the receptor compartment was kept below 30% of the solubility of C2E5 at pH7.4, which is about 2.2 mg/mL at room temperature (17). Therefore, steady-state flux condition and sink condition were maintained for the duration of the experiment.

Absorption of C2E5 Administered as a Neat Oil or as a Nonaqueous Gel

All animal studies were conducted according to a protocol approved by the University of North Carolina at Chapel Hill Institutional Animal Care and Use Committee. Ten-week-old adult female Sprague–Dawley (SD) rats weighing 200–300 g were used in these studies (Charles River Labs, Raleigh, NC, USA). Food and water were provided *ad libitum*. The animal room was kept at a controlled temperature on a 12 h/12 h light/dark cycle (light exposure from 7 AM to 7 PM). For the duration of the study, the rats were individually housed in metabolic cages until euthanasia at 24 h after neat C2E5 oil or C2E5 gel application.

In all animals, the dorsal skin between the cervical vertebrae and anterior thoracic vertebrae of SD rats was carefully clipped prior to drug application to remove hair. C2E5 nonaqueous gel was applied at a C2E5 dose of 200 mg/kg to a 2×3 cm region using a cotton swab. For comparison, neat C2E5 oil (200 mg/kg) was applied using a 1-mL syringe to the same size area on a control group of rats. For each rat, the mass of the drug and applicator was recorded before and after application with the difference being the delivered dose. Finally, a jacket with a dermal insert (VWR International, Radnor, PA, USA) was placed on the rats to protect the applied treatments. Blood samples (0.4 mL) were collected from the tail vein using SurFlash® polyurethane i.v. catheters (Terumo, Somerset, NJ, USA) at either before or 0.5 h after treatment and then at 1, 2, 4, 8, 12, and 24 h after treatment. The collected samples were immediately transferred from the syringes into prechilled sampling tubes containing 5 mg sodium fluoride and 4 mg potassium oxalate (BD Vacutainer product number 367921). The tubes were inverted eight times per manufacturer's recommendation and centrifuged (1,300×*g* for 10 min at 4°C). Plasma samples were then portioned into two 1.7-mL Eppendorf tubes, which contained an equal amount of a 20% formic acid aqueous solution. These tubes were immediately vortexed and placed on dry ice until transfer to storage at −80°C until analysis. The animals were transferred to individual housing in metabolic cages after C2E5 treatment. Animals were euthanized 24 h after C2E5 gel or neat C2E5 oil application. The animals were observed during the study period, and the body weight of each animal was recorded at predose and prior to necropsy.

A liquid chromatography–tandem mass spectrometry (LC/MS/MS) method was developed for the analysis of C2E5 and metabolites except for the fully de-esterified metabolite, DTPA, in these samples. Acidified plasma samples (100 μL) were first treated with 25 μL of ^{13}C-C2E5 stable-label internal standard (1,000 ng/mL), followed by precipitation with acetonitrile (400 μL). The supernatant (400 μL) was removed and evaporated to dryness, and the residue was reconstituted with 500 μL of 85/15/0.1% water/acetonitrile/formic acid. A 10-μL injection was used for LC/MS/MS analysis. Reverse-phase chromatography was performed at 0.3 mL/min on a YMC® ODS-AM C18 (100×2 mm, 3 μm) column with mobile phases A (0.1% formic acid in water) and B (0.1% formic acid in acetonitrile) using a 10-min gradient (isocratic at 13% mobile phase B for 1 min, linear gradient to 50% mobile phase B at 6 min, linear gradient to 60% mobile phase A at 6.5 min, linear gradient to 90% mobile phase B at 8 min, return to initial 13% mobile phase B at 8.1 min, and equilibrate at 13% mobile phase B until 10 min). After separation by liquid chromatography, the analytes and internal standard were detected on a triple quadrupole mass spectrometer using heated electrospray ionization (HESI-II) (Thermo Scientific) in the positive-ion mode. Suitable reference standard material was available to provide reliable results for C2E5, C2E4, and C2E2. Although reference standard material was not available for C2E3 and C2E1, these analytes were present as trace impurities in the reference standards for C2E5, C2E4, and C2E2. The assumption of response factors for C2E3 and C2E1 equal to those of the reference standards afforded an estimate of the concentrations of C2E3 and C2E1 in calibration standards; this allowed the generation of calibration curves for C2E3 and C2E1 that were used to estimate the levels of these analytes in samples. Due to lack of pure internal standards for C2E3 and C2E1, the plasma concentrations of C2E3 and

C2E1 in the samples were considered as estimates. The lower limit of quantification (LLQ) for C2E5, C2E4, C2E3, C2E2, and C2E1 were determined to be 5.0, 10.0, 1.0, 10.0, and 5.0 ng/mL, respectively.

For detection of DTPA, acidified plasma samples (100 μL) were first treated with 50 μL of 2 mM iron(III) chloride hexahydrate, followed by addition of 400 μL of ^{13}C-DTPA stable-label internal standard (100 ng/mL in 0.1% acetic acid in acetonitrile). This solution was vortexed for 5 min and then centrifuged at 3,000 rpm for 10 min. The supernatant (350 μL) was removed, evaporated to dryness, and reconstituted with 100 μL of 0.1% aqueous acetic acid. A 10-μL aliquot of the reconstituted sample was used for LC/MS/MS analysis. The highly polar nature of DTPA required the incorporation of ion-pairing chromatography to produce acceptable LC peak shape and retention. Mobile phase A was 90:10 water/methanol with 1 mM ammonium formate and 1 mM tributylamine, and mobile phase B was 50:50 acetonitrile/(5:95 water/methanol) with 1 mM acetic acid and 1 mM tributylamine. A 10 min gradient was used to afford separation (isocratic at 5% mobile phase B for 1 min, linear gradient to 80% mobile phase B at 7 min, linear gradient to 90% mobile phase B at 7.1 min, maintaining at 90% mobile phase B through 8 min, return to initial 5% mobile phase B at 8.1 min, and equilibrate at 5% mobile phase B until 10 min). Reverse-phase chromatography was performed at 0.3 mL/min on an Advanced Materials Technology HALO® Phenyl-Hexyl column (50×2.1 mm, 2.7 μm). The analyte and internal standard were detected on a triple quadrupole mass spectrometer using HESI-II in the negative-ion mode. The LLQ for DTPA was determined to be 10.0 ng/mL.

For C2E5 and its metabolites in the pharmacokinetic samples, plasma concentrations below the limit of quantification were labeled as not detected (ND) and assigned a value of zero for the area under the curve (AUC) analysis. The AUCs were calculated using the trapezoidal method.

Statistical Analyses

The concentrations of C2E2 and C2E3 in plasma samples collected at different times from the two C2E5 dosage forms (neat oil and nonaqueous gel) were compared by unbalanced two-way analysis of variance (ANOVA). Analysis of the calculated exposure to C2E3 and C2E2 was by two-tailed *t* test. All measurements are expressed as mean±standard deviation (SD). The level of significance was set at $p<0.05$.

RESULTS

Preparation of C2E5 Nonaqueous Gels

The solvent evaporation method was used to prepare the C2E5 nonaqueous gel formulations. To maximize C2E5 loading in the gel and achieve desirable rheological and mechanical properties, a formulation that contained 40% C2E5, 20% EC10, and 40% Miglyol 840 was prepared and yielded a slightly yellow translucent gel, which was determined to have a density of 1.02 g/cm^3. Based on the HPLC analysis, the C2E5 content in nonaqueous gel samples stored at 4°C for 6 months contained 98.2% of the C2E5 content in a freshly prepared C2E5 nonaqueous gel, with C2E4 being as the main degradant.

Thermal Analysis by DSC

The DSC thermogram of predried EC10 showed one minor endothermic peak appearing at 63°C and one major endothermic peak at 120°C. The endothermic peak at 120°C is the EC10 glass transition temperature (30). The endothermic peak at 63°C may be the result of the presence of glyoxal, an impurity in ethyl cellulose (19), or glyoxal reaction products. However, further investigation is necessary for confirmation of this peak. The DSC thermogram of the C2E5 nonaqueous gel containing 20% EC10, 40% C2E5, and 40% Miglyol 840 prepared using the solvent evaporation method showed no prominent endothermic peaks in the range from −10 to 160°C. Complete dissolution of the EC10 in ethanol prior to gel formation eliminated the EC10 glass transition endothermic peak at 120°C. The impurity in EC10, which showed the endothermic peak at 63°C on the DSC thermogram of predried EC10, could possibly have been dissolved in ethanol and later removed during the solvent evaporation process, either through direct evaporation (the boiling point of glyoxal is 51°C) or by formation of an azeotrope with ethanol. The residual water content in the gel components could also have been effectively removed during the solvent evaporation process by formation of an azeotrope with ethanol.

Rheological Measurement Results

Rheograms derived from continuous shear rheometry (Fig. 2) demonstrated that the C2E5 nonaqueous gel is a typical shear-thinning system at both 25 and 32°C. The shear stress *versus* shear rate rheogram exhibits a convex shape and a hysteresis loop. The rheological properties of the 40% C2E5 nonaqueous gel at different temperatures are

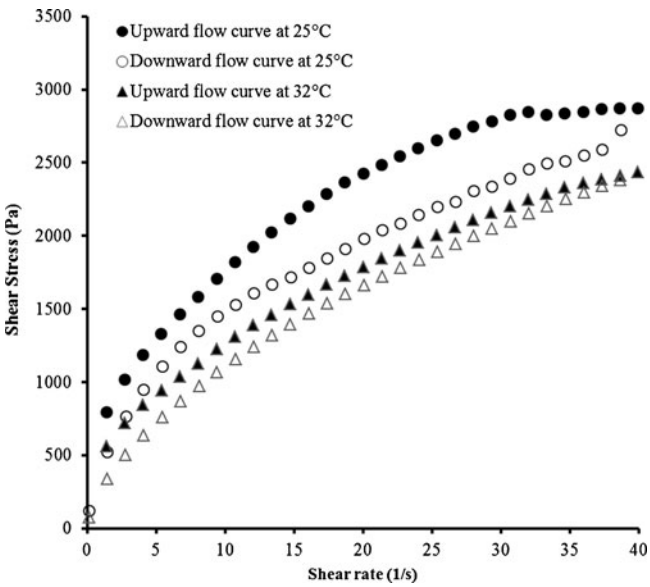

Fig. 2. Continuous shear rheogram showing shear rate *versus* shear stress at 25°C and 32°C of C2E5 nonaqueous gel comprised of 20% EC10, 40% C2E5, and 40% Miglyol 840 prepared using the solvent evaporation method

summarized in Table I. The flow behavior index values (n) were below 1 for both the 25 and 32°C measurements, indicating a shear-thinning gel structure under each of these temperature conditions (31). Yield stress and hysteresis area are parameters representing the rigidity and cohesion between the molecules forming a three-dimensional gel structure and the extensiveness of this three-dimensional gel structure (32,33).

In Vitro Release of C2E5 Nonaqueous Gel

A plot of the cumulative amount of C2E5 released per unit membrane area *versus* the square root of time, for the lead nonaqueous gel (20% EC10, 40% C2E5, and 40% Miglyol 840), is presented in Fig. 3. The cumulative amount of C2E5 released per unit membrane area from the lead nonaqueous gel *versus* the square root of time yielded a linear plot with $y=1.57x-0.78$ and $R^2=0.996$. The amounts of C2E5 released after 6 h from the five individual *in vitro* release runs ranged from 2.89 to 3.33 mg/cm^2, with an average value of 3.11±0.17 mg/cm^2 (coefficient of variance=5.5%). The average release rate constant k and average steady-state flux J_{ss} per unit area of the 40% C2E5 nonaqueous gel were determined to be 1.57±0.09 mg cm^{-2} h$^{-0.5}$ and 0.556±0.031 mg cm^{-2} h^{-1}, respectively, with both having a coefficient of variance of 5.6%. For each individual run, an acceptable linear regression fit was achieved for the release rate constant k per unit area ($R^2 \geq 0.994$) and the steady-state flux J_{ss} per unit area ($R^2 \geq 0.969$).

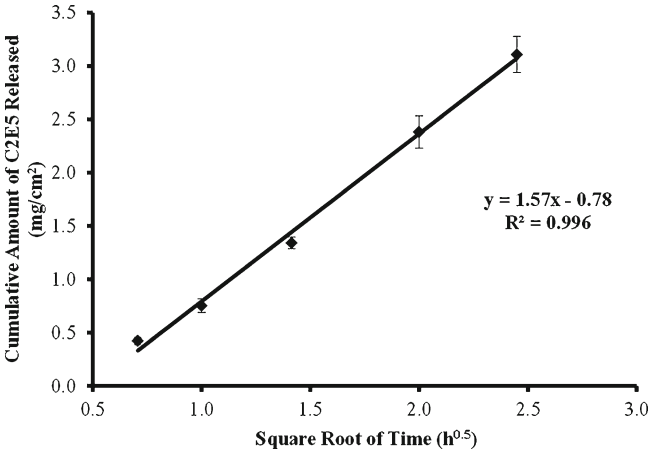

Fig. 3. Relationship between square root of time and cumulative amount of C2E5 released through a cellulose membrane into 0.1 M phosphate buffer after application of C2E5 nonaqueous gel (n=5). The C2E5 nonaqueous gel consisted of 20% EC10, 40% C2E5, and 40% Miglyol 840. The release rate constant k is determined from the slope of the cumulative amount of C2E5 released per unit membrane area from the tested nonaqueous gel *versus* square root of time defined in Eq. 4

Absorption of C2E5 Administered as a Neat Oil or as a Nonaqueous Gel

Following topical application of either the neat C2E5 oil or the 40% C2E5 nonaqueous gel, the principal circulating metabolites detected in plasma were C2E3 and C2E2. The concentrations of C2E3 and C2E2 detected in the rat plasma samples plotted *versus* time for the neat C2E5 oil and the 40% C2E5 nonaqueous gel groups are presented in Figs. 4 and 5, respectively. Two-way ANOVA showed that the C2E5 dosage form had a significant effect on the plasma concentration of both C2E2 [$F_{Formulation(1,36)}=13.3$, $p<0.001$] and C2E3 [$F_{Formulation(1,36)}=6.91$, $p<0.05$]. The time the plasma was sampled was not a significant factor for either metabolite [C2E2, $F_{Time(7,36)}=1.06$, $p=0.41$ and C2E3, $F_{Time(7,36)}=0.84$, $p=0.56$], and no interaction between dosage form and time was observed [C2E2, $F_{Interaction(7,36)}=0.84$, $p=0.56$ and C2E3, $F_{Interaction(7,36)}=1.04$, $p=0.42$]. The pharmacokinetic parameters of C2E3 and C2E2 after application of neat C2E5 oil or 40% C2E5 nonaqueous gel at 200 mg/kg dose (n=4) are shown in Table II. We observed a trend for increased exposure to the metabolites C2E3 and C2E2 following C2E5 application as a nonaqueous gel compared with application as the neat oil; however, this trend did not reach statistical significance for either metabolite alone (AUC_{C2E2}, $p=0.073$ and AUC_{C2E3}, $p=0.087$; both two-tailed t test). Enhancement ratios based on the AUCs for C2E3 and C2E2 were determined to compare the AUC obtained from the 40% C2E5 nonaqueous gel group to the neat C2E5 oil group.

There was only two plasma samples in which C2E5 was detected with a concentration above the LLQ among the 56 samples, one from the neat C2E5 oil group (28.4 ng/mL at 2 h) and one from the C2E5 nonaqueous gel group (7.2 ng/mL at 24 h). There were five plasma samples in which C2E4 was detected with a concentration above the LLQ among 56 samples, three from the neat C2E5 oil group (13.5 ng/mL at 0.5 h, 52.7 ng/mL at 2 h and 45.1 ng/mL at 24 h), and two from the C2E5 nonaqueous gel group (59.9 ng/mL at 1 h and 83.8 ng/mL at 2 h).

C2E3 and C2E2 species were consistently detected in the plasma samples from both groups throughout the experimental period with the C_{max} values ranging from 85.3 to 485 ng/mL for C2E3 and from 17.4 to 413 ng/mL for C2E2, indicating that C2E3 and C2E2 are stable C2E5 metabolites *in vivo*. The concentrations of C2E3 and C2E2 reported in

Table I. Rheological Properties of a 40% C2E5 Nonaqueous Gel at Different Temperatures

Temperature (°C)	Flow behavior index, n	Consistency index, m (Pas^n)	Apparent viscosity[a] (Pas)	Yield stress (Pa)	Hysteresis area (kPas^{-1})
	Mean±SD				
25	0.407±0.013	691±17	177±1	663±18	16.7±0.7
32	0.462±0.005	446±13	129±3	381±14	7.71±0.28

[a] Apparent viscosity at a shear rate of 10 s^{-1}

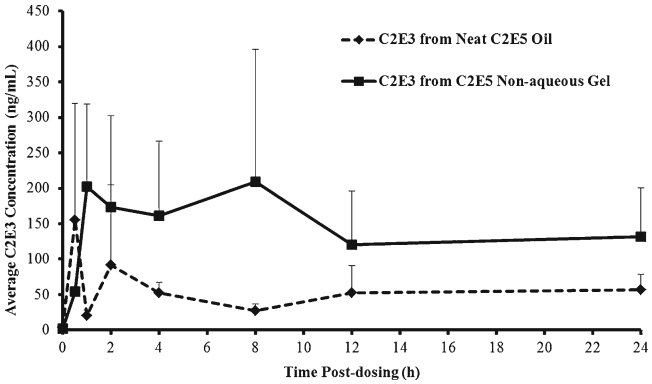

Fig. 4. Concentration of C2E3 detected in rat plasma *versus* time after topical administration of the neat C2E5 oil and the 40% C2E5 nonaqueous gel (mean±SD) (n=4)

the rat plasma samples *versus* time figures showed a sustained release profile from transdermal neat C2E5 oil and C2E5 nonaqueous gel formulations. Average steady-state concentrations (C_{ss}) for both C2E3 and C2E2 were between 100 and 200 ng/mL for the C2E5 nonaqueous gel group and between 20 and 80 ng/mL for the neat C2E5 oil group. Overall systemic exposures to C2E3 and C2E2 were approximately 2.9- and 4.2-fold (based on $AUC_{0-24\ h}$) higher for the C2E5 nonaqueous gel group compared to the neat C2E5 oil group.

There was no C2E1 detected above the quantification limit in any rat plasma samples for either the neat C2E5 oil group or the C2E5 nonaqueous gel group during the experimental period. DTPA was frequently detected in the plasma samples at time points after 4 h postdosing for both the neat C2E5 oil group and the C2E5 nonaqueous gel group. Most of the detected DTPA plasma concentrations were in the range of 10 ng/mL to 30 ng/mL, which is just above the LLQ of DTPA (10 ng/mL). The maximum DTPA concentration detected in plasma in the neat C2E5 oil group was 61.4 ng/mL, compared with 693 ng/mL in the C2E5 nonaqueous gel group.

DISCUSSION

Nonaqueous gel formulations have been a useful vehicle for moisture-sensitive drugs for topical and transdermal application (20–24). Critical components for the successful development of a semisolid product for topical and transdermal applications include the stability of the active pharmaceutical ingredient (API) in the delivery matrix, product uniformity, and the release profile of API from the delivery matrix. In this study, we report on the development and characterization of a nonaqueous gel formulation that stabilizes the hydrolysis-prone API, enhances its percutaneous permeation flux, and improves its pharmacokinetic profile following topical application to rats.

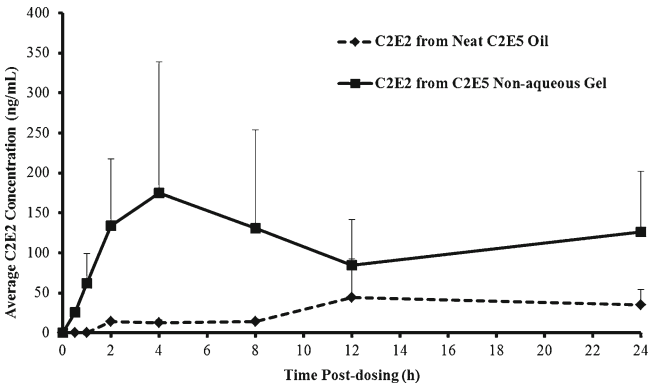

Fig. 5. Concentration of C2E2 detected in rat plasma *versus* time after topical administration of the neat C2E5 oil and the 40% C2E5 nonaqueous gel (mean±SD) (n=4)

Candidate nonaqueous gel formulations showed improved stability of C2E5 under various storage conditions when compared with the neat API and other tested delivery vehicles, such as creams and ointments (34,35), suggesting a clear benefit of the ethyl cellulose based nonaqueous gel for this moisture-sensitive compound. The enhanced stability profile of C2E5 in the nonaqueous gel matrix is probably due to decreased interactions with the hydroxyl groups on the ethyl cellulose polymer chains. These hydroxyl groups are not readily available to interact with other molecules compared to the hydroxyl groups in small molecule due to steric and rotational hindrance. The use of Miglyol 840 neutral oil as a dispersion medium also contributes to the enhanced stability of C2E5 in the gel matrix because Miglyol 840 is nonhygroscopic, possesses high stability against oxidation, and contains no free hydroxyl groups (23).

Modification of the published direct mixing method for gel preparation (23), using anhydrous ethanol to dissolve the ethyl cellulose before forming the gel and then evaporating the ethanol from the gel mixture, resulted in a significant improvement in gel uniformity. Although the solvent evaporation method is a commonly used technique for making films, microspheres, and solid dispersions (36–38), to our knowledge, this method has not been reported previously for preparation of ethyl cellulose based nonaqueous gels. To minimize the amount of solvent used in the gel preparation, EC7 and EC10 were selected because much more ethanol is needed to dissolve EC100 than for equal amounts of EC7 or EC10. Our method of gel preparation requires simple evaporation of the solvent and is suitable for scale-up, with ethanol content in the gels readily reduced to below 2% of gel weight. The solvent evaporation method was successfully scaled up to prepare 400 g of C2E5 nonaqueous gels in one batch. Any residual ethanol present in the gel system would not interact with the C2E5 molecules and might possibly retard its hydrolysis. Ethanol is approved for human use in commercial topical and transdermal products at relatively high concentrations as a basic component and can act as a permeation enhancer by changing the characteristics of the skin (23,39). A C2E5 formulation screening study was carried out and phase separation was observed in gels with low EC content (<10%) and particularly in gels with lower molecular weight EC chains. This phase separation may be due to a decrease in the interactions between the gel matrix and the C2E5 dissolved in it (data not shown). A C2E5 nonaqueous gel formulation comprised of 20% EC10, 40% C2E5, and 40% Miglyol 840 was chosen as a candidate formulation for further physical characterization and *in vivo* pharmacokinetic evaluation.

The stability study with the 40% C2E5 nonaqueous gel showed that <2% of C2E5 had degraded after being stored at 4°C for 6 months, suggesting an acceptable stability profile of

Table II. Pharmacokinetic Parameters of C2E3 and C2E2 After Application of Neat C2E5 Oil or 40% C2E5 Nonaqueous gel at a C2E5 Dose of 200 mg/kg (n=4) and the Enhancement Ratio of C2E3 and C2E2 Based on the Formula $AUC_{0–24\ h\ (C2E5\ gel)}/AUC_{0–24\ h\ (neat\ C2E5)}$

Treatment	C2E3				C2E2			
	C_{max} (mean±SD, μg/mL)	T_{max} (mean± SD, h)	$AUC_{0\text{-}24h}$ (mean±SD, h×μg/mL)	Enhancement ratio ($AUC_{0–24\ h\ (C2E5\ gel)}$/ $AUC_{0–24\ h\ (neat\ C2E5)}$)	C_{max} (mean±SD, μg/mL)	T_{max} (mean± SD, h)	$AUC_{0\text{-}24h}$ (mean±SD, h×μg/mL)	Enhancement ratio [$AUC_{0–24\ h\ (C2E5\ gel)}$/ $AUC_{0–24\ h\ (neat\ C2E5)}$]
Neat C2E5 oil at 200 mg/kg	0.181±0.097	9.6±10.9	1.21±0.16		0.059±0.041	17.0±8.2	0.660±0.351	
40% C2E5 nonaqueous gel at 200 mg/kg	0.281±0.159	4.5±4.0	3.52±2.26	2.9	0.203±0.161	4.5±2.5	2.75±1.89	4.2

C_{max} maximum plasma concentration during 0–24 h period, T_{max} time of maximum plasma concentration during 0–24 h period, $AUC_{0–24\ h}$ area under the curve during 0–24 h period

this formulation. As demonstrated by the DSC thermograms, the slightly yellow translucent C2E5 nonaqueous gel possessed acceptable uniformity. This was a result of EC10 being completely solubilized in ethanol before incorporation into the gel matrix and thus eliminating the problems related to residual EC particulates encountered when using the direct mixing method.

The rheological and mechanical properties of the nonaqueous gel matrices containing ethyl cellulose and Miglyol 840 were investigated in detail by the Heng group (23). The rheological properties of the C2E5 nonaqueous gel comprised of 20% EC10, 40% C2E5, and 40% Miglyol 840 (Table I) exhibited characteristics and flow patterns similar to nonaqueous gels comprised of ethyl cellulose and Miglyol 840, suggesting that an adequate adhesion force to the skin surface for prolonged periods could be maintained, a critical property for the sustained delivery of drug substance from the gel (40). Other characteristics, such as a 36.6% decrease in viscosity from 177 (Pas) to 129 (Pas) and a 117% decrease in hysteresis area with a temperature increase from 25 to 32° C, are good indicators that the gel is suitable for application on human skin with a surface temperature of 32–34°C. The *in vivo* pharmacokinetic studies using this gel formulation confirmed the predictions based on these physical measurements; the gel spread easily during application and remained at the application site for the entire study. In contrast, neat C2E5 oil presented a challenge for application to the skin and retention at the application site due to its lower viscosity.

In vitro release testing is widely used to assess content uniformity and drug release from semisolid products and can also be used to compare performance across different batches and after storage or changes in the manufacturing process (41,42). Although transdermal delivery of C2E5 to the systemic circulation is a multistep process, *in vitro* release results suggest that C2E5 is readily released from the nonaqueous gel matrix and the steady state flux (0.556± 0.031 $mgcm^{-2}h^{-1}$) associated with this release is expected provide the required sustained concentration of drug in plasma. The narrow distribution of the release rate constant (1.57±0.09, coefficient of variance=5.6%) confirmed the optimal content uniformity of the 40% C2E5 nonaqueous gel prepared by solvent evaporation method.

Pharmacokinetic data obtained from *in vivo* studies confirmed our observations from the *in vitro* release testing, with metabolites of C2E5 detected in plasma throughout the collection period. Additionally, an improved plasma pharmacokinetic profile for drug released from the C2E5 nonaqueous gel compared with the neat C2E5 oil suggests that Miglyol 840, a major component of the gel, perhaps along with residual ethanol in the gel, are working as permeation enhancers (23,39,43). The enhanced ratios of systemic exposure to major C2E5 metabolites (C2E3 and C2E2) with C2E5 nonaqueous gel were greater than those observed with neat C2E5 oil. The pharmacokinetic data also support our hypothesis that the mismatch between the biokinetics of transuranic contaminants and the pharmacokinetics of DTPA used to treat contamination could be overcome using a transdermal prodrug strategy.

C2E5 and C2E4 were only detected in concentrations above their respective LLQs in <10% of all samples; detection of C2E4 suggests that it is a direct metabolite of C2E5 *in vivo*, generated by a stepwise de-esterification process involving esterases in the rat skin and plasma (44,45). C2E2 and C2E3 were observed as the principal metabolites detected in circulation throughout the 24 h study period, matching the findings of the C2E5 *in vitro* metabolism study (44,45). C2E1 was not detected above the LLQ in any plasma samples throughout the study, but is likely present transiently resulting from the stepwise de-esterification of C2E5 to DTPA. Detection of DTPA at low concentrations, close to the 10 ng/mL LLQ, was not unexpected as DTPA has a short half-life ranging from 18.5 to 31.8 min (8,9).

In addition to DTPA, other metabolites, such as C2E3, C2E2, and C2E1, may effectively sequester transuranic radionuclides and form stable complexes. For example, ^{241}Am, an abundant transuranic radionuclide, forms complexes with various chelators, including DTPA and other molecules structurally similar to C2E3, C2E2, and C2E1, with stability constants ranging from 10.7 to 24.0 M^{-1} (46). Although stability constants for americium binding to C2E5 metabolites are not known, the binding of Gd^{3+} with DTPA mono-propyl ester and DTPA di-propyl ester (compounds analogous to C2E1 and C2E2) are reported to be 18.91 and 16.30 M^{-1} (47). Because gadolinium is viewed as a biochemical analogue of americium and Gd^{3+} ion is structurally very similar to $^{241}Am^{3+}$ (48,49), comparable binding constants and thermodynamic stability can be

expected for the binding of $^{241}Am^{3+}$ with C2E1 and C2E2 *in vivo*. Furthermore, studies in americium-contaminated rats demonstrated that C2E5 administered orally enhanced ^{241}Am decorporation (17,50).

CONCLUSIONS

The penta-ethyl ester of DTPA (C2E5) was incorporated into a nonaqueous gel comprised of ethyl cellulose and Miglyol 840 using the solvent evaporation method, and was characterized by thermal and rheological analysis and *in vitro* release. A superior pharmacokinetic profile of C2E5 metabolites, including DTPA, was achieved when C2E5 was administered as a nonaqueous gel as opposed to a neat oil, perhaps as a result of permeation enhancement by Miglyol 840 and ethanol. These findings demonstrate that transdermal delivery of a chelator prodrug is a viable approach for delivering DTPA and other chelating agents to the circulation as a potential treatment of transuranic radionuclide contamination and provide additional understanding of the properties of nonaqueous gel formulations as well as their utility in applications requiring transdermal and topical delivery of moisture-sensitive drugs.

ACKNOWLEDGMENTS

The authors thank Dr. Richard Superfine and UNC Center for Computer Integrated Systems for Microscopy and Manipulation at UNC-Chapel Hill for access to the rheometer, which was funded by NIBIB/NIH award number P41-EB002025, and Dr. Joseph DeSimone for access to the differential scanning calorimeter. The authors also thank Mrs. Shraddha Shapariya for her help with pharmacokinetic studies, Dr. Jeremy Cribb for his help with the rheometer measurements, and Ms. Sara White for help with the differential scanning calorimeter. This work was funded in part by the National Institute of Health, US Department of Health and Human Services under contract HHSN266200500045C.

REFERENCES

1. Howard WL, Wilson D. Chelating agents. Kirk–Othmer Encyclopedia of Chemical Technology. New York:Wiley; 2000.
2. Taylor DM, Stradling GN, Hengé-Napoli M-H. The scientific background to decorporation. Radiat Prot Dosim. 2000;87 (1):11–8.
3. Taylor DM, Volf V. Oral chelation treatment of injected ^{241}Am or ^{239}Pu in rats. Heal Phys. 1980;38(2):147–58.
4. Volf V. Effect of drinking Zn-DTPA on 238-Pu and 241-Am in rat bones. Radiat Environ Biophys. 1984;23(2):141–3.
5. Stradling GN, Gray SA, Ellender M, Pearce M, Wilson I, Moody JC, *et al*. Removal of inhaled plutonium and americium from the rat by administration of ZnDTPA in drinking water. Hum Exp Toxicol. 1993;12(3):233–9. Comparative Study.
6. FDA approves drugs to treat internal contamination from radioactive elements (2004) http://www.fda.gov/NewsEvents/Newsroom/PressAnnouncements/2004/ucm108339.htm. Accessed 30 May 2012.
7. National Council on Radiation Protection and Measurements; National Council on Radiation Protection and Measurements. Scientific Committee 57–17 on Radionuclide Dosimetry Model for Wounds. Development of a biokinetic model for radionuclide-contaminated wounds and procedures for their assessment, dosimetry, and treatment: recommendations of the National Council on Radiation Protection and Measurements, December 14, 2006. Bethesda: National Council on Radiation Protection and Measurements; 2007. pp. 35–117.
8. Crawley FE, Haines JW. The dosimetry of carbon-14 labelled compounds: the metabolism of diethylenetriamine pentaacetic acid (DTPA) in the rat. Int J Nucl Med Biol. 1979;6(1):9–15.
9. Phan G, Herbet A, Cholet S, Benech H, Deverre JR, Fattal E. Pharmacokinetics of DTPA entrapped in conventional and long-circulating liposomes of different size for plutonium decorporation. J Control Release. 2005;110(1):177–88.
10. Brown L, Langer R. Transdermal delivery of drugs. Annu Rev Med. 1988;39(1):221–9.
11. Sloan KB. Prodrugs: topical and ocular drug delivery. New York: Marcel Dekker; 1992.
12. Chien YW. Novel drug delivery systems. 2nd ed. New York: Marcel Dekker; 1992.
13. Walters KA. Dermatological and transdermal formulations: London: Informa HealthCare; 2002.
14. Diethylenetriaminepentaacetic acid (DTPA) Material safety data sheet. www.sigmaaldrich.com, Version 4.8. Accessed 30 May 2012.
15. Cassatt DR, Kaminski JM, Hatchett RJ, DiCarlo AL, Benjamin JM, Maidment BW. Medical countermeasures against nuclear threats: radionuclide decorporation agents. Radiat Res. 2008;170 (4):540–8.
16. Jay M, Mumper RJ. Methods and pharmaceutical compositions for decorporation of radioactive compounds. United States Patent 8,030,358; 2011.
17. Sueda K, Sadgrove MP, Fitzsimmons JM, Jay M. Physicochemical characterization of a prodrug of a radionuclide decorporation agent for oral delivery. J Pharm Sci. 2012;101 (8):2844–53.
18. Langner M, Maibach H. Many common drugs in dermatology are light, temperature, or moisture-sensitive. Skin Therapy Lett. 2009;14(1):3–5.
19. Crowley P, Martini LG. Drug–excipient interactions. Pharm Technol Eur. 2001;13(3):26–34.
20. Claramonte M, Parera Vialard A, Vilchez FG. *In vitro* percutaneous absorption of naproxen from gels using a double-layer artificial membrane. Int J Pharm. 1993;98(1–3):37–43.
21. Lee C, Kitagawa K, Uchida T, Kim N, Goto S. Transdermal delivery of theophylline using an ethanol/panasate 800-ethylcellulose gel preparation. Biol Pharm Bull. 1995;18(1):176.
22. Lizaso E, Muñoz ME, Santamaría A. Formation of gels in ethylcellulose solutions. an interpretation from dynamic viscoelastic results. Macromolecules. 1999;32(6):1883–9.
23. Heng PWS, Chan LW, Chow KT. Development of novel nonaqueous ethylcellulose gel matrices: rheological and mechanical characterization. Pharm Res. 2005;22(4):676–84.
24. Chow K, Chan L, Heng P. Formulation of hydrophilic nonaqueous gel: drug stability in different solvents and rheological behavior of gel matrices. Pharm Res. 2008;25(1):207–17.
25. Chan L, Chow K, Heng PWS. Investigation of wetting behavior of nonaqueous ethylcellulose gel matrices using dynamic contact angle. Pharm Res. 2006;23(2):408–21.
26. Chow KT, Chan LW, Heng PWS. Characterization of spreadability of nonaqueous ethylcellulose gel matrices using dynamic contact angle. J Pharm Sci. 2008;97(8):3467–82.
27. Macosko CW. Rheology: principles, measurements, and applications. New York: VCH; 1994. p. 65–108.
28. Higuchi T. Physical chemical analysis of percutaneous absorption process from creams and ointments. J Soc Cosmet Chem. 1960;11 (2):85–97.
29. Higuchi W. Analysis of data on the medicament release from ointments. J Pharm Sci. 1962;51(8):802–4.
30. Rekhi GS, Jambhekar SS. Ethylcellulose—a polymer review. Drug Dev Ind Pharm. 1995;21(1):61–77.
31. Chang JY, Oh YK, Choi HG, Kim YB, Kim CK. Rheological evaluation of thermosensitive and mucoadhesive vaginal gels in physiological conditions. Int J Pharm. 2002;241(1):155–63.
32. Pena LE, Lee BL, Stearns JF. Structural rheology of a model ointment. Pharm Res. 1994;11(6):875–81.
33. Contreras MD, Sanchez R. Application of a factorial design to the study of the flow behavior, spreadability and

transparency of a Carbopol ETD 2020 gel. Part II. Int J Pharm. 2002;234(1–2):149–57.
34. Zhang Y, Sadgrove M, Jay M. Transdermal delivery of DTPA prodrug for continuous decorporation of transuranic elements. Abstract T2248. AAPS Annual Meeting and Exposition, Washington, October, 2011. http://www.aapsj.org/abstracts/AM_2011/T2248.pdf.
35. Yang Y-T, Di Pasqua AJ, He W, Tsai T, Sueda K, Zhang Y, *et al*. Preparation of alginate beads containing a prodrug of diethylenetriaminepentaacetic acid. Carbohydrate Polymers. 2012;92:1915–1920. doi:10.1016/j.carbpol.2012.11.071.
36. Banker GS. Film coating theory and practice. J Pharm Sci. 1966;55(1):81–9.
37. Bodmeier R, McGinity JW. The preparation and evaluation of drug-containing poly (dl-lactide) microspheres formed by the solvent evaporation method. Pharm Res. 1987;4(6):465–71.
38. Leuner C, Dressman J. Improving drug solubility for oral delivery using solid dispersions. Eur J Pharm Biopharm. 2000;50(1):47–60.
39. Lachenmeier DW. Safety evaluation of topical applications of ethanol on the skin and the oral cavity. J Occup Med Toxicol. 2008;3:26.
40. Barry BW. Dermatological formulations: percutaneous absorption. New York: Marcel Dekker; 1983. pp. 296–440.
41. Shah VP, Elkins J, Hanus J, Noorizadeh C, Skelly JP. *In vitro* release of hydrocortisone from topical preparations and automated procedure. Pharm Res. 1991;8(1):55–9.
42. Shah VP. *In vitro* release from semisolid dosage forms? What is its value? Percutaneous absorption. London: Informa Healthcare; 2005. pp. 481–8.
43. Pharmacopoeia E. 2002 European Pharmacopoeia. 4th ed. Strasbourg: Council of Europe; 2002.
44. Zhang Y, Yang Y-T, Jay M. Species-dependent metabolism of a DTPA prodrug by skin esterases. Abstract T2424. AAPS Annual Meeting and Exposition, Washington, October, 2011. http://www.aapsj.org/abstracts/AM_2011/T2424.pdf.
45. Pacyniak E, M. Leed, M. Sadgrove, Jay M. Interspecies differences in metabolism of a multi-ester prodrug by carboxylesterases. Abstract W4419. AAPS Annual Meeting and Exposition. Washington, October, 2011. http://www.aapsj.org/abstracts/AM_2011/W4419.pdf.
46. Morss LR, Edelstein NM, Fuger J, Katz JJ. The chemistry of the actinide and transactinide elements, vol. 2. 3rd ed. Dordrecht: Springer; 2006. p. 1265–395.
47. Sherry AD, Cacheris WP, Kuan KT. Stability constants for Gd3+ binding to model DTPA-conjugates and DTPA-proteins: implications for their use as magnetic resonance contrast agents. Magn Reson Med. 1988;8(2):180–90.
48. Shutt A, Youngman M, Raine C, Stradling G, Etherington G, Kreyling W. A study of the human biokinetics of inhaled gadolinium oxide. Ann Occup Hyg. 2002;46 suppl 1:320–2.
49. Schulz WW. Chemistry of Americium. Richland: Atlantic Richfield Hanford; 1976.
50. Sadgrove MP, Leed MGD, Shapariya S, Madhura DB, Jay M. Evaluation of a DTPA prodrug, C2E5 as an orally bioavailable radionuclide decorporation agent. Drug Dev Res. 2012;73 (5):243–51.

APPENDIX C Transdermal Prodrug Delivery for RadionuclideDecorporation: Non-aqueous Gel Formulation Development and In Vitro and In Vivo Assessment

Research Article

Transdermal Prodrug Delivery for Radionuclide Decorporation: Nonaqueous Gel Formulation Development and In Vitro and In Vivo Assessment

Yong Zhang, Matthew P. Sadgrove, Russell J. Mumper, and Michael Jay*

Division of Molecular Pharmaceutics, UNC Eshelman School of Pharmacy, University of North Carolina at Chapel Hill, Chapel Hill, NC 27599-7362, USA

Strategy, Management and Health Policy				
Enabling Technology, Genomics, Proteomics	Preclinical Research	Preclinical Development Toxicology, Formulation Drug Delivery, Pharmacokinetics	Clinical Development Phases I-III Regulatory, Quality, Manufacturing	Postmarketing Phase IV

ABSTRACT The penta-ethyl ester of diethylenetriamine pentaacetic acid (DTPA), a DTPA prodrug designated as C2E5 intended for transdermal delivery for radionuclide decorporation, was first screened with a prototype cream formulation and a hydrocarbon base ointment with C2E5 concentration ranging from 1% to 20%. C2E5 experienced rapid degradation in the cream matrix and C2E5 ointment formulation underwent phase separation due to components incompatibility. Nonaqueous gel matrix comprised of ethyl cellulose/Miglyol 840® was utilized to formulate C2E5 at different ethyl cellulose and C2E5 content levels. Differential scanning calorimetry (DSC) and scanning electron microscope (SEM) imaging were applied for analysis of the prepared C2E5 gel formulation. C2E5 was stabilized in the nonaqueous gel matrix and ethyl cellulose solubilization by dispersion media was confirmed by DSC and SEM results. Selected C2E5 nonaqueous gel formulations were evaluated in a rodent ^{241}Am wound contamination model at a dose level of 200 mg C2E5/kg. The enhanced decorporation over no treatment control on total decorporation, decorporation by urine, and decorporation by feces was 142%, 181%, and 86%, respectively. The nonaqueous gel matrix composed of ethyl cellulose/Miglyol 840 was successfully employed to stabilize the hydrolysis prone C2E5. C2E5 was delivered transdermally and achieved enhanced decorporation for the proof of hypothesis. Drug Dev Res •• : ••–••, 2013. © 2013 Wiley Periodicals, Inc.

Key words: DTPA; radionuclide decorporation; transdermal drug delivery; nonaqueous gel; Americium

INTRODUCTION

The United States and many other countries face increasing threats from terrorist groups with respect to the use of weapons of mass destruction against civilian populations. Of particular concern is that some of these groups are intensifying their efforts to acquire and develop nuclear and radiological weapons, such as radiological dispersal devices (RDDs) which, when spread by means of conventional explosives, constitutes what is referred to as a "dirty bomb." Among the radionuclides of greatest concern that may be incorporated in an RDD are isotopes of americium (Am), curium (Cm), and plutonium (Pu). Internalization of these radioactive materials may result in acute radiation sickness or chronic injuries including an increased risk of developing tumors.

The calcium (Ca) and zinc (Zn) trisodium salts of diethylenetriamine pentaacetic acid (DTPA) are the only agents that have been approved by the US Food

The authors have no Conflicts of Interest to declare.

*Correspondence to: Michael Jay, Division of Molecular Pharmaceutics, UNC Eshelman School of Pharmacy, University of North Carolina at Chapel Hill, CB# 7362, 120 Mason Farm Rd, Chapel Hill, NC 27599-7362, USA.
E-mail: mjay@unc.edu

Received 31 January 2013; Accepted 18 March 2013

Published online in Wiley Online Library (wileyonlinelibrary.com). DOI: 10.1002/ddr.21082

© 2013 Wiley Periodicals, Inc.

and Drug Administration as chelating agents for internal contamination by Am, Cm, and Pu radionuclides. The primary goal of these agents is to chelate those radionuclides before they become fixed in tissues such as liver and bone while enhancing their elimination. Because of the fact that Ca-DTPA and Zn-DTPA are highly hydrophilic and have a low oral bioavailability of 2–3% [Stradling et al., 1993], these products must be prepared as sterile injectable solutions. Most sterile injectable products are expensive to manufacture and require administration by a skilled professional, which render current Ca/Zn-DTPA treatment unsuitable for facile use in a mass casualty situation. Furthermore, there is a mismatch between the pharmacokinetic profile of intravenously (i.v.) administered DTPA and the biokinetic profile of transuranic radionuclides [Guilmette et al., 1979; Guilmette and Muggenburg, 1988; Phan et al., 2005]. Stevens et al. [1962] studied the clearance of ^{14}C-labeled DTPA in man after i.v. administration and observed that the i.v. administered ^{14}C-labeled DTPA was quantitatively excreted intact in urine within 24 h. The total body clearance of ^{14}C-labeled DTPA in rats 24 h after i.v. injection has been reported to range from 94% to 100% with half-lives from 0.28 to 0.53 h with no metabolic degradation [Crawley and Haines, 1979; Phan et al., 2005]. In contrast, the release rates of internalized Am, Pu, and Cm contaminants from wounds sites to the systemic circulation in various animal species range from 0.052% to 6.3% of the injected dose per day, a relatively slow and steady transfer process [National Council on Radiation Protection and Measurements, 2007]. It has been suggested that a chelating agent must be maintained at a concentration of at least 10–25 μM for a sustained duration to ensure an optimal chelation effect of transuranic radionuclides, both in extracellular and intercellular fluids [Ansoborlo et al., 2007]. A sustained DTPA plasma concentration cannot be achieved by i.v. Ca/Zn-DTPA and is not readily achievable by conventional sustained-release oral dosage forms. In addition, there are some patient populations that cannot take drugs orally, e.g., patients experiencing severe nausea following radiation exposure and very young pediatric patients.

A zero-order release profile can be achieved via transdermal drug delivery [Brown and Langer, 1988; Chien, 1992]. Topical and transdermal drug delivery provides many clinical advantages over the oral route, such as avoidance of first path metabolism, sustained release of drug with more uniform plasma concentration, and improved patient acceptance and compliance [Brown and Langer, 1988; Chien, 1992]. To be a good topical and transdermal drug delivery candidate, the compound needs to possess suitable physicochemical properties, such as a molecular weight generally less than 500 Dalton, a partition coefficient (log P) between 1 and 3, and a melting point below 200°C [Brown and Langer, 1988; Chien, 1992]. DTPA is highly hydrophilic (log P = –4.90) with high melting point (219–220°C), thus making it unsuitable for transdermal delivery. We have reported on the preparation of a lipophilic DTPA prodrug, designated as C2E5, in which the five carboxylic groups on DTPA were esterified with ethanol. C2E5 is a clear, light yellow, slightly viscous Newtonian liquid with a viscosity of ~175 cP (175 mPa s) and possesses desirable physicochemical properties for transdermal delivery [Jay and Mumper, 2011; Sueda et al., 2012]. The structures of C2E5 and the parent compound (DTPA) are depicted in Figure 1. Transdermal delivery of C2E5 may provide a sustained release of DTPA in the circulation following metabolism of the prodrug by esterases present in the skin and plasma. The semisolid dosage forms for topical and transdermal drug delivery include creams, ointments, gels, and lotions. Unlike transdermal patches that require highly specialized expertise on patch design and sophisticated manufacturing systems, semisolid dosage forms can easily be screened in a lab setting. Previous reports showed that approximately 68% of C2E5 remained intact for the neat C2E5 oil containing 0.6% α-tocopherol stored at 25°C/80% relative humidity for 3 months [Yang et al., 2013], indicating that C2E5 is prone to degradation. The aims of these studies were to screen candidate cream, ointment, and gel dosage forms to identify a semisolid matrix to stabilize and be compatible with C2E5, investigate the relevant physical properties of a lead C2E5 formulation, and evaluate the decorporation

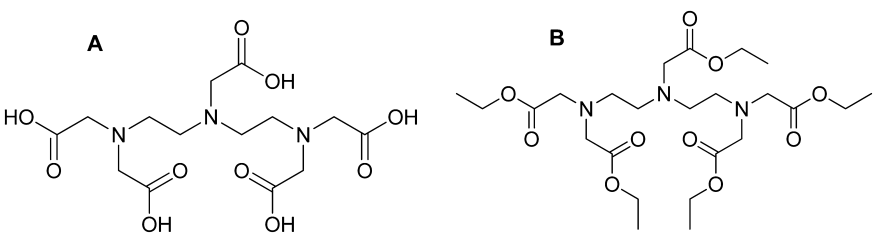

Fig. 1. Structures of DTPA (**A**) and its prodrug C2E5 (**B**).

efficiency of the lead C2E5 formulation in a simulated ^{241}Am wound contamination model.

METHODS AND MATERIALS

Materials

Miglyol 812® and Miglyol 840® were gifts from Sasol (Witten, Germany). The Capmul MCM® was a gift from Abitec Corp (Columbus, OH, USA). Ethylcellulose polymers of increasing chain length with ethoxyl content of 48.0–49.5% (ETHOCEL® Std 7 FP Premium [EC7], ETHOCEL® Std 10 FP Premium [EC10], and ETHOCEL® Std 100 FP Premium [EC100]) were gifts from Dow Chemical (Midland, MI, USA). C2E5 was prepared based on the Fischer esterification method by reacting DTPA with ethanol under reflux in the presence of a hydrochloric acid catalyst delivery [Sueda et al., 2012]. Propylene glycol (USP), sorbitol, 70% solution (USP), sorbic acid (NF), butylated hydroxytoluene (NF), simethicone (USP), white petrolatum (USP), cetostearyl alcohol (NF), polyoxyethylene (20) cetyl ether (Brij 58®), glyceryl monostearate (cosmetic grade), polyethylene glycol 400 monostearate (NF), butylated hydroxyanisole (NF), 1N NaOH solution, acetonitrile, trifluoroacetic acid, anhydrous ethanol, and isopropyl alcohol were purchased from VWR International (Radnor, PA, USA) and Fisher Scientific (Fairlawn, NJ, USA. [^{241}Am]-Americium nitrate solution for intramuscular (i.m.) contamination of adult female Sprague-Dawley (SD) rats was prepared from [^{241}Am]-Americium chloride (Eckert & Ziegler Isotope Products, Valencia, CA, USA) by dilution with a solution of concentrated nitric acid. Double-distilled water was obtained from a Milli-Q system (Millipore, Billerica, MA, USA).

Preparation of C2E5 Cream Formulations

The oil-in-water emulsion-based cream formulation was composed of an aqueous phase (85.2% w/w of base cream; components: distilled water 79.8% w/w, propylene glycol 3.0% w/w, sorbitol 70% solution 2.0% w/w, sorbic acid 0.2% w/w, butylated hydroxytoluene 0.1% w/w, simethicone 0.1% w/w) and an oil phase (14.8% w/w of base cream; components: petrolatum 5.6% w/w, cetostearyl alcohol 4.4% w/w, Brij 58 4.0% w/w, glyceryl monostearate 0.2% w/w, polyethylene glycol 400 monostearate 0.6% w/w). The topical cream was prepared by first preparing the aqueous phase in a 200 mL glass jar. The ingredients were weighed into the jar and subsequently heated to 70°C in a water bath. When all ingredients were fully dissolved, the pH was adjusted to 3.5, 4.5, or 5.5 by addition of a 1N NaOH solution. The oil phase was prepared by weighing the various components into a 100 mL beaker and then heating at 60°C. The emulsion was formed by decanting the melted oil phase into the jar containing the aqueous phase and which was equipped with a Caframo BDC1850 mechanical stirrer (Caframo Ltd, Wiarton, ON, Canada). The mixer was positioned in the center of the jar approximately 1/3 from the bottom and the stirring speed was set at 1,000 rpm. The emulsion was stirred for 30 min while heated at 70°C. The heating was then stopped and the emulsion was stirred for an additional 2 h. The final emulsion was prepared by direct addition of C2E5 and subsequent mixing for 5 min at 500 rpm so that the final concentration of C2E5 was 1, 5, 10, or 15% w/w. All emulsions were sealed in vials with an airtight cap, covered with aluminum foil to protect from light, and stored at room temperature for stability testing.

Preparation of C2E5 Ointment Formulations

The nonaqueous hydrocarbon base ointment was composed of white petrolatum (79.9% w/w), Miglyol 812 (15.4% w/w), Capmul MCM (4.6% w/w), and butylated hydroxyanisole (0.1% w/w). The base ointment was prepared by liquefying the white petrolatum using heat while mixing and then adding the Miglyol 812, Capmul MCM, and butylated hydroxyanisole; a white ointment was produced upon cooling. C2E5 containing ointment formulations with C2E5 concentrations of 5%, and 10% and 20% w/w were prepared by adding the C2E5 directly to the base ointment and then mixing for 5 min at 1,000 rpm using a Caframo BDC1850 mechanical stirrer with a mixer with 8 points and 1 inch in diameter. The final C2E5 containing ointment formulations were transferred to 20 mL scintillation vials, sealed with an airtight cap, covered with aluminum foil to protect from light, and stored at room temperature for subsequent stability testing.

Preparation of C2E5 Nonaqueous Gels

The C2E5 nonaqueous gels were prepared according to a previously described method with minor modifications [Heng et al., 2005]. Miglyol 840 and C2E5 were first heated to 60°C, followed by the slow addition of the fine particles of EC7, EC10, and EC100 into the solvent under constant stirring. The EC, Miglyol 840, and C2E5 mixtures were held under stirring until the mixtures turned into clear viscous solutions, typically in 2–12 h. Nonaqueous gels were formed after cooling to ambient temperature. Four formulations were prepared from each EC polymer: 7, 8, 14,

and 16% w/w for EC7, and 7, 8, 10, and 12% w/w for EC10 and EC100. The nonaqueous gel samples were put under vacuum to remove air bubbles trapped in the gels and subsequently crimped with an airtight cap, covered with aluminum foil to protect from light, and stored at room temperature for stability testing.

High Pressure Liquid Chromatography (HPLC) Assay for C2E5

The C2E5 concentration in these cream, ointment, and nonaqueous gel formulations was determined using a Shimadzu Prominence HPLC system equipped with an Alltech 3300 Evaporative Light Scattering Detector (ELSD). A reverse-phase gradient separation was performed using a Chromolith® Fast-Gradient RP-18e column (50 × 2.0 mm) coupled with an Alltima Alltech HP All-Guard Cartridge (C18, 5 μm particle size, 2.1 × 7.5 mm) at 40°C and at a flow rate of 0.25 mL/min. The solvents that comprised the mobile phase were water with 0.1% trifluoroacetic acid (A) and acetonitrile with 0.1% trifluoroacetic acid (B). The linear gradient for the mobile phase mixture (A : B) was first an equilibration phase at 95:5 for 1 min, then from 95:5 to 5:95 over 9 min, followed by an equilibration phase at 95:5 for 10 min, and ending with a reversal to 95:5 in 3 min and an equilibration phase of 95:5 for 3 min. The ELSD was operated at 40°C with 1.9 L/min nitrogen gas flow and the retention time of C2E5 was 9 min. The extraction of C2E5 from the cream, ointment, and nonaqueous gel samples was followed the method of Tashtoush with minor modifications [Tashtoush et al., 2008]. Approximately 50–200 mg of the formulation samples were weighed into a 50 mL conical centrifugation tube, followed by addition of 20 –30 mL of acetonitrile. The mixture was then vortexed for 1–10 min followed by centrifugation for 5 min at 10,000×g at 20°C. One milliliter of the supernatant was filtered through a 0.2 μm polyvinylidene difluoride filter into an HPLC vial for analysis. A 10 μL injection for each sample was performed. Samples were held at ambient temperature during analysis and analyzed using standard curves over a concentration range of 0.05–1.00 mg/mL which had a power regression fit of $R^2 \geq 0.997$.

Viscosity Measurement of C2E5 Nonaqueous Gels

The apparent viscosity of the C2E5 nonaqueous gels were measured at a shear rate of 1,000 s at 25°C using an Brookfield R/S Plus rheometer (Brookfield Engineering, Middleboro, MA, USA), which was equipped with a 25 mm diameter cone and plate assembly. The gel samples were carefully loaded to the lower plate to reduce shearing effects and equilibrated for 5 min at 25°C prior to measurement. Triplicate measurements were performed for the formulation and data are reported as mean ± standard deviation.

Thermal Analysis by Differential Scanning Calorimetry (DSC)

The EC10 polymer particles that had been dried overnight at 60°C before analysis, and the C2E5 nonaqueous gel samples were analyzed using a TA Instruments DSC Model Q200 (Newcastle, DE) under a nitrogen flow of 50 mL/min. Samples (5–10 mg) were heated in a sealed aluminum pan at a ramp rate of 10°C/min, cooled at a rate of 5°C/min, and subsequently heated at 10°C/min in heat/cool/heat mode from −10 to 160°C. The glass transition (Tg), and melting (Tm) temperatures in the third heating cycle were determined using TA Universal Software.

Scanning Electron Microscope (SEM) Imaging

The pre-dried EC10 polymer particles and C2E5 nonaqueous gel samples were observed and recorded using a Hitachi S-4700 SEM at an accelerated voltage of 15 kV. All images were taken at a scan rate of 100 ms per line. The EC10 polymer particles and C2E5 nonaqueous gel samples were deposited directly over double-sided carbon tape and imaged without further treatment. The C2E5 nonaqueous gel samples were imaged on the stub which was tilted 45° toward the lower scanning election detector for better imaging results.

Americium Decorporation in a Rodent Wound Model of Contamination

All animal studies were conducted according to a protocol approved by the University of North Carolina at Chapel Hill Institutional Animal Care and Use Committee. Adult female SD rats weighing from 200 to 400 g were used in these studies (Charles River Labs, Raleigh, NC, USA). Food and water were given ad libitum. The animal room was kept at a controlled temperature (23°C) and light cycle (light exposure from 8 AM to 8 PM). For the duration of the study, the rats were individually housed in metabolic cages.

To evaluate the efficacy of transdermal delivery of the C2E5 nonaqueous gel, a proof of principle radionuclide decorporation efficacy study was conducted in rats contaminated with ^{241}Am. Adult female

SD rats were anesthetized with 2–3% isoflurane. Dorsal skin between the cervical vertebrae and anterior thoracic vertebrae was clipped with caution before all animals were contaminated with [^{241}Am]-Americium nitrate solution (250 nCi, 0.1 mL) via an i.m. injection in the anterior thigh muscle. Freshly prepared C2E5 nonaqueous gel formulations containing 30% C2E5, 63% Miglyol 840, and 7% of EC7, EC10, or EC100 (formulations N-1, N-5, and N-9; see Table 2) were applied at a dose of 200 mg C2E5/kg (375 μmol C2E5/kg) using a cotton swab to approximately 6–8 cm^2 of the clipped dorsal region immediately after contamination. The mass of C2E5 gel applied was recorded for each animal to permit the actual dose determination. Negative control included animals without any treatment. The animals were observed once daily and their body weights recorded at pre-dose and prior to necropsy. Urine and feces were collected daily until the animals were euthanized on day 7 at which time the cage washes were collected. As ~35% of the decay of ^{241}Am is associated with photon emissions of 59.7 keV, ^{241}Am in samples was quantified using a gamma counter (2470 Wizard 2, Perkin Elmer, Waltham, MA). The samples were counted for 1 min using a 40–80 keV energy detection window and were background corrected. Additionally, ^{241}Am activity was quantified in 2×0.1 mL aliquots of the dosing solution to determine the initial administered dose of ^{241}Am. For all samples, ^{241}Am content was expressed as a percentage of the initial injected dose. The percent of enhanced decorporation for animals treated with transdermal C2E5 nonaqueous gels compared to the no treatment control animals were calculated from Equation 1 [Guilmette et al., 1979].

$$\textit{Percentage Enhanced Decorporation} = \frac{\%ID(Treatment) - \%ID(No\ Treatment)}{\%ID(No\ Treatment)} * 100$$

In this equation, *%ID* represents the percent of the initial injected dose.

Statistical Analysis

Comparisons between nonaqueous gel formulations were made using one-way analysis of variance (ANOVA). Having determined by one-way ANOVA that gel formulation was not a significant effect, two-tailed *t*-tests were used to compare decorporation efficacy between C2E5 treated and untreated animals. All measurements are expressed as mean ± standard deviation. The level of significance was set at $P < 0.05$.

RESULTS

Stability of C2E5 Cream and Ointment Formulations

The composition and stability testing results of C2E5 cream formulations are presented in Table 1. The base cream is white and the C2E5 containing cream became more yellow with increasing C2E5 content. No phase separation was observed for the C2E5 cream formulations for the 2-month stability testing period at 25 ± 2°C/60 ± 5% relative humidity. Because of the high concentrations of C2E5 in these formulations and the fact that C2E5 is self-buffering, the final pH of all of the cream formulations was in the range of pH 5–6. Based on the stability testing results of the C2E5 oil-in-water cream-based formulations, it indicated that higher C2E5 content in the creams resulted in a better stability profile, ranging from 52.6% to 61.6% C2E5 remaining for 1% C2E5 cream formulations, to 77.1% to 90.6% C2E5 remaining for 16.7% C2E5 cream formulations. The major degradants of C2E5 in the cream formulations were partially hydrolyzed products of C2E5, such as the tri- and tetra-ethyl esters of DTPA. Although the cream formulations with higher C2E5 content showed improved C2E5 stability over lower C2E5 containing cream formulations, they failed to deliver an acceptable C2E5 stability profile for a reasonable product shelf life.

The C2E5 ointment formulations showed a similar trend in terms of physical appearance as C2E5 containing cream formulations. The ointment formulation containing 20% C2E5 underwent phase separation within the first month after storage at 25 ± 2°C/60 ± 5% relative humidity; the C2E5 ointment formulation with 5 and 10% C2E5 contents experiencing phase separation within 3 months under the same storage conditions.

TABLE 1. C2E5 Cream Formulation Composition, Physical Appearance and Stability Results after Storage at 25 ± 2°C and 60 ± 5% Relative Humidity for 2 Months

Formulation	pH of base cream	C2E5 (%)	C2E5 cream appearance	% C2E5 remaining
C-1	3.5	1.0	White	61.6
C-2	3.5	4.8	Off-white	72.2
C-3	3.5	9.1	Pale yellow	77.0
C-4	3.5	16.7	Yellow	77.1
C-5	4.5	1.0	White	53.0
C-6	4.5	4.8	Off-white	71.4
C-7	4.5	9.1	Pale yellow	80.5
C-8	4.5	16.7	Yellow	87.3
C-9	5.6	1.0	White	52.3
C-10	5.6	4.8	Off-white	76.9
C-11	5.6	9.1	Pale yellow	81.7
C-12	5.6	16.7	Yellow	90.6

Stability of C2E5 Nonaqueous Gels

The composition and stability data of C2E5 nonaqueous gel formulations after 3-month storage at 25 ± 2°C/60 ± 5% relative humidity are presented in Table 2. The C2E5 nonaqueous gel formulations appeared to be yellow and opaque. During the 3-month storage period, no phase separation was observed for the nonaqueous gel formulations. The improved C2E5 stability in the nonaqueous gel matrix was achieved over the C2E5 cream formulations with greater than 93% of the original C2E5 remaining for most of the nonaqueous gel formulations stored at the same storage condition for 3 months. Clumps were observed for formulations associated with C2E5 nonaqueous gel using EC100 as the gelling agent possibly due to EC100's longer polymer chain and higher molecular weight, which make the solubilization of EC100 in C2E5 and Miglyol 840 inadequate. Lack of content uniformity in these gels may explain the higher than expected C2E5 concentration observed in the formulation of N-10.

Viscosity of C2E5 Nonaqueous Gels

The apparent viscosity measurements of C2E5 nonaqueous gel formulations are reported in Table 2. An increase in concentration of the ethyl cellulose, the gelling agent, resulted in the increase in the apparent viscosity of the nonaqueous gel formed, as well as the same trend in the ethyl celluloses with higher molecular weight and polymeric chain length, an indication of a stronger gel structure as a result of stronger interaction between the ethyl cellulose chains and between the ethyl cellulose chain and the dispersion media molecules. This observation is consistent with the result reported by Heng et al. [2005]. The nonaqueous gels containing 10% and 12% EC100 failed to yield a stable reading at this shear year due to the breakup of the gel samples.

Thermal Analysis by DSC

The DSC spectrum of pre-dried EC10 showed one minor endothermic peak appearing at 63°C and one major endothermic peak at 120°C. The latter peak was determined to be the EC10 glass transition temperature [Rekhi and Jambhekar, 1995]. The endothermic peak at 63°C appeared to be glyoxal, which is a major impurity in ethyl cellulose [Crowley and Martini, 2000], or reaction products associated with glyoxal. However, further investigation is necessary for confirmation of this peak. The DSC spectrum of the C2E5 nonaqueous gel formulation N-7 showed one major endothermic peak appearing at 106°C and one minor endothermic peak at 120°C. The presence of a minor EC10 glass transition endothermic peak at 120°C indicated that there was nearly complete solubilization of EC10 particles in Miglyol 840 and C2E5 and a minuscule amount of partially solubilized EC10 particles present in the gel sample was expected. The endothermic peaks at 106°C might be due to water trapped in the EC10 material, which could be a result of use of the EC10 that was not dried before incorporated in the gel preparation.

SEM Imaging

Figure 2 shows the SEM images of pre-dried EC10 particles and the C2E5 nonaqueous gel (formulation N-7). In Figure 2A and B, the SEM images showed tightly clumped EC10 particles with a relatively uniform size distribution averaging 1–5 μm in length.

TABLE 2. Ethyl Cellulose-Containing C2E5 Nonaqueous Gel Formulation Composition, Related Physical Characterization Data and Stability Results after Storage at 25 ± 2°C and 60 ± 5% Relative Humidity for 3 Months

Formulation	EC type (%)	C2E5 (%)	Miglyol 840 (%)	Gel appearance	% C2E5 remaining	Apparent viscosity (Pa s)*
N-1	EC7 (7)	30	63	Yellow and opaque	94.0 ± 2.6	0.51 ± 0.01
N-2	EC7 (8)	20	72	Yellow and opaque	97.7 ± 7.6	0.55 ± 0.00
N-3	EC7 (14)	30	56	Yellow and opaque	94.8 ± 8.3	3.82 ± 0.04
N-4	EC7 (16)	20	64	Yellow and opaque	84.0 ± 1.1	4.74 ± 0.08
N-5	EC10 (7)	30	63	Yellow and opaque	93.9 ± 7.1	0.72 ± 0.01
N-6	EC10 (8)	20	72	Yellow and opaque	96.7 ± 6.6	0.73 ± 0.01
N-7	EC10 (10)	30	60	Yellow and opaque	92.9 ± 3.4	2.56 ± 0.02
N-8	EC10 (12)	20	68	Yellow and opaque	97.4 ± 5.4	3.26 ± 0.05
N-9	EC100 (7)	30	63	Yellow and opaque	101.0 ± 5.9	2.38 ± 0.02
N-10	EC100 (8)	20	72	Yellow and opaque	106.2 ± 5.1	2.89 ± 0.03
N-11	EC100 (10)	30	60	Yellow and opaque	99.0 ± 7.8	N/A
N-12	EC100 (12)	20	68	Yellow and opaque	102.7 ± 11.1	N/A

*Apparent viscosity at a shear rate of 1,000 s^{-1}; N/A: No stable viscosity reading available.

TABLE 3. Distribution of Americium-241 in Excreta 7 Days after Different Treatments Immediate Post Contamination at a Dose of 200 mg C2E5/kg

Treatment groups	Cumulative excretion (% of ID, mean ± standard deviation)					
	In urine	Enhanced decorporation	In feces	Enhanced decorporation	Total eliminated	Enhanced decorporation
Untreated[†] ($n = 4$)	4.2 ± 0.6	181%	2.9 ± 1.0	86%	7.1 ± 1.4	142%
Transdermal C2E5 nonaqueous gels ($n = 6$)	11.8 ± 2.3***		5.4 ± 1.7*		17.2 ± 3.5***	

Significant difference by *t*-test comparison of means, *$P < 0.05$, **$P < 0.01$, and ***$P < 0.001$ against no treatment control.
[†]From previously published results [Sadgrove et al., 2012].

The SEM images of the C2E5 nonaqueous gel (Fig. 2C and D) displayed a relatively smooth gel surface that was embedded with small particles. The small particles were determined to be residual EC10 material that failed to be completely solubilized by Miglyol 840 and C2E5 during the gel preparation process. This assessment is supported by the DSC spectrum of the C2E5 nonaqueous gel in which a minor EC10 glass transition endothermic peak appeared at 120°C.

Radionuclide Decorporation

The excretion of ^{241}Am in urine and feces after 7 days in untreated rats and in rats treated with a single 200 mg/kg dose of C2E5 applied topically in different nonaqueous gel formulations immediately after radionuclide contamination are summarized in Table 3. The mean total decorporation observed following treatment with C2E5 nonaqueous gels formulated with EC7, EC10 and EC100 was not significantly different ($F_{\text{Formulations}}[2,3] = 0.15$, $P = 0.87$) and clearance in the urine and feces were consistent across all formulations ($F_{\text{Urine}}[2,3] = 0.41$, $P = 0.70$ and $F_{\text{Feces}}[2,3] = 0.72$, $P = 0.56$), indicating that the type of the ethyl cellulose polymers used in formulating C2E5 nonaqueous gels did not affect decorporation efficacy in a statistical manner. Therefore, the C2E5 treatment groups were combined into one C2E5 treated animal group and compared with untreated animals. The daily excretion of ^{241}Am in contaminated animals treated with the

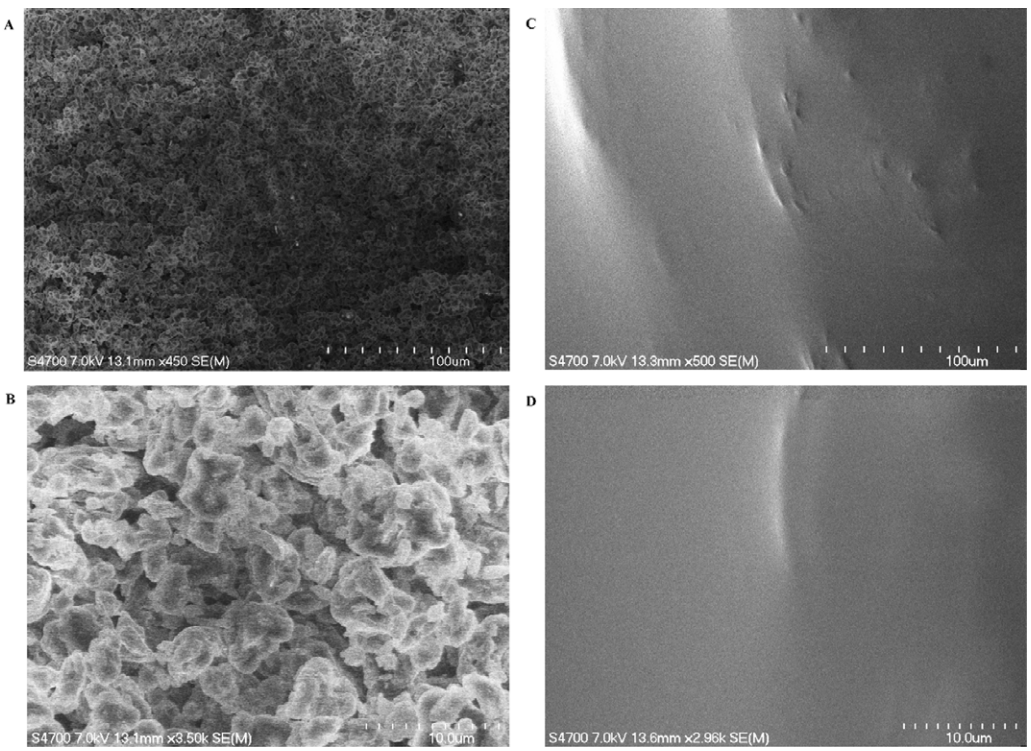

Fig. 2. SEM images of EC10 particles (**A** and **B**) and a C2E5 nonaqueous gel formulation consisting of 10% EC10, 30% C2E5, and 60% Miglyol 840 (**C** and **D**) at magnifications of ~500× and 3000×.

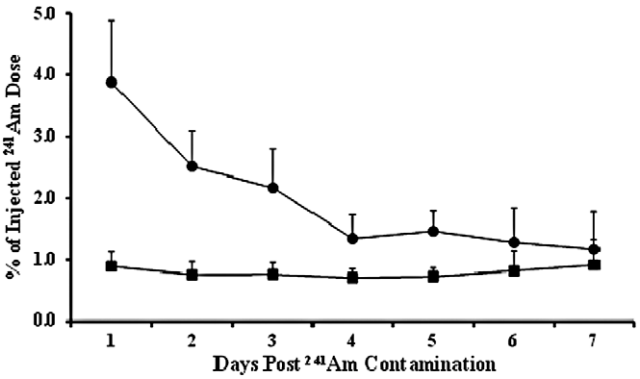

Fig. 3. Daily excretion of ^{241}Am after a single dose topical application of 40% C2E5 nonaqueous gels (—●—, $n = 6$) versus untreated control (—■—, $n = 4$; from Sadgrove et al., 2012). Data are means ± standard deviations.

C2E5 gel and untreated control animals is presented in Figure 3. Application of a single dose of the C2E5 gel immediately after contamination resulted in enhanced excretion of ^{241}Am for a period of at least 3 days compared with untreated animals. Treatment with C2E5 transdermal gels enhanced total decorporation compared with untreated controls. The enhanced decorporation was primarily due to urinary, but significantly increased fecal decorporation was also observed. The enhanced decorporation over no treatment control on total decorporation, decorporation by urine, and decorporation by feces was 142%, 181% and 86%, respectively.

DISCUSSION

In the present study, by testing the stability and compatibility of C2E5 in different transdermal drug delivery vehicles, we demonstrate that a nonaqueous gel matrix composed of ethyl cellulose/Miglyol 840 can be used to protect a hydrolysis prone compound while retaining the drug's efficacy for transdermal delivery. DSC and SEM results confirmed the nearly complete solubilization of ethyl cellulose in the dispersion media.

C2E5 possesses suitable physicochemical properties for transdermal delivery [Sueda et al., 2012], but it suffers from a poor stability profile due to hydrolysis, which is one of the major degradation pathways for pharmaceutical formulations [Waterman et al., 2002]. The pH of the water phase for the cream formulations was set at 3.5, 4.5, and 5.5 based on C2E5 preformulation data which demonstrated that C2E5 degradation in buffered aqueous solution follows a pseudo-first order kinetics and C2E5 is most stable at approximately pH 4.2 [Sueda et al., 2012]. From the C2E5 cream stability testing results, it suggests that the C2E5 content in the cream plays a more important role for the stability of the C2E5 incorporated in the cream matrix than the pH of the water phase, with a much higher percent of C2E5 remaining intact in the cream formulation with higher C2E5 content. However, the cream formulation failed to stabilize the C2E5 incorporated in the cream matrix for sufficient storage stability at 25°C.

As a consequence of poor stability of the cream formulations, ointment formulations comprising white petrolatum, Miglyol 812 and Capmul MCM was developed. The C2E5 ointment formulations were physically unstable and underwent phase separation within 3 months after storage at 25 ± 2°C/60 ± 5% relative humidity, which demonstrates the instability of C2E5 ointment formulations as a result of incompatibility and lack of interaction between the white petrolatum, the main component of the ointment matrix, and the C2E5. White petrolatum consists of saturated hydrocarbons with carbon numbers mainly greater than 25 [Petrolatum (White)]. In order to maintain the physical stability of ointment structure, interactions between petrolatum molecules and dispersion medium molecules are necessary. Because the major force existing between petrolatum molecules are hydrophobic-hydrophobic interaction, and considerable interactions of this type exist between the C-8 and C-10 chains of Miglyol 812 and Capmul MCM, and the petrolatum molecules, addition of the C2E5 molecules that lack hydrophobic-hydrophobic interaction potential would destabilize the ointment matrix, with the expectation that the higher the C2E5 content in the ointment formulation, the faster the ointment formulation would undergo phase separation. The limited physical stability of the C2E5 ointment formulations could be well explained by these observations.

Because of the high hydrolytic tendency of the C2E5 ester bonds and incompatibility of C2E5 with the hydrocarbon base ointment matrix, the focus of the C2E5 formulation development was shifted to select a semisolid dosage form that contains a dispersion medium lacking functional groups such as hydroxyl and carboxylic groups that facilitate the hydrolysis of the C2E5 ester bonds and a gelling agent that is compatible with C2E5. Furthermore, the process to make this semisolid dosage form should not expose C2E5 to harsh conditions that accelerate its degradation. Nonaqueous gel formulations were pursued as a viable dosage form candidate to stabilize C2E5 in the delivery vehicles. In contrast to extensive research on traditional semisolid dosage forms such as creams, ointments, and hydrogels, there are far fewer reports on the development of nonaqueous gel matrices intended for topical and transdermal drug delivery [Claramonte et al., 1993; Lee et al.,

1995; Lizaso et al., 1999; Heng et al., 2005; Chow et al., 2008a]. Advantages of nonaqueous gel dosage form include matrix components that stabilize the moisture-sensitive drug substance and candidate nonaqueous gel matrices that possess the suitable rheological and mechanical properties for topical and transdermal drug delivery. The Heng group reported on nonaqueous gel matrices containing ethyl cellulose and Miglyol 840 by directly mixing the ethyl cellulose and Miglyol 840 at 60°C [Heng et al., 2005]. ETHOCEL, an ethyl cellulose polymer suitable for pharmaceutical application, contains ~50% hydroxyl content on the polymer chain. Miglyol 840, a neutral oil mixture of propylene glycol dicaprylate and dicaprate, has excellent penetration-promoting, emollient and skin-smoothing properties as well as a high stability against oxidation [European Pharmacopoeia, 2002]. The C2E5 stability profile in the nonaqueous gel formulations demonstrated pronounced improvement compared to that of neat C2E5 containing 0.6% α-tocopherol in which less than 70% of C2E5 remained intact after 3 months of storage under similar conditions [Yang et al., 2013], as well as that of C2E5 incorporated in the cream formulations. The improved stability profile of C2E5 in this ethyl cellulose/Miglyol 840 matrix may be attributed to steric and rotational hindrance of the hydroxyl groups on the ethyl cellulose polymer backbone resulting in decreased interactions with C2E5 molecules. In addition, Miglyol 840 neutral oil is nonhygroscopic, possesses high stability against oxidation and contains no free hydroxyl groups. No phase separation observed in the 3-month storage period for the C2E5 containing nonaqueous gel formulations indicated that a stable and extensive three-dimensional reversible physical crosslinks were formed within the gel structures [Heng et al., 2005]. Based on the initial report on the viscosity of the prepared C2E5 nonaqueous gels and previous studies on an ethyl cellulose/Miglyol 840 nonaqueous gel matrix [Heng et al., 2005; Chan et al., 2006; Chow et al., 2008b], further investigation may the relationship between the viscosity and the ratios of the ethyl cellulose, Miglyol 840 and C2E5 could yield the ideal C2E5 nonaqueous formulations with suitable rheological and mechanical properties for the transdermal delivery of C2E5. To improve the quality of the C2E5 nonaqueous formulations, procedures such as pre-drying the ethyl cellulose before use to remove water and volatile impurities and milling the ethyl cellulose particles before use to improve EC10 solubilization were applied. To reduce the potential C2E5 degradation in the gel preparation stage, addition of C2E5 after ethyl cellulose/Miglyol 840 gel formation and filling the head space of the gel preparation vessel with nitrogen could retard C2E5 degradation.

C2E5, applied topically to contaminated rats, in nonaqueous gel formulations at 200 mg/kg was able to enhance ^{241}Am decorporation. A preliminary pharmacokinetic study conducted by this research group on SD rats using a C2E5 nonaqueous gel at a dose of 200 mg C2E5/kg demonstrated that C2E5 was converted into DTPA in vivo [Zhang et al., 2013], confirming that C2E5 is indeed a prodrug of DTPA. We had previously reported on the enhanced decorporation of ^{241}Am after oral delivery of C2E5 [Sadgrove et al., 2012]; decorporation efficacy achieved by transdermal delivery of C2E5 at the same dose level is comparable. Analysis of the in vivo data showed that changing the ethyl cellulose polymer chain length in the nonaqueous gel matrix did not alter C2E5 efficacy. Together, these data suggest that ethyl cellulose based nonaqueous gels can be readily optimized to provide effective delivery of C2E5 in a stable vehicle. As the first report using ethyl cellulose/Miglyol 840 gel matrix developed by the Heng group to incorporate a hydrolytically sensitive drug, we believe this nonaqueous delivery vehicle may find useful applications for moisture and hydrolysis sensitive compounds intended for topical and transdermal drug delivery.

In summary, C2E5, a DTPA prodrug for transdermal delivery, was formulated in cream, ointment, and nonaqueous gel delivery vehicles. Because of the hydrolysis labile nature of C2E5, it rapidly degraded in a cream matrix composed of an aqueous phase. Incompatibility between hydrophobic petrolatum and C2E5 resulted in the phase separation of C2E5 containing ointment formulations. C2E5 was shown to be stable in a nonaqueous gel composed of ethyl cellulose and Miglyol 840. This nonaqueous gel matrix has the potential for use with current and future moisture-sensitive drug molecules intended for topical and transdermal delivery. Enhanced ^{241}Am decorporation in a wound contamination animal model was demonstrated following topical application of C2E5 nonaqueous gels. Future studies including pharmacokinetic and dose-dependent decorporation studies are being conducted to evaluate this novel treatment option for internal radionuclide contamination by transuranic elements.

ACKNOWLEDGMENTS

The authors thank Dr. Richard Superfine and University of North Carolina (UNC) Center for Computer Integrated Systems for Microscopy and Manipulation at UNC-Chapel Hill for access to the Hitachi S-4700 SEM which was funded by NIBIB/NIH award number P41-EB002025, and Dr. Joseph DeSimone for access to the differential scanning calorimeter. The authors also thank Maciej Szymczyk and Kevin Chu for

their help on cream and ointment formulation preparation, Ms. Nadira Williams for her help with Hitachi S-4700 SEM and Ms. Sara White for her help with the differential scanning calorimeter. This work was funded in part by the National Institutes of Health, US Department of Health and Human Services under contract HHSN266200500045C.

REFERENCES

Ansoborlo E, Amekraz B, Moulin C, Moulin V, Taran F, Bailly T, Burgada R, Henge-Napoli MH, Jeanson A, Den Auwer C. 2007. Review of actinide decorporation with chelating agents. Comptes Rendus Chimie 10:1010–1019.

Brown L, Langer R. 1988. Transdermal delivery of drugs. Ann Rev Med 39:221–229.

Chan L, Chow K, Heng PWS. 2006. Investigation of wetting behavior of nonaqueous ethylcellulose gel matrices using dynamic contact angle. Pharm Res 23:408–421.

Chien YW. 1992. Novel drug delivery systems. New York: M. Dekker, p vii, 797.

Chow K, Chan L, Heng P. 2008a. Formulation of hydrophilic nonaqueous gel: drug stability in different solvents and rheological behavior of gel matrices. Pharm Res 25:207–217.

Chow KT, Chan LW, Heng PWS. 2008b. Characterization of spreadability of nonaqueous ethylcellulose gel matrices using dynamic contact angle. J Pharm Sci 97:3467–3482.

Claramonte MDC, Vialard AP, Vilchez FG. 1993. An application of regular solution theory in the study of the solubility of naproxen in some solvents used in topical preparations. Int J Pharm 94:23–30.

Crawley FE, Haines JW. 1979. The dosimetry of carbon-14 labelled compounds: the metabolism of diethylenetriamine pentaacetic acid (DTPA) in the rat. Int J Nucl Med Biol 6:9–15.

Crowley P, Martini LG. 2000. Drug-excipient interactions. Pharm Technol Eur 13:26–34.

European Pharmacopoeia. 2002. 2002 european pharmacopoeia, 4th edn. Strasbourg, France: Council of Europe.

Guilmette R, Muggenburg B. 1988. Reducing the radiation dose from inhaled americium-241 using continuously administered DTPA therapy. Int J Radiat Biol 53:261–271.

Guilmette RA, Moretti ES, Lindenbaum A. 1979. Toward an optimal DTPA therapy for decorporation of actinides: time-dose relationships for plutonium in the dog. I. Radiat Res 78:415–428.

Heng PW, Chan LW, Chow KT. 2005. Development of novel nonaqueous ethylcellulose gel matrices: rheological and mechanical characterization. Pharm Res 22:676–684.

Jay M, Mumper RJ. 2011. Methods and pharmaceutical compositions for decorporation of radioactive compounds. United States Patent 8,030,358.

Lee C, Kitagawa K, Uchida T, Kim N, Goto S. 1995. Transdermal delivery of theophylline using an ethanol/panasate 800-ethylcellulose gel preparation. Biol Pharm Bull 18:176–180.

Lizaso E, Muñoz ME, Santamaría A. 1999. Formation of gels in ethylcellulose solutions. an interpretation from dynamic viscoelastic results. Macromolecules 32:1883–1889.

National Council on Radiation Protection and Measurements. 2007. Scientific committee 57-17 on radionuclide dosimetry model for wounds. 2007 NCRP Report N. 156:35–117.

Petrolatum (White). ICSC 1440 - PETROLATUM (WHITE). http://www.inchem.org/documents/icsc/icsc/eics1440.htm. Accessed 8 January 2013.

Phan G, Herbet A, Cholet S, Benech H, Deverre JR, Fattal E. 2005. Pharmacokinetics of DTPA entrapped in conventional and long-circulating liposomes of different size for plutonium decorporation. J Control Release 110:177–188.

Rekhi GS, Jambhekar SS. 1995. Ethylcellulose-A polymer review. Drug Dev Ind Pharm 21:61–77.

Sadgrove MP, Leed MGD, Shapariya S, Madhura DB, Jay M. 2012. Evaluation of a DTPA prodrug, C2E5 as an orally bioavailable radionuclide decorporation agent. Drug Dev Res 73:243–251.

Stevens E, Rosoff B, Weiner M, Spencer H. 1962. Metabolism of the chelating agent diethylenetriamine pentaacetic acid (C14DTPA) in man. New York: Proceedings of the Society for Experimental Biology and Medicine; volume 111.

Stradling GN, Gray SA, Ellender M, Pearce M, Wilson I, Moody JC, Hodgson A. 1993. Removal of inhaled plutonium and americium from the rat by administration of ZnDTPA in drinking water. Hum Exp Toxicol 12:233–239.

Sueda K, Sadgrove MP, Fitzsimmons JM, Jay M. 2012. Physicochemical characterization of a prodrug of a radionuclide decorporation agent for oral delivery. J Pharm Sci 101:2844–2853.

Tashtoush BM, Jacobson EL, Jacobson MK. 2008. Validation of a simple and rapid HPLC method for determination of metronidazole in dermatological formulations. Drug Dev Ind Pharm 34:840–844.

Waterman KC, Adami RC, Alsante KM, Antipas AS, Arenson DR, Carrier R, Hong J, Landis MS, Lombardo F, Shah JC. 2002. Hydrolysis in pharmaceutical formulations. Pharm Dev Technol 7:113–146.

Yang Y-T, Di Pasqua AJ, He W, Tsai T, Sueda K, Zhang Y, Jay M. 2013. Preparation of alginate beads containing a prodrug of diethylenetriaminepentaacetic acid. Carbohydr Poly 92:1915–1920.

Zhang Y, Sadgrove MP, Sueda K, Yang YT, Pacyniak EK, Kagel JR, Braun BA, Zamboni WC, Mumper RJ, Jay M. 2013. Non-aqueous gel for the transdermal delivery of a DTPA penta-ethyl ester prodrug. AAPS J in press; doi: 10.1208/s12248-013-9459-5.

REFERENCES

1. Nuclear Trafficking Abstracts Database at the Nuclear Threat Initiative. http://www.nti.org/db/nistraff/index.html. Accessed on 03 April 2013.

2. International Atomic Energy Agency (IAEA). Assessing the Chernobyl Consequences. http://www.iaea.org/Publications/Magazines/Bulletin/Bull383/boxp6.html. Accessed on 03 April 2013.

3. International Atomic Energy Agency (IAEA). The Radiological Accident in Goiania. http://www-pub.iaea.org/MTCD/publications/PDF/Pub815_web.pdf. Accessed on 03 April 2013.

4. International Atomic Energy Agency (IAEA). Fukushima Nuclear Accident. http://www.iaea.org/newscenter/focus/fukushima/. Accessed on 03 April 2013.

5. Lawrence Berkeley National Laboratory. The Discovery of Radioactivity (http://www.lbl.gov/abc/wallchart/chapters/03/4.html). Accessed on 03 April 2013.

6. International Commission on Radiological Protection (ICRP). ICRP publications: http://www.icrp.org/publications.asp. Accessed on 03 Apr 2013

7. National Council on Radiation Protection and Measurements (NCRP). NCRP reports: http://www.ncrppublications.org/Reports/. Accessed on 03 Apr 2013

8. U.S. Nuclear Regulatory Commission (NRC). Biological Effects of Radiation by NRC www.nrc.gov/reading-rm/basic-ref/teachers/09.pdf. Accessed on 04 April 2013.

9. Wiseman H, Halliwell B. Damage to DNA by reactive oxygen and nitrogen species: role in inflammatory disease and progression to cancer. Biochemical Journal. 1996;313(Pt 1):17.

10. Cadet J, Berger M, Douki T, Ravanat J-L. Oxidative damage to DNA: formation, measurement, and biological significance. Reviews of Physiology Biochemistry and Pharmacology, Volume 131: Springer; 1997. p. 1-87.

11. Mikkelsen RB, Wardman P. Biological chemistry of reactive oxygen and nitrogen and radiation-induced signal transduction mechanisms. Oncogene. 2003;22(37):5734-54.

12. Cadet J, Douki T, Gasparutto D, Ravanat J-L. Radiation-induced damage to cellular DNA: measurement and biological role. Radiation Physics and Chemistry. 2005;72(2–3):293-9.

13. Shah DJ, Sachs RK, Wilson DJ. Radiation-induced cancer: a modern view. British Journal of Radiology. 2012 December 1, 2012;85(1020):e1166-e73.

14. Stone HB, Moulder JE, Coleman CN, Ang KK, Anscher MS, Barcellos-Hoff MH, et al. Models for Evaluating Agents Intended for the Prophylaxis, Mitigation and Treatment of Radiation Injuries Report of an NCI Workshop, December 3–4, 2003. Radiation Research. 2004;162(6):711-28.

15. Riley PA. Free-radicals in biology – oxidative stress and the effects of ionizing-radiation. International Journal of Radiation Biology. 1994;65(1):27-33.

16. Robbins MEC, Zhao W. Chronic oxidative stress and radiation-induced late normal tissue injury: a review. International Journal of Radiation Biology. 2004;80(4):251-9.

17. Weiss JF, Landauer MR. History and development of radiation-protective agents. International Journal of Radiation Biology. 2009;85(7):539-73.

18. Seed TM. Radiation protectants: Current status and future prospects. Health physics. 2005;89(5):531-45.

19. Xiao M, Whitnall MH. Pharmacological countermeasures for the acute radiation syndrome. Curr Mol Pharmacol. 2009;2(1):122-33.

20. Hosseinimehr SM. Foundation review: Trends in the development of radioprotective agents. Drug Discov Today. 2007;12(19-20):794-805.

21. Mönig H, Messerschmidt O, Streffer C. Chemical radioprotection in mammals and in man. Radiation exposure and occupational risks: Springer; 1990. p. 97-143.

22. Rubin GJ, Page L, Morgan O, Pinder RJ, Riley P, Hatch S, et al. Public information needs after the poisoning of Alexander Litvinenko with polonium-210 in London: cross sectional telephone survey and qualitative analysis. British Medical Journal. 2007;335(7630):1143.

23. Plant JA, Smith B, Phoon X, Ragnarsdottir KV. Radioactivity and Radioelements. Pollutants, Human Health and the Environment: John Wiley & Sons, Ltd; 2011. p. 115-46.

24. Greenwood NN, Earnshaw A. Chemistry of the Elements: Butterworth-Heinemann Oxford; 1997.

25. Lawrence Livermore National Laboratory. Uncovering the Secrets of the Actinides. https://www.llnl.gov/str/pdfs/06_00.2.pdf#search=%22actinide%20series%22 (Accessed on 05 April 2013).

26. Martin RC, Kos SE. Applications and Availability of Californium-252 Neutron Sources for Waste Characterization. Oak Ridge National Laboratory, Submitted in 2001.

27. HHS Public Health Emergency Medical Countermeasure Enterprise Implementation Plan for Chemical, Biological, Radiological and Nuclear Threats. Office of Public Health Emergency Medical Countermeasures, U.S. Department of Health and Human Services, Washington, DC, 2007

28. Guidance for Industry Calcium DTPA and Zinc DTPA Drug Products —Submitting a New Drug Application. U.S. Food and Drug Administration, Washington, DC, 2004. [Available online at www.fda.gov/downloads/Drugs/GuidanceComplianceRegulatoryInformation/Guidances/UCM071320.pdf] 2004.

29. Guidance for Industry, Internal Radioactive Contamination—Development of decorporation Agents. U.S. Food and Drug Administration, Washington, DC, 2006. [Available online at http://www.fda.gov/CDER/guidance/6983fnl.htm].

30. Guidance for Industry: Animal Models-Essential Elements to Address Efficacy Under the Animal Rule U.S. Food and Drug Administration, Washington, DC, 2009. [Available online at http://www.fda.gov/downloads/Drugs/GuidanceComplianceRegulatoryInformation/Guidances/ucm078923.pdf].

31. Cassatt DR, Kaminski JM, Hatchett RJ, DiCarlo AL, Benjamin JM, Maidment BW. Medical Countermeasures against Nuclear Threats: Radionuclide Decorporation Agents. Radiation Research. 2008;170(4):540-8.

32. Assessing Medical Preparedness to Respond to a Terrorist Nuclear Event: Workshop Report. Benjamin GC, McGeary M, McCutchen SR, editors: The National Academies Press; 2009.

33. Wizemann T, Altevogt BM, Claiborne AB. Advancing Regulatory Science for Medical Countermeasure Development: Workshop Summary: National Academies Press; 2011.

34. Howard WL, Wilson D. Chelating Agents. Kirk-Othmer Encyclopedia of Chemical Technology: John Wiley & Sons, Inc.; 2000.

35. FDA Approves Drugs to Treat Internal Contamination from Radioactive Elements. 2004. Available from: http://www.fda.gov/NewsEvents/Newsroom/PressAnnouncements/2004/ucm108339.htm (Accessed on 30 May 2012).

36. Breitenstein Jr B, Fry S, Lushbaugh C. DTPA Therapy: the US experience 1958-1987. The medical basis of radiation accident preparedness2nd ed, R Ricks, SA Fry Elsevier Science, New York. 1990:397-406.

37. Grappin L, Berard P, Menetrier F, Carbone L, Courtay C, Castagnet X, et al. Treatment of actinide exposures: a review of Ca-DTPA injections inside CEA-COGEMA plants. Radiation Protection Dosimetry. 2007;127(1-4):435-9.

38. Radiation Emergency Assistance Center/Training Site (REAC/TS). https://orise.orau.gov/reacts/ (Accessed on 06 April 2013).

39. Hameln Pharma GmbH. Package insert: pentetate calcium trisodium injection and pentetate zinc trisodium injection. Hameln Pharma GmbH. 2009.

40. National Council on Radiation Protection and Measurements. Management of Persons Accidentally Contaminated with Radionuclides: Recommendations of the National Council on Radiation Protection and Measurements: NCRP; 1980.

41. Fukuda S. Chelating agents used for plutonium and uranium removal in radiation emergency medicine. Current medicinal chemistry. 2005;12(23):2765-70.

42. Pellmar TC, Rockwell S. Priority list of research areas for radiological nuclear threat countermeasures. Radiation Research. 2005;163(1):115-23.

43. Jay M, Mumper RJ. Methods and pharmaceutical compositions for decorporation of radioactive compounds. United States Patent 8,030,358; 2011.

44. Sueda K, Sadgrove MP, Fitzsimmons JM, Jay M. Physicochemical characterization of a prodrug of a radionuclide decorporation agent for oral delivery. Journal of Pharmaceutical Sciences. 2012;101(8):2844-53.

45. Sadgrove MP, Leed MGD, Shapariya S, Madhura DB, Jay M. Evaluation of a DTPA Prodrug, C2E5 as an Orally Bioavailable Radionuclide Decorporation Agent. Drug Development Research. 2012;73(5):243-51.

46. Yang Y-T, Di Pasqua AJ, He W, Tsai T, Sueda K, Zhang Y, et al. Preparation of alginate beads containing a prodrug of diethylenetriaminepentaacetic acid. Carbohydrate polymers. 2013;92(2):1915-20.

47. Zhang Y, Sadgrove M, Sueda K, Yang Y-T, Pacyniak E, Kagel J, et al. Nonaqueous Gel for the Transdermal Delivery of a DTPA Penta-ethyl Ester Prodrug. The AAPS Journal. 2013;15(2):523-32.

48. Zhang Y, Sadgrove MP, Mumper RJ, Jay M. Transdermal Prodrug Delivery for Radionuclide Decorporation: Nonaqueous Gel Formulation Development and In Vitro and In Vivo Assessment. Drug Development Research. 2013: Early view. DOI: 10.1002/ddr.21082.

49. Shankar GN, Parish HJ. Oral DTPA for radionuclide chelation. United States Patent 7,914,767; 2011.

50. Shankar GN, Weber W, Doyle-Eisele M, Guilmette RA. Efficacy of a Novel Orally Administered Formulation of DTPA Tablets for Decorporating an Intravenously Injected Radionuclide: A Comparison with Intravenously Administered Licensed DTPA. Drug Development Research. 2012;73(5):290-8.

51. Reddy JD, Cobb RR, Dungan NW, Matthews LL, Aiello KV, Ritter G, et al. Preclinical Toxicology, Pharmacology, and Efficacy of a Novel Orally Administered Diethylenetriaminepentaacetic acid (DTPA) Formulation. Drug Development Research. 2012;73(5):232-42.

52. Talton JD. Process for milling and preparing powders and compositions produced thereby. United States Patent 8,074,906; 2011.

53. Miller SC, Liu G, Bruenger FW, Lloyd RD. Efficacy of orally administered amphipathic polyaminocarboxylic acid chelators for the removal of plutonium and americium: Comparison with injected Zn-DTPA in the rat. Radiation Protection Dosimetry. 2006;118(4):412-20.

54. Miller SC, Wang X, Bowman BM. Pharmacological properties of orally available, amphipathic polyaminocarboxylic acid chelators for actinide decorporation. Health physics. 2010;99(3):408.

55. Neilands JB. Siderophores: Structure and Function of Microbial Iron Transport Compounds. Journal of Biological Chemistry. 1995;270(45):26723-6.

56. Bergeron RJ. Desferrithiocin Analogue Actinide Decorporation Agents. US Patent 20100137346 (PCT/US2007/025377); 2007.

57. Bergeron RJ, Wiegand J, Singh S. Desferrithiocin analogue uranium decorporation agents. International Journal of Radiation Biology. 2009;85(4):348-61.

58. Raymond KN, Scarrow RC, White DL. Hydroxypyridonate chelating agents. United States Patent 4,698,431; 1987.

59. Gorden AE, Xu J, Raymond KN, Durbin P. Rational design of sequestering agents for plutonium and other actinides. Chem Rev. 2003;103(11):4207-82.

60. Durbin-Heavey P, Raymond K, Abergel R, Shuh D. Combination treatment of hydroxypyridonate actinide/lanthanide decorporation agents. WO Patent 2,010,129,962; 2010.

61. Stradling G, Gray S, Moody J, Pearce M, Wilson I, Burgada R, et al. Comparative efficacies of 3, 4, 3-LIHOPO and DTPA for enhancing the excretion of plutonium and americium from the rat after simulated wound contamination as nitrates. International Journal of Radiation Biology. 1993;64(1):133-40.

62. Volf V, Burgada R, Raymond K, Durbin P. Decorporation of Plutonium-238 and Americium-241 in Rats. Toxicology Letters. 1995;78(1001):84.

63. Volf V. Chelation therapy by DFO-HOPO and 3, 4, 3-LIHOPO for injected Pu-238 and Am-241 in the rat: effect of dosage, time and mode of chelate administration. International Journal of Radiation Biology. 1996;70(6):765-72.

64. Durbin PW, Kullgren B, Xu J, Raymond KN. New agents for in vivo chelation of uranium (VI): efficacy and toxicity in mice of multidentate catecholate and hydroxypyridinonate ligands. Health physics. 1997;72(6):865-79.

65. W. Durbin BK, J. Xu, KN Raymond, P. Multidentate hydroxypyridinonate ligands for Pu (IV) chelation in vivo: comparative efficacy and toxicity in mouse of ligands containing 1, 2-HOPO or Me-3, 2-HOPO. International Journal of Radiation Biology. 2000;76(2):199-214.

66. Paquet F, Chazel V, Houpert P, Guilmette R, Muggenburg B. Efficacy of 3, 4, 3-LI (1, 2-HOPO) for decorporation of Pu, Am and U from rats injected intramuscularly with high-fired particles of MOX. Radiation Protection Dosimetry. 2003;105(1-4):521-5.

67. Ramounet-Le Gall B, Grillon G, Rataeu G, Burgada R, Bailly T, Fritsch P. Comparative decorporation efficacy of 3, 4, 3-LIHOPO, 4, 4, 4-LIHOPO and DTPA after contamination of rats with soluble forms of 238Pu and 233U. Radiation Protection Dosimetry. 2003;105(1-4):535-8.

68. Abergel RJ, Durbin PW, Kullgren B, Ebbe SN, Xu J, Chang PY, et al. Biomimetic actinide chelators: an update on the preclinical development of the orally active hydroxypyridonate decorporation agents 3, 4, 3-LI (1, 2-HOPO) and 5-LIO (Me-3, 2-HOPO). Health physics. 2010;99(3):401.

69. Abergel RJ, Raymond KN. Multidentate terephthalamidate and hydroxypyridonate ligands: towards new orally active chelators. Hemoglobin. 2011;35(3):276-90.

70. Jarvis EE, An DD, Kullgren B, Abergel RJ. Significance of Single Variables in Defining Adequate Animal Models to Assess the Efficacy of New Radionuclide Decorporation Agents: Using the Contamination Dose as an Example. Drug Development Research. 2012;73(5):281-9.

71. Bunin DI, Chang PY, Doppalapudi RS, Riccio ES, An D, Jarvis EE, et al. Dose-Dependent Efficacy and Safety Toxicology of Hydroxypyridinonate Actinide Decorporation Agents in Rodents: Towards a Safe and Effective Human Dosing Regimen. Radiation Research. 2013;179(2):171-82.

72. Brown L, Langer R. Transdermal delivery of drugs. Annual review of medicine. 1988;39(1):221-9.

73. Chien YW. Novel drug delivery systems. 2nd ed. New York: M. Dekker; 1992.

74. Walters KA. Dermatological and transdermal formulations: Informa HealthCare; 2002.

75. Guy RH, Hadgraft J. Transdermal drug delivery. 2nd ed. New York: M. Dekker; 2003.

76. Williams A. Transdermal and topical drug delivery: From theory to clinical practice. London ; Chicago: Pharmaceutical Press; 2003.

77. Goosen C, Du Plessis J, Müller D, Janse van Rensburg L. Correlation between physicochemical characteristics, pharmacokinetic properties and transdermal absorption of NSAID's. International journal of pharmaceutics. 1998;163(1):203-9.

78. Andrews SN, Jeong E, Prausnitz MR. Transdermal Delivery of Molecules is Limited by Full Epidermis, Not Just Stratum Corneum. Pharmaceutical Research. 2012;30(4):1099-1109.

79. Crawley FE, Haines JW. The dosimetry of carbon-14 labelled compounds: the metabolism of diethylenetriamine pentaacetic acid (DTPA) in the rat. Int J Nucl Med Biol. 1979;6(1):9-15.

80. National Council on Radiation Protection and Measurements., National Council on Radiation Protection and Measurements. Scientific Committee 57-17 on Radionuclide Dosimetry Model for Wounds. Development of a biokinetic model for radionuclide-contaminated wounds and procedures for their assessment, dosimetry, and treatment : recommendations of the National Council on Radiation Protection and Measurements, December 14, 2006. Bethesda, MD: National Council on Radiation Protection and Measurements; 2007 pp. 35-117.

81. International Commission on Radiological Protection. Human respiratory tract model for radiological protection: A report of a task group of the International Commission on Radiological Protection: Elsevier Health Sciences; 1994.

82. Bailey M. The new ICRP model for the respiratory tract. Radiation Protection Dosimetry. 1994;53(1-4):107-14.

83. Birchall A, Bailey M, Jarvis N, editors. Application of the new ICRP respiratory tract model to inhaled plutonium nitrate using experimental biokinetic data. Proceedings of the international conference on radiation dose management in the nuclear industry, Windermere, UK; 1995.

84. Etherington G, Shutt A, Stradling G, Fifield L, Newton D. A study of the human biokinetics of inhaled plutonium nitrate. Annals of Occupational Hygiene. 2002;46(suppl 1):350-2.

85. K. Bull R, T. Morrison R, Talbot R, A. Roberts G. An intake of americum oxide powder: Implications for biokinetic models for americum. Radiation Protection Dosimetry. 2003 July 1, 2003;105(1-4):369-73.

86. Bailey M, Ansoborlo E, Guilmette R, Paquet F. Updating the ICRP human respiratory tract model. Radiation Protection Dosimetry. 2007;127(1-4):31-4.

87. Leggett R, Eckerman K, Khokhryakov V, Suslova K, Krahenbuhl M, Miller S. Mayak worker study: an improved biokinetic model for reconstructing doses from internally deposited plutonium. 2009.

88. Ansoborlo E, Amekraz B, Moulin C, Moulin V, Taran F, Bailly T, et al. Review of actinide decorporation with chelating agents. Cr Chim. 2007;10(10-11):1010-9.

89. Volf V. Treatment of Incorporated Transuranium Elements: A Report Sponsored by WHO and the IAEA: International Atomic Energy Agency; 1978.

90. Guilmette RA, Moretti ES, Lindenbaum A. Toward an optimal DTPA therapy for decorporation of actinides: time-dose relationships for plutonium in the dog. I. Radiat Res. 1979;78(3):415-28.

91. Ménétrier F, Taylor DM, Comte A. The biokinetics and radiotoxicology of curium: A comparison with americium. Applied Radiation and Isotopes. 2008;66(5):632-47.

92. Guilmette RA, Muggenburg BA. Reducing the radiation dose from inhaled americium-241 using continuously administered DTPA therapy. Int J Radiat Biol Relat Stud Phys Chem Med. 1988;53(2):261-71.

93. Anderegg G, Arnaud-Neu F, Delgado R, Felcman J, Popov K. Critical evaluation of stability constants of metal complexes of complexones for biomedical and environmental applications*(IUPAC Technical Report). Pure and applied chemistry. 2005;77(8):1445-95.

94. Phan G, Herbet A, Cholet S, Benech H, Deverre JR, Fattal E. Pharmacokinetics of DTPA entrapped in conventional and long-circulating liposomes of different size for plutonium decorporation. J Control Release. 2005;110(1):177-88.

95. Phan G, Le Gall B, Grillon G, Rouit E, Fouillit M, Benech H, et al. Enhanced decorporation of plutonium by DTPA encapsulated in small PEG-coated liposomes. Biochimie. 2006;88(11):1843-9.

96. Diethylenetriaminepentaacetic acid (DTPA) Material Safety Data Sheet from www.sigmaaldrich.com, Version 4.8, Revision date 04/12/2012. (Accessed on 30 May 2012)

97. Beaumont K, Webster R, Gardner I, Dack K. Design of ester prodrugs to enhance oral absorption of poorly permeable compounds: challenges to the discovery scientist. Current Drug Metabolism. 2003;4(6):461-85.

98. Ettmayer P, Amidon GL, Clement B, Testa B. Lessons learned from marketed and investigational prodrugs. Journal of Medicinal Chemistry. 2004;47(10):2393.

99. Rautio J, Kumpulainen H, Heimbach T, Oliyai R, Oh D, Järvinen T, et al. Prodrugs: design and clinical applications. Nature Reviews Drug Discovery. 2008;7(3):255-70.

100. Stella V, Borchardt R, Hageman M, Oliyai R, Maag H, Tilley J. Prodrugs: Challenges and rewards: Springer; 2007.

101. Testa B, Mayer JM. Hydrolysis in drug and prodrug metabolism: Vch Verlagsgesellschaft Mbh; 2003.

102. Sloan KB. Prodrugs : topical and ocular drug delivery. New York: M. Dekker; 1992.

103. Jacobson EL, Kim H, Kim M, Williams JD, Coyle DL, Coyle WR, et al. A topical lipophilic niacin derivative increases NAD, epidermal differentiation and barrier function in photodamaged skin. Experimental dermatology. 2007;16(6):490-9.

104. Jacobson EL, Jacobson MK, Kim H, Kim M, Qasem JG. Topical formulations for the transdermal delivery of niacin and methods of treating hyperlipidemia. United States Patent 6,677,361; 2004.

105. Wang J-J, Sung KC, Huang J-F, Yeh C-H, Fang J-Y. Ester prodrugs of morphine improve transdermal drug delivery: a mechanistic study. Journal of Pharmacy and Pharmacology. 2007;59(7):917-25.

106. Fang J-Y, Leu Y-L. Prodrug strategy for enhancing drug delivery via skin. Current drug discovery technologies. 2006;3(3):211-24.

107. Prausnitz MR, Langer R. Transdermal drug delivery. Nature biotechnology. 2008;26(11):1261-8.

108. Oesch F, Fabian E, Oesch-Bartlomowicz B, Werner C, Landsiedel R. Drug-metabolizing enzymes in the skin of man, rat, and pig. Drug metabolism reviews. 2007;39(4):659-98.

109. Beisson F, Aoubala M, Marull S, Moustacas-Gardies AM, Voultoury R, Verger R, et al. Use of the tape stripping technique for directly quantifying esterase activities in human stratum corneum. Analytical Biochemistry. 2001;290(2):179-85.

110. Liederer BM, Borchardt RT. Enzymes involved in the bioconversion of ester-based prodrugs. J Pharm Sci. 2006;95(6):1177-95.

111. Prusakiewicz JJ, Ackermann C, Voorman R. Comparison of skin esterase activities from different species. Pharm Res. 2006;23(7):1517-24.

112. IMAI T. Human carboxylesterase isozymes: catalytic properties and rational drug design. Drug metabolism and pharmacokinetics. 2006;21(3):173-85.

113. Jewell C, Prusakiewicz JJ, Ackermann C, Payne N, Fate G, Voorman R, et al. Hydrolysis of a series of parabens by skin microsomes and cytosol from human and minipigs and in whole skin in short-term culture. Toxicology and applied pharmacology. 2007;225(2):221-8.

114. Sugibayashi K, Hayashi T, Morimoto Y. Simultaneous transport and metabolism of ethyl nicotinate in hairless rat skin after its topical application: the effect of enzyme distribution in skin. Journal of Controlled Release. 1999;62(1):201-8.

115. Kim M-K, Lee C-H, Kim D-D. Skin Permeation of Testosterone and its Ester Derivatives in Rats. Journal of Pharmacy and Pharmacology. 2000;52(4):369-75.

116. Zhang Y, Yang Y-T, Jay M. Species-Dependent Metabolism of a DTPA Prodrug by Skin Esterases. Abstract T2424. AAPS Annual Meeting and Exposition. Washington, DC, October, 2011. Available from: http://www.aapsj.org/abstracts/AM_2011/T2424.pdf.

117. Pacyniak E, M. Leed, M. Sadgrove, Jay M. Interspecies Differences in Metabolism of a Multi-Ester Prodrug by Carboxylesterases. Abstract W4419. AAPS Annual Meeting and Exposition. Washington, DC, October, 2011. Available from: http://www.aapsj.org/abstracts/AM_2011/W4419.pdf.

118. Sherry AD, Cacheris WP, Kuan KT. Stability constants for Gd3+ binding to model DTPA-conjugates and DTPA-proteins: implications for their use as magnetic resonance contrast agents. Magn Reson Med. 1988;8(2):180-90.

119. Morss LR, Edelstein NM, Fuger J, Katz JJ. The chemistry of the actinide and transactinide elements, Vol. 2. 3rd ed. Dordrecht: Springer; 2006, pp. 1265-1395.

120. Guilmette RA, Parks JE, Lindenbaum A. Synthesis and therapeutic testing of mono- and dialkyl esters of pentetic (diethylenetriaminepentaacetic) acid for decorporation of polymeric plutonium. Journal of Pharmaceutical Sciences. 1979;68(2):194-6.

121. Stradling GN, Gray SA, Moody JC, Hodgson A, Raymond KN, Durbin PW, et al. The Efficacy of DFO-HOPO, DTPA-DX and DTPA for Enhancing the Excretion of Plutonium and Americium from the Rat. International Journal of Radiation Biology. 1991;59(5):1269-77.

122. Volf V, Burgada R, Raymond KN, Durbin PW. Early Chelation Therapy for Injected Pu-238 and Am-241 in the Rat: Comparison of 3,4,3-LIHOPO, DFO-HOPO, DTPA-DX, DTPA and DFOA. International Journal of Radiation Biology. 1993;63(6):785-93.

123. Zhu D, Lu X, Hardy PA, Leggas M, Jay M. Nanotemplate-engineered nanoparticles containing gadolinium for magnetic resonance imaging of tumors. Investigative radiology. 2008;43(2):129-40.

124. Stradling GN, Gray SA, Ellender M, Pearce M, Wilson I, Moody JC, et al. Removal of inhaled plutonium and americium from the rat by administration of ZnDTPA in drinking water. Hum Exp Toxicol. [Comparative Study]. 1993;12(3):233-9.

125. Stevens E, Rosoff B, Weiner M, Spencer H, editors. Metabolism of the chelating agent diethylenetriamine pentaacetic acid (C14DTPA) in man. Proceedings of the Society for Experimental Biology and Medicine Society for Experimental Biology and Medicine (New York, NY); 1962: Royal Society of Medicine.

126. Heng PWS, Chan LW, Chow KT. Development of Novel Nonaqueous Ethylcellulose Gel Matrices: Rheological and Mechanical Characterization. Pharmaceutical Research. 2005;22(4):676-84.

127. Tashtoush BM, Jacobson EL, Jacobson MK. Validation of a simple and rapid HPLC method for determination of metronidazole in dermatological formulations. Drug development and industrial pharmacy. 2008;34(8):840-4.

128. Rekhi GS, Jambhekar SS. Ethylcellulose-A polymer review. Drug Development and Industrial Pharmacy. 1995;21(1):61-77.

129. Crowley P, Martini LG. Drug–excipient interactions. reactions. Pharm. Technol. Eur. 2001;13:26–34.

130. Waterman KC, Adami RC, Alsante KM, Antipas AS, Arenson DR, Carrier R, et al. Hydrolysis in pharmaceutical formulations. Pharmaceutical development and technology. 2002;7(2):113-46.

131. Langner M, Maibach H. Many common drugs in dermatology are light, temperature, or moisture-sensitive. Skin Therapy Lett. 2009;14(1):3-5.

132. Petrolatum (White). http://www.inchem.org/documents/icsc/icsc/eics1440.htm (Accessed on 8 January 2013).

133. Chow K, Chan L, Heng P. Formulation of Hydrophilic Non-Aqueous Gel: Drug Stability in Different Solvents and Rheological Behavior of Gel Matrices. Pharmaceutical Research. 2008;25(1):207-17.

134. Claramonte M, Parera Vialard A, Vilchez FG. In vitro percutaneous absorption of naproxen from gels using a double-layer artificial membrane. International journal of pharmaceutics. 1993;98(1-3):37-43.

135. Lee C, Kitagawa K, Uchida T, Kim N, Goto S. Transdermal delivery of theophylline using an ethanol/panasate 800-ethylcellulose gel preparation. Biological & pharmaceutical bulletin. 1995;18(1):176.

136. Lizaso E, Muñoz ME, Santamaría A. Formation of Gels in Ethylcellulose Solutions. An Interpretation from Dynamic Viscoelastic Results. Macromolecules. 1999;32(6):1883-9.

137. European Pharmacopoeia, 2002 European Pharmacopoeia (4th Edition) Council of Europe, Strasbourg, France. 2002.

138. Chan L, Chow K, Heng PWS. Investigation of wetting behavior of nonaqueous ethylcellulose gel matrices using dynamic contact angle. Pharmaceutical Research. 2006;23(2):408-21.

139. Chow KT, Chan LW, Heng PWS. Characterization of spreadability of nonaqueous ethylcellulose gel matrices using dynamic contact angle. Journal of Pharmaceutical Sciences. 2008;97(8):3467-82.

140. Taylor DM, Stradling GN, Hengé-Napoli M-H. The Scientific Background to Decorporation. Radiation Protection Dosimetry. 2000;87(1):11-8.

141. Taylor DM, Volf V. Oral Chelation Treatment of Injected 241Am Or 239Pu in Rats. Health physics. 1980;38(2):147-58.

142. Volf V. Effect of Drinking Zn-DTPA on 238-Pu and 241-Am in rat bones. Radiation and Environmental Biophysics. 1984;23(2):141-3.

143. Macosko CW. Rheology : principles, measurements, and applications. New York: VCH; 1994, pp. 65-108.

144. Higuchi T. Physical chemical analysis of percutaneous absorption process from creams and ointments. J Soc Cosmet Chem. 1960;11(2):85-97.

145. Higuchi W. Analysis of data on the medicament release from ointments. Journal of Pharmaceutical Sciences. 1962;51(8):802-4.

146. Chang JY, Oh YK, Choi HG, Kim YB, Kim CK. Rheological evaluation of thermosensitive and mucoadhesive vaginal gels in physiological conditions. Int J Pharm. 2002;241(1):155-63.

147. Pena LE, Lee BL, Stearns JF. Structural rheology of a model ointment. Pharm Res. 1994;11(6):875-81.

148. Contreras MD, Sanchez R. Application of a factorial design to the study of the flow behavior, spreadability and transparency of a Carbopol ETD 2020 gel. Part II. Int J Pharm. 2002;234(1-2):149-57.

149. Zhang Y, Sadgrove M, Jay M. Transdermal Delivery of DTPA Prodrug for Continuous Decorporation of Transuranic Elements. Abstract T2248. AAPS Annual

Meeting and Exposition. Washington, DC, October, 2011. Available from: http://www.aapsj.org/abstracts/AM_2011/T2248.pdf.

150. Yang Y-T, Di. Pasqua AJ, He W, Tsai T, Sueda K, Zhang Y, et al. Preparation of alginate beads containing a prodrug of diethylenetriaminepentaacetic acid. Carbohydrate polymers. 2013;92(2):1915-1920.

151. Banker GS. Film coating theory and practice. Journal of Pharmaceutical Sciences. 1966;55(1):81-9.

152. Bodmeier R, McGinity JW. The preparation and evaluation of drug-containing poly (dl-lactide) microspheres formed by the solvent evaporation method. Pharmaceutical Research. 1987;4(6):465-71.

153. Leuner C, Dressman J. Improving drug solubility for oral delivery using solid dispersions. European Journal of Pharmaceutics and Biopharmaceutics. 2000;50(1):47-60.

154. Lachenmeier DW. Safety evaluation of topical applications of ethanol on the skin and inside the oral cavity. J Occup Med Toxicol. 2008;3:26.

155. Barry BW. Dermatological formulations: percutaneous absorption. M. Dekker; 1983. p. 296-440.

156. Shah VP, Elkins J, Hanus J, Noorizadeh C, Skelly JP. <i>In Vitro</i> Release of Hydrocortisone from Topical Preparations and Automated Procedure. Pharmaceutical Research. 1991;8(1):55-9.

157. Shah VP. In Vitro Release from Semisolid Dosage Forms?ÄîWhat Is Its Value? Percutaneous Absorption: Informa Healthcare; 2005. p. 481-8.

158. Shutt A, Youngman M, Raine C, Stradling G, Etherington G, Kreyling W. A study of the human biokinetics of inhaled gadolinium oxide. Annals of Occupational Hygiene. 2002;46(suppl 1):320-2.

159. Schulz WW. Chemistry of americium: Atlantic Richfield Hanford Co., Richland, Wash.(USA)1976.

160. International Commission on Radiological Protection. 1990 recommendations of the International Commission on Radiological Protection : user's edition. 1st ed. Oxford ; New York: :Published for the International Commission on Radiological Protection by Pergamon Press; 1992.

161. Wood R, Sharp C, Gourmelon P, Le Guen B, Stradling GN, Taylor DM, et al. Decorporation Treatment - Medical Overview. Radiation Protection Dosimetry. 2000;87(1):51-6.

162. Harrison JD, Muirhead CR. Quantitative comparisons of cancer induction in humans by internally deposited radionuclides and external radiation. Int J Radiat Biol. 2003;79(1):1-13.

163. Moysich KB, Menezes RJ, Michalek AM. Chernobyl-related ionising radiation exposure and cancer risk: an epidemiological review. Lancet Oncol. 2002;3(5):269-79.

164. Stradling GN, Taylor DM, Hengé-Napoli M-H, Wood R, Silk TJ. Treatment for Actinide-bearing Industrial Dusts and Aerosols. Radiation Protection Dosimetry. 2000;87(1):41-50.

165. Stradling GN, Hengé-Napoli M-H, Paquet F, Poncy J-L, Fritsch P, Taylor DM. Approaches for Experimental Evaluation of Chelating Agents. Radiation Protection Dosimetry. 2000;87(1):19-28.

166. Volf V. Chelation therapy of incorporated plutonium-238 and americium-241: comparison of LICAM(C), DTPA and DFOA in rats, hamsters and mice. Int J Radiat Biol Relat Stud Phys Chem Med. 1986;49(3):449-62.

167. Lloyd RD, Bruenger FW, Mays CW, Atherton DR, Jones CW, Taylor GN, et al. Removal of Pu and Am from Beagles and Mice by 3,4,3-LICAM(C) or 3,4,3-LICAM(S). Radiation Research. 1984;99(1):106-28.

168. Sérandour AL, Grémy O, Fréchou M, Renault D, Poncy JL, Fritsch P. In Vitro and In Vivo Assessment of Plutonium Speciation and Decorporation in Blood and Target Retention Tissues after a Systemic Contamination followed by an Early Treatment with DTPA. Radiation Research. 2008;170(2):208-15.

169. Taylor D. Some aspects of the comparative metabolism of plutonium and americium in rats. Health physics. 1962;8(6):673-7.

170. Turner G, Taylor D. The Transport of Plutonium, Americium and Curium in the Blood of Rats. Physics in Medicine and Biology. 1968;13:535-46.

171. Markley JF. Removal of Polymeric Plutonium from Mice by Combined Therapy with the Calcium Chelate and Penta-Ethyl Ester of Dtpa. Int J Radiat Biol Relat Stud Phys Chem Med. 1963;7:405-7.

172. Taylor GN, Lloyd RD, Mays CW, Angus W, Miller SC, Shabestari L, et al. Plutonium- Or Americium-induced Liver Tumors and Lesions in Beagles. Health physics. 1991;61(3):337-47.

173. International Commission on Radiological Protection. Limits for intakes of radionuclides by workers. ICRP 30, Part 1. Ann. ICRP 2 (3-4): Pergamon Press; 1979.

174. Roberts R, McCune S. Animal studies in the development of medical countermeasures. Clinical Pharmacology & Therapeutics. 2008;83(6):918-20.

175. Snoy PJ. Establishing Efficacy of Human Products Using Animals: The US Food and Drug Administration's "Animal Rule". Veterinary Pathology Online. 2010;47(5):774-8.

176. Farriol M, Rosselló J, Schwartz S. Body surface area in Sprague-Dawley rats. Journal of Animal Physiology and Animal Nutrition. 1997;77(1-5):61-5.

177. Wang C, Cunningham G, Dobs A, Iranmanesh A, Matsumoto AM, Snyder PJ, et al. Long-term testosterone gel (AndroGel) treatment maintains beneficial effects on sexual function and mood, lean and fat mass, and bone mineral density in hypogonadal men. Journal of Clinical Endocrinology & Metabolism. 2004;89(5):2085-98.

178. Durbin P, Schmidt C. Predicting the kinetics of chelating agents in man from animal data. Health physics. 1989;57:165-74.

179. Sueda K. Sadgrove MP, Jay M. Di Pasqua AJ. Species-dependent effective concentration of DTPA in plasma for chelation of ^{241}Am. Health Physics. In press, 2013.